

# **Evaluation and Improvement of Particle Number/Mass Size Distribution Modelling in WRF-Chem over Europe**

An der Fakult ä für Physik und Geowissenschaften  
der Universit ä Leipzig  
genehmigte

DISSERTATION  
zur Erlangung des akademischen Grades  
DOCTOR RERUM NATURALIUM  
(Dr. rer. nat.)  
vorgelegt  
von M. Sc. Ying Chen

geboren am 27.10.1984 in Fujian, China

Gutachter: Prof. Dr. Alfred Wiedensohler  
Prof. Dr. Gregory Carmichael

Tag der Verleihung: 10 Juli 2017

The present study was prepared between August 2013 and June 2017

at the Leibniz Institute for Tropospheric Research (TROPOS)  
Department of Experimental Aerosol and Cloud Microphysics  
Permoserstraße 15  
04318 Leipzig  
Germany

The work was supervised by  
Prof. Dr. Alfred Wiedensohler

## **Bibliographic Description**

Ying Chen

### **Evaluation and Improvement of Particle Number/Mass Size Distribution Modelling in WRF-Chem over Europe**

University of Leipzig, Faculty of Physics and Earth Sciences, Doctoral thesis

88 Pages, 136 References, 7 Figures, 2 Tables

#### **Abstract:**

Atmospheric aerosol particles play an important role in global climate change, via direct and indirect radiative forcing. Elemental carbon (EC) and nitrate are important contributors to anthropogenic aerosol radiative forcing over Europe, since they strongly absorb and/or scatter solar radiation, respectively. However, the evaluation of their climate effects remains highly uncertain. Improvements on the simulation of particle number/mass size distribution (PSD) in modelling will help us to refine model assessments of climate change. The simulations were performed over Europe with a fully online-coupled regional air quality model (WRF-Chem) for the time period of September 10-20<sup>th</sup>, 2013. Measurements in the HOPE-Melpitz campaign and other datasets in Europe were adopted to evaluate the model uncertainties.

The meteorological conditions were well reproduced by the simulations. However, a remarkable overestimation of coarse mode PSD was found in the simulations. The overestimation was mainly contributed by EC, sodium nitrate and sea salt (SSA), stemming from the inadequate emission of EC and SSA. The EC inventory overestimates EC point sources in Germany and the fractions of coarse mode EC emissions in Eastern Europe and Russia. Allocating too much EC emission into the coarse mode could shorten EC lifetime and reduce its long-range transport, thus partly (~20-40%) explaining the underestimation of EC in Germany, when air masses came from eastern direction in previous studies. Furthermore, WRF-Chem overestimated coarse mode SSA mass concentrations by factors of about 8-20 over northwestern and central Europe in this study, due to the shortcoming of its emission scheme. This could facilitate the coarse mode sodium nitrate formation and lead to ~140% overestimation of coarse mode nitrate. Under such circumstances, nitric acid was exhausted, and fine mode ammonium nitrate formation was inhibited. The overestimated SSA shaped the PSD of nitrate towards larger sizes, which might influence the optical properties, lifetime and climate effect of nitrate accordingly. A transport mechanism would broaden the influence of SSA on nitrate PSD to central Europe, where a considerable amount of nitrate precursors and ammonium nitrate is present.

## **Bibliographic Description**

Ying Chen

### **Bewertung und Entwicklung der Modellierung von Aerosolpartikelgrößen- und massenverteilungen über Europa mit WRF-Chem**

Universität Leipzig, Fakultät für Physik und Geowissenschaften, Dissertation

88 Seiten, 136 Literaturzitate, 7 Abbildungen, 2 Tabellen

#### **Referat:**

Atmosphärische Aerosolpartikel können sich direkt und indirekt auf den Strahlungshaushalt der Erde auswirken und spielen somit eine wichtige Rolle für das globale Klima. Elementarer Kohlenstoff (EC) und Nitrat haben die Eigenschaft Licht stark zu absorbieren beziehungsweise zu streuen. Durch ihre hohen Konzentrationen stellen sie in Europa wichtige Faktoren für den anthropogenen Strahlungsantrieb dar. Die Unsicherheiten in Bezug auf die Abschätzung ihres Klimaeffektes sind jedoch sehr hoch. Eine Verbesserung der Simulation von Partikelgrößen- und massenverteilung (PSD) hilft dabei Modellabschätzungen zum Klimawandel zu optimieren. Dazu wurden Modellsimulationen mit einem online-gekoppelten regionalen Luftqualitätsmodell (WRF-Chem) über Europa für den Zeitraum von 10. bis 20. September 2013 durchgeführt. Messungen der HOPE-Melpitz Kampagne und andere Datensätze aus Europa wurden verwendet, um die Unsicherheiten des Modells zu bewerten.

Es zeigte sich, dass die meteorologischen Verhältnisse gut durch das Modell reproduziert werden konnten. Jedoch wurde der Grobmod der PSD durch das Modell überschätzt. Hauptsächlich trugen EC, Natriumnitrat und Seesalz (SSA) zur Überschätzung bei. Ursache ist die unzureichend beschriebene Emission von EC und Seesalz. Das verwendete Emissionskataster überschätzt die EC-Quellen in Deutschland sowie den Grobmod des EC in Osteuropa und Russland. Dadurch wird dem Grobmod eine zu hohe Emission von EC zugeordnet. Dies könnte die Verweildauer des EC verkürzen und damit den großräumigen Transport reduzieren, was teilweise (~20-40%) die Unterschätzung des EC in Deutschland bei Ostanströmung, wie sie in früheren Studien erwähnt wird, erklären könnte. Des Weiteren wurde wegen des unzureichend charakterisierten Emissionsschemas, die Grobmod-Massenkonzentration des Seesalzes über Nordwest- und Zentraleuropa durch WRF-Chem um einen Faktor von 8 bis 20 überschätzt. Im Grobmod führt dies zu einer erhöhten Bildung von Natriumnitrat und schließlich zu einer Überschätzung des Nitrates um  $\approx 140\%$ . Dadurch wird Salpetersäure verbraucht, was eine Hemmung der Bildung von Ammoniumnitrat im Feinmod nach sich zieht. Die Überschätzung von SSA führt zur Verschiebung der Nitratmasse hin zu höheren Partikelgrößen. Dies kann die optischen Eigenschaften, die Verweildauer und den Klimaeinfluss von Nitrat beeinflussen. Ein Transportmechanismus würde den Einfluss von SSA auf die PSD des Nitrates in Zentraleuropa erweitern, wo Ausgangsstoffe des Nitrates und Ammoniumnitrates in hohem Maße vorhanden sind.



# Table of Contents

List of Figures .....	I
List of Tables.....	I
Abbreviations .....	II
<b>1. Introduction .....</b>	<b>1</b>
1.1 Particle size distribution .....	2
1.2 Elemental carbon particle size distribution simulation .....	5
1.3 Chemical pathways for particulate nitrate .....	7
1.4 Influence of sea salt on nitrate particle mass size distribution .....	8
1.5 Objectives.....	9
<b>2. Methodology .....</b>	<b>11</b>
2.1. WRF-Chem model .....	11
2.1.1. General description.....	11
2.1.2. Model configuration .....	12
2.1.3 Anthropogenic source emissions .....	16
2.1.4 Natural source emissions.....	17
2.2 HOPE-Melpitz campaign .....	17
2.3 GUAN network over Germany .....	19
2.4 Other datasets .....	20
<b>3. Results and Discussion .....</b>	<b>21</b>
3.1 First publication.....	21
3.1.1 Evaluation of the size segregation of elemental carbon (EC) emission in Europe: influence on the simulation of EC long-range transportation .....	21
3.1.2 Supporting information .....	35
3.2 Second publication .....	39
3.2.1 Sea salt emission, transport and influence on size-segregated nitrate simulation: a case study in northwestern Europe by WRF-Chem .....	39
3.2.2 Supporting information .....	57
<b>4. Summary and Conclusions.....</b>	<b>64</b>
<b>5. Outlook.....</b>	<b>68</b>
<b>Appendix A .....</b>	<b>69</b>
<b>Bibliography .....</b>	<b>70</b>
<b>Acknowledgements</b>	

## List of Figures

<b>Figure 1.</b> The size-resolved particle mass light extinction efficiency. The results are integrated over a typical solar spectrum. The solid and dashed black line indicates the result of particles with complex refractive index of 1.5-0.005i and 1.37-0.001i. Available at: <a href="https://www.ipcc.ch/ipccreports/tar/wg1/fig5-1.htm">https://www.ipcc.ch/ipccreports/tar/wg1/fig5-1.htm</a> . (Last access: 10 May 2016) ....	2
<b>Figure 2.</b> Size segregated mass concentration of particle compositions observed at Bologna, Italy. OM: organic matter; unacc.: the remaining unaccounted mass fraction; min. dust: mineral dust; nnsSO <sub>4</sub> : non-sea-salt sulfate. Source: Putaud et al., (2004). ....	6
<b>Figure 3.</b> Schematic diagram of the scientific questions.....	10
<b>Figure 4.</b> Setup of domains in WRF-Chem.....	13
<b>Figure 5.</b> Observation sites of the GUAN network. Source: Birmili et al. (2016).....	19
<b>Figure 6.</b> Aerosol mass residential rate in relation to the transport time and lifetime. Source: Chen et al. (2016a).....	65
<b>Figure 7.</b> Schematic of sea salt transportation and its influence on coarse mode nitrate formation and nitrate particle mass size distribution. Source: Chen et al. (2016b).....	67

## List of Tables

<b>Table 1.</b> Configurations of WRF-Chem.....	14
<b>Table 2.</b> Comparison between EMEP and TNO emission inventory of Germany .....	16

# Abbreviations

ACTRIS	Aerosols, Clouds, and Trace gases Research InfraStructure Network
AERONET	Aerosol Robotic Network
AOD	Aerosol Optical Depth
APS	Aerodynamic Particle Size spectrometer
AQMEII	Air Quality Model Evaluation International Initiative project
ARW	Advanced Research Weather Research and Forecasting model
BC	Black Carbon
CBMZ	The Carbon-Bond Mechanism version Z
CCN	Cloud Condensation Nuclei
CIT	California Institute of Technology model
COSMO	Consortium for Small-scale Modeling model
DMA	Differential Mobility Analyzer
DRF	Direct Radiative Forcing
EC	Elemental Carbon
ECc	Coarse mode Elemental Carbon
EEA	European Environment Agency
EMEP	European Monitoring and Evaluation Programme
EPA	Environmental Protection Agency, United States
EUCAARI	European Integrated project on Aerosol, Cloud, Climate and Air Quality Interactions
FINN	Fire Inventory from National Center of Atmospheric Research
FNL	Final Operational Global Analysis
GATOR	Gas, Aerosol, TranspOrt, Radiation model
GUAN	German Ultrafine Aerosol Network
GO03	the sea salt emission parameterization according to Gong (2003)

HOPE	HD(CP)2 Observational Prototype Experiment
IMPACT	Integrated Massively Parallel Atmospheric Chemical Transport model
IPCC	Intergovernmental Panel on Climate Change
IRF	Indirect Radiative Forcing
MAAP	Multi-Angle Absorption Photometers
MAC	Mass Absorption Cross-section
MADE	Modal Aerosol Dynamics model for Europe
MADE-IN	Modal Aerosol Dynamics model including Insoluble Modes
MAM	A Modal Aerosol Model
MARGA	Monitor for AeRosols and Gases in ambient Air system
MEGAN	Model of Emissions of Gases and Aerosols from Nature
MOSAIC	MOdel for Simulating Aerosol Interactions and Chemistry
MOZART	Model for Ozone and Related chemical Tracers
MUSCAT	Multi-Scale Chemistry Aerosol Transport model
NCAR	National Center of Atmospheric Research
NCEP	National Center for Environmental Prediction
NMM	Non-hydrostatic Mesoscale Model
NMVOCs	non-methane volatile organic compounds
OC	Organic Carbon
RACM	Regional Atmospheric Chemistry Mechanism
RADM2	The second generation Regional Acid Deposition Model
PBL	Planetary Boundary Layer
PM	Particulate Matter
PM <sub>10</sub>	Particulate Matter with an aerodynamic diameter less than 10 µm
PM <sub>2.5</sub>	Particulate Matter with an aerodynamic diameter less than 2.5 µm
PM <sub>1</sub>	Particulate Matter with an aerodynamic diameter less than 1 µm
PMSD	Particle Mass Size Distribution

PNSD	Particle Number Size Distribution
PSD	Particle number/mass Size Distribution
SAPRC99	Statewide Air Pollution Research Center chemical mechanism
SMPS	Scanning Mobility Particle Sizer spectrometer
SNAP	Selected Nomenclature of Air Pollution
SORGAM	Secondary ORGanic Aerosol Model
SSA	Sea Salt Aerosol
SST	Sea Surface Temperature
TROPOS	Leibniz Institute for Tropospheric Research
UAM-AERO	Urban Airshed Model with Aerosols
UAM-AIM	Urban Airshed Model with Aerosol Inorganics Model
UCM	Urban canopy model
WRF-Chem	Weather Research and Forecasting model coupled with Chemistry
WMO-GAW	World Meteorological Organization – Global Atmospheric Watch
YSU	Yonsei University



### 1. Introduction

Atmospheric aerosol particles play an important role in global climate, via direct radiative forcing (DRF, light scattering and absorption) and indirect radiative forcing (IRF, participating in cloud processes). However, aerosol radiative forcing still has the highest uncertainty among all climate change agents according to the recent Intergovernmental Panel on Climate Change (IPCC) assessment (IPCC AR5, 2013), with a wide range of  $-0.77$  to  $+0.23$   $\text{W/m}^2$  and  $-1.33$  to  $-0.06$   $\text{W/m}^2$  for DRF and IRF, respectively. The particle number/mass size distribution (PSD) is a key parameter that determines both direct and indirect radiative forcing of aerosol particles (IPCC AR5, 2013; Shiraiwa et al., 2013; Zhang et al., 2010a; Aquila et al., 2011).

The optical properties of an aerosol particle are strongly related to its size. As illustrated in Fig. 1, fine mode particles usually have larger mass extinction efficiency than the coarse mode particles (IPCC AR5, 2013; Seinfeld and Pandis, 2006). For example, the mass extinction efficiency of a particle with a diameter of 600 nm is about 10-15 times higher than that of 6  $\mu\text{m}$ , therefore it has a more important effect in direct radiative forcing. In the polluted urban atmosphere, fine mode particles are responsible for more than 90% of the total scattering coefficient (Seinfeld and Pandis, 2006). Aerosol particles have both a warming and a cooling effect in climate change. Within all anthropogenic aerosol chemical compounds, black carbon (BC, Bond et al., 2013) and nitrate (Schaap et al., 2002; Schaap et al., 2007) play the most important roles in climate warming and cooling over Europe, respectively. This is due to the considerable burden of BC (Bond et al., 2013) and nitrate (Schaap et al., 2002) over Europe (Putaud et al., 2004; see also Fig. 2), as well as the strong ability of BC for absorbing and nitrate for scattering solar radiation. Therefore, aiming to improve the evaluation of anthropogenic aerosol radiative forcing over Europe, a key question is to improve the PSD simulations of BC and nitrate in current modelling studies.

In addition, the particle size also influences its hygroscopic growth and ability as cloud condensation nuclei (CCN) significantly (Köhler, 1936). Therefore, the IRF of aerosol particles are not only determined by aerosol chemical properties, but also strongly related to the PSD (IPCC AR5, 2013; Zhang et al., 2010a). Moreover, fine particles have a longer lifetime than coarse particles (Petzold and Krämer, 2012; Croft et al., 2014; IPCC AR5, 2013) and therefore have higher chances to accumulate in the atmosphere, participate in long-range transport, and contribute to the global-scale climate forcing (Foret et al., 2006).

## Introduction

Furthermore, the PSD is also crucial for the health effect of particles. Several studies have shown a strong relation between human health effects (e.g., mortality rate, lung and heart diseases, diabetes, etc.) and fine particles in European cities (e.g., Timonen et al., 2004; Rosenthal et al., 2011; Meister et al., 2012). Fine particles are easily inhaled deep into the lungs where they can remain embedded for long periods of time (U.S. EPA, 1996). Therefore, fine particles are especially harmful to people with lung diseases such as chronic obstructive pulmonary disease and asthma (Zanobetti et al., 2000). Even worse, a recent study reported that nano-particles can be transported directly into the brain and pose a hazard to human health (Maher et al., 2016).

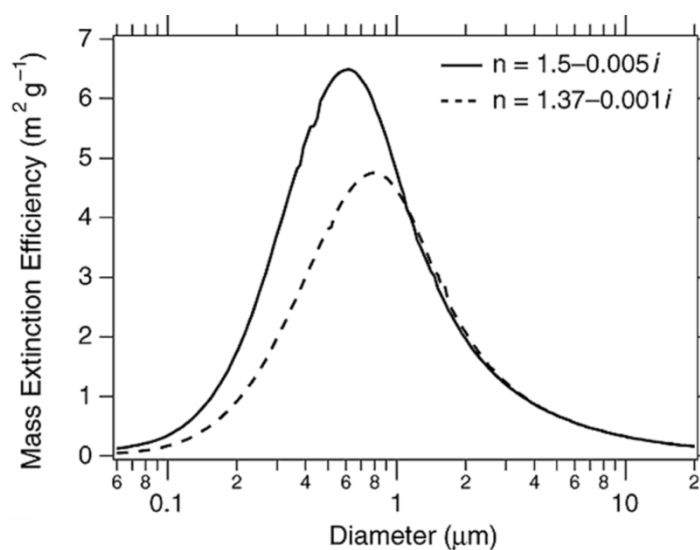


**Figure 1.** The size-resolved particle mass light extinction efficiency. The results are integrated over a typical solar spectrum. The solid and dashed black line indicates the result of particles with complex refractive index of  $1.5-0.005i$  and  $1.37-0.001i$ .

Available at: <https://www.ipcc.ch/ipccreports/tar/wg1/fig5-1.htm> (last access: May 10, 2016)

### 1.1 Particle size distribution

The diameter of aerosol particles covers a wide range from  $10^{-3}$   $\mu\text{m}$  to  $100$   $\mu\text{m}$ . The size distribution of the aerosol population varies strongly in space and time (e.g., Zhang et al., 2010a). In 1976, Knutson (1976) firstly presented submicron PSD measurements with a Differential Mobility Analyzer (DMA). Later that year, TSI Inc. (USA) introduced a commercial DMA (model 3071). Since then measurements of PSD have been performed all over the world (e.g., Wang et al., 2013; Birmili et al., 2001; Birmili et al., 2016). Based on field measurements, Whitby (1978) introduced a classical trimodal model consisting of three additive log-normal



## Introduction

---

modes to describe the PSD in the atmosphere, including Aitken mode (10 to 100 nm), accumulation mode (100 nm to 1-2  $\mu\text{m}$ ) and coarse mode (1-2  $\mu\text{m}$  to 100  $\mu\text{m}$ ). In the past twenty years, the simulation of PSD has commonly been developed in fully online-coupled 3-D atmospheric models (e.g., Ackermann et al., 1998; Zhang et al., 2010a; Zhang et al., 2010b; Aquila et al., 2011). Two major approaches are currently used to represent the PSD in the 3-D atmospheric models: the sectional approach and the modal approach (Zhang et al., 2010a).

In the sectional approach, the PSD is approximated by a discrete number of size sections (Gelbard and Seinfeld 1980; Gelbard et al. 1980). This discretization can be conducted based on number, surface area, or volume/mass, depending on the particle property of interest (Zhang et al., 1999). The sectional representation is used in many air quality models. For example, UAM-AIM (**Urban Airshed Model with Aerosol Inorganics Model**), GATOR (**Gas, Aerosol, TranspOrt, Radiation Model**), UAM-AERO (**Urban Airshed Model with AEROsols**), CIT (**California Institute of Technology Model**), WRF-Chem (**Weather Research and Forecasting model coupled with Chemistry**; with MOSAIC aerosol module: **Model for Simulating Aerosol Interactions and Chemistry**), etc.

The modal technique represents the aerosol as multiple, independent populations of aerosol particles, called modes (Whitby and McMurry, 1997). The aerosol within each mode is represented by a separate mode size distribution function, generally a log-normal distribution (Zhang et al., 1999; Whitby and McMurry, 1997). The modal approach is also commonly used in many models. For example, EMEP (air pollutants model of **European Monitoring and Evaluation Programme**), IMPACT (**Integrated Massively Parallel Atmospheric Chemical Transport Model**), COSMO-MUSCAT (**Consortium for Small-scale Modeling and Multi-Scale Chemistry Aerosol Transport**), WRF-Chem (with MADE-SORGAM aerosol module: **Modal Aerosol Dynamics Model for Europe with Secondary ORGanic Aerosol Model**), etc.

The sectional approach is usually more computationally intensive than the modal approach and its accuracy is dependent on the number of sections used to discretize the size distribution (Whitby and McMurry, 1997; Zhang et al., 1999; Textor et al., 2006; Foret et al., 2006; Zhang et al., 2010a). Foret et al. (2006) reported that at least eight isogradient size bins are necessary for a reasonable size distribution simulation. The accuracy of the modal approach is dependent on the degree to which the size distribution functions represent the actual size distribution (Whitby and McMurry, 1997). The uncertainties of the simulated PSD can stem from primary emissions of

## Introduction

---

particles, secondary formation processes, transport, deposition, coagulation and nucleation (Zhang et al., 1999; Aquila et al., 2011). The simulation of the PSD is very challenging and still has very high uncertainties (Aquila et al., 2011; Textor et al., 2006). For example, Textor et al. (2006) compared the particle sizes simulated by 13 different aerosol models, and reported very high uncertainties of the modelled PSD. The mass fractions of fine particles were in a range of about 15-73%, with a standard deviation of 55% (Textor et al., 2006). Zhang et al. (2010a) compared PSD results of three models, which represented PSD by a modal approach, with ground measurements (10-800 nm) over Europe (Van Dingenen et al., 2004). In Zhang et al. (2010a), although the characteristic shape of the distribution patterns were reasonably reproduced, the uncertainties of PSD simulations over Europe were at least a factor of 2, and can reach up to an order of magnitude. Later, Aquila et al. (2011) proposed a modal approach aerosol module (MADE-IN: **M**odal **A**erosol **D**ynamics model including **I**nsoluble modes), incorporated it into an atmospheric chemistry global model, and compared the PSD results with ground measurements (10-800 nm) over Europe (Van Dingenen et al., 2004). Similar to Zhang et al. (2010a), uncertainties up to 1-2 orders of magnitudes can still be observed, although the distribution pattern of fine mode can be captured by the model.

Improving the simulation of the PSD could help to improve the evaluation of the radiative forcing, and thus refine the model assessments of climate change (Aquila et al., 2011). Field campaign measurements are highly valuable for evaluating the uncertainties of PSD simulations. The HOPE-Melpitz (HD(CP)2 Observational Prototype Experiment at Melpitz) campaign (September 10-20<sup>th</sup>, 2013) provided extensive measurements regarding size-resolved particle microphysical and chemical properties. This dataset was used in this thesis to address the uncertainties of PSD simulations by the state-of-the-art fully online-coupled model WRF-Chem. WRF-Chem simulates the emission, transport, mixing, and chemical transformation of trace gases and aerosols simultaneously with the meteorology. WRF-Chem is one of the most commonly used models for the investigation of regional-scale air quality, field program analysis, and cloud-scale interactions between clouds and chemistry, in the Continental US (e.g., Grell et al., 2011; Ntelekos et al., 2009), China (e.g., Chen et al., 2009; Cheng et al., 2016; Zheng et al., 2015) as well as in Europe (e.g., Tuccella et al., 2012; Archer-Nicholls et al., 2014; Nordmann et al., 2014). In this study, the PSD in WRF-Chem is represented in detail by a sophisticated sectional approach (MOSAIC, Zaveri et al., 2008), which specially focuses on gas-particle partitioning on size distributed particles with a fully dynamic mass transfer approach (Zaveri et al., 2008). The German Ultrafine Aerosol Network (GUAN), which provides the BC online

measurements over Germany, will also be used for model validation. More details of the HOPE-Melpitz campaign, the WRF-Chem model, the GUAN network and other used datasets in this thesis will be given in Chapter-2.

### 1.2 Elemental carbon particle size distribution simulation

Elemental carbon (EC) is defined as the refractory fraction of soot particles that remain stable at high temperatures, as opposed to organic carbon (OC). BC accounts for the light absorbing components of soot particles (Nordmann et al., 2013). The soot particles, measured with photometric methods based on the change in light transmittance through a particle laden filter medium, are defined as BC. However, in modelling studies and emission inventories, EC can be used as the best approximation of BC (Nordmann et al., 2013; Nordmann et al., 2014; Denier van der Gon et al., 2015). A previous study reported that the measured EC and BC are highly correlated over Germany, with  $R^2$  often better than 0.9 (Nordmann et al., 2013).

EC/BC is characterized by its strong absorbing/warming effect (Hansen et al., 2000; Jacobson et al., 2000; Cheng et al., 2012; Bond et al., 2013). EC is the second strongest contributor to current global warming with a total radiative forcing of about  $+1.1 \text{ W/m}^2$ , just after carbon dioxide (Bond et al., 2007; Ramanathan and Carmichael, 2008). As mentioned above, the radiative forcing of EC is strongly related to its PSD. Hence, the accuracy of the PSD simulation of EC can have a significant influence on the assessments of the aerosol warming effect. Uncertainties of EC emission can strongly impact its PSD simulation.

EC particles are exclusively from primary emissions. Globally, biomass burning (40 %), fossil fuel combustion (40 %) and biofuel combustion (20 %) are the major sources of EC emissions (Ramanathan and Carmichael, 2008). Although EC is a crucial contributor to climate warming, its emission inventory is significantly uncertain (Denier van der Gon et al., 2015). The European Environment Agency report (EEA, 2013) indicated that it was almost impossible to evaluate the overall uncertainty at European level. The uncertainty of EC emissions is at least  $\pm 50\%$  on global scales, and a factor of 2 to 5 on a regional scale (Ramanathan and Carmichael, 2008).

In addition to the high uncertainties of EC emission rates in the inventories, modelling studies investigating the PSD of emitted EC are rare and limited. Global emission inventories of EC have been published (e.g., Bond et al., 2004; Lamarque et al., 2010; Streets et al., 2004; Wang et al., 2014) without size segregation information. An emission inventory for UNECE-Europe of

## Introduction

EC (EUCAARI 42-Pan-European Carbonaceous aerosol inventory) has been published with a high resolution ( $1/8^\circ \times 1/16^\circ$ , about  $7 \times 7$  km) and separated size mode ( $PM_{10}$ ,  $PM_{1-2.5}$  and  $PM_{2.5-10}$ ; PM: particulate matter) (Visschedijk and Denier van der Gon, 2008). How well does this EUCAARI inventory represent European EC emissions and especially its size-segregation? This question needs to be answered by modelling validation using in-situ measurements.

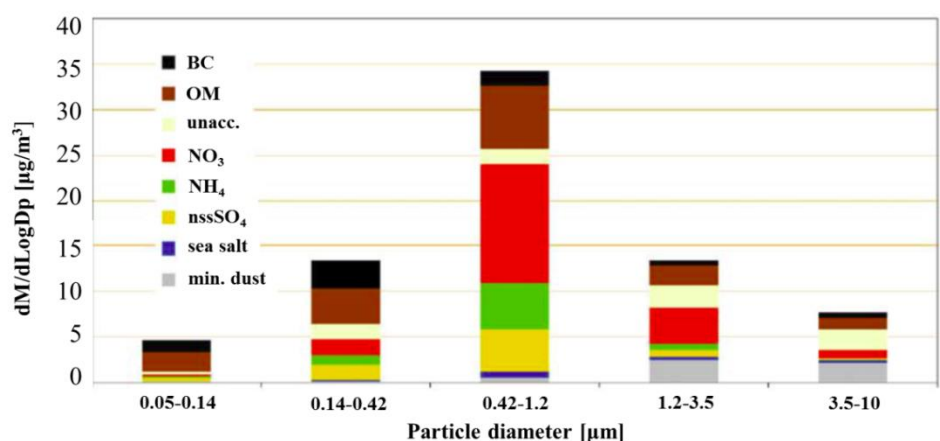


**Figure 2.** Size segregated mass concentration of particle compositions observed at Bologna, Italy. OM: organic matter; unacc.: the remaining unaccounted mass fraction; min. dust: mineral dust; nssSO<sub>4</sub>: non-sea-salt sulfate. Source: Putaud et al., (2004).

The uncertainties of allocating EC emissions in different modes can influence the modelled PSD of EC, and thus can exert a strong influence on its transport. The PSD of EC is crucial for climate change not only due to its influence on the optical properties, but also due to the influence on the long-range transport and deposition of EC particles. Long-range transport of EC particles to remote areas and the deposition on ice could contribute to the glacier melting in the Himalayan (Ming et al., 2008) and Arctic regions (McConnell et al., 2007; Ramanathan and Carmichael, 2008). This can change the surface albedo and hence the absorption of solar radiation, and thus causes positive climate forcing. Despite the importance of the PSD of EC, related studies are rare and limited. Rose et al. (2006) reported that the EC particles freshly emitted from incomplete combustion have sizes around 100 nm. Several field measurement studies reported that about 80-95% EC should be presented as fine particles over Europe (Spindler et al., 2013; Reddington et al., 2013; Hitzenberger et al., 2006; Hitzenberger et al., 2001; Putaud et al., 2004; see Fig. 2). Many modelling studies have evaluated EC emission inventories and its transport in Europe, however, without considering its PSD and the influence on its transport. Koch et al. (2009) evaluated 17 global models and found out that 13 of 17

models overestimate EC in Europe. Stern et al. (2008) compared five model results with observations from northern Germany, and none of the models could reproduce the high EC concentration at the central Europe background station Melpitz. Nordmann et al. (2014) reported that the EUCAARI inventory may underestimate the Eastern European EC emission by a factor of 2, resulting in the underestimation of EC in Germany. However, the size segregation uncertainty of EC emission and the influence on its transport was not considered in these studies.

Evaluating the EC emission inventory and its size-segregation over Europe is one sub-topic of the present thesis. The further influence on long-range transport of EC particles will also be investigated in the present work.

### 1.3 Chemical pathways for particulate nitrate

Nitrate is one of the most important anthropogenic aerosol components that scatters solar radiation and exhibits a considerable cooling effect in climate change, just following sulfate on a global scale (IPCC AR5, 2013). The DRF of nitrate is about  $-0.11 \text{ W/m}^2$ , with a wide range from  $-0.03$  to  $-0.3 \text{ W/m}^2$  (IPCC AR5, 2013; Adams et al., 2001; Bauer et al., 2007; Jacobson, 2001; Liao and Seinfeld, 2005; Myhre et al., 2013; Streets et al., 2013; van Dorland et al., 1997; Xu and Penner, 2012). Especially in western and central Europe, nitrate is the dominant component and may be a more important contributor to aerosol burden than sulfate (Schaap et al., 2002; Schaap et al., 2007; Schaap et al., 2011; Putaud et al., 2004; see also Fig. 2). Therefore, a reduction of uncertainties of nitrate particle mass size distribution simulation can significantly improve the evaluation of its cooling effect, especially over Europe. The particulate nitrate has different major chemical pathways in fine and coarse modes.

Particulate nitrate is mainly secondarily formed by neutralization of gas-phase nitric acid. Ammonia is one of the main precursors of particulate nitrate. It can neutralize nitric acid to form the semi-volatile ammonium nitrate. Ammonium nitrate is mainly present in the accumulation mode (Schaap et al., 2011), which is a part of fine particles. This is because the accumulation mode particles facilitate the gas-particle partitioning processes of ammonium nitrate due to the dominance over particle surface area concentration (Jacobson, 2002). In western and central Europe, particulate nitrate is mainly present as ammonium nitrate in fine mode (ten Brink et al., 1997; Schaap et al., 2002).

## Introduction

---

Nitric acid can also be neutralized by sea salt (sodium chloride) with the depletion of chloride. The heterogeneous reaction of nitric acid on the surface of sea salt aerosol (SSA) promotes the formation of sodium nitrate in the coarse mode, which dominates particulate nitrate formation in northern and southern Europe (Pakkanen et al., 1999; Putaud et al., 2004). However, SSA has the largest uncertainty among all aerosols (Grythe et al., 2014). No emission scheme of sea salt is recommended according to IPCC AR5 (2013). One of the commonly used parameterization schemes of SSA emissions (Gong, 2003; Monahan et al., 1986; hereafter GO03), which is incorporated in WRF-Chem, may largely overestimate the emission of SSA (Neumann et al., 2016a and 2016b; Nordmann et al., 2014; Archer-Nicholls et al., 2014; Zhang et al., 2013; Saide et al., 2012; Saide et al., 2013; de Leeuw et al., 2011). Saide et al. (2012) demonstrated that GO03 overestimated SSA by a factor of 10 for sub-micron particles and a factor of 2 for super-microns in the southeast Pacific Ocean. Jaegl   et al. (2011) found that GO03 overestimated the coarse mode SSA mass concentrations by factors of 2–3 at high wind speeds over the cold waters of the South Pacific, North Pacific and North Atlantic Oceans. Other studies also indicated an overestimation of SSA emissions to varying degrees (Zhang et al., 2013; de Leeuw et al., 2011; Yang et al., 2011; Neumann et al., 2016b). Inaccurate SSA emissions may lead to the uncertainties of coarse mode nitrate simulation.

In this study, the GO03 scheme is adopted into WRF-Chem to describe the SSA emission. The influence of the inadequate SSA emission scheme (GO03) on the nitrate formation modelling and to what extent will this influence be spread over Europe will be explored in this thesis.

### 1.4 Influence of sea salt on nitrate particle mass size distribution

The overestimation of sea salt due to its emission scheme could promote the formation of sodium nitrate in coarse mode, by consuming nitric acid. This was discussed in recent modelling studies (Neumann et al., 2016a; Liu et al., 2015; Im, 2013; Athanasopoulou et al., 2008). However, these previous studies mainly focused on the influence of sea salt on bulk nitrate mass concentration, but not enough on nitrate particle mass size distribution.

Sodium nitrate, which is thermodynamically stable, will not transfer to the gas-phase nitric acid (Schaap et al., 2011). However, a gas-particle equilibrium exists between ammonium nitrate and its gas-phase precursors (ammonia and nitric acid). This equilibrium is built up with dependence on ambient conditions and precursor concentrations (Schaap et al., 2011), therefore, would be altered through the consumption of nitric acid in the formation of sodium nitrate on the surface

of coarse mode sea salt. As illustrated in Fig. 3, the equilibrium will be pushed towards gas-phase precursors, and then nitric acid will be further consumed by the overestimated sea salt. Eventually, the simulated nitrate particle mass size distribution is expected to shift towards larger sizes due to the overestimation of sea salt.

The mechanism of modifying nitrate particle mass size distribution due to sea salt is important, because the lifetime and optical properties of particulate nitrate, and nitrogen cycle will be changed accordingly. In the present thesis, the influence of sea salt on nitrate particle mass size distribution will be quantitatively analyzed. Though the effect of this mechanism may be thought only to be significant in the coast areas where sea salt is abundant, it is of interest to investigate the effect of this mechanism in the central Europe, where a considerable amount of NO<sub>x</sub> and ammonium nitrate is present.

### 1.5 Objectives

The overall objective of the present dissertation is to determine the gaps between the simulated and measured PSD, for the purpose of reducing those gaps. Summarizing the above mentioned topics, this thesis can be divided into three main scientific questions (Fig. 3):

- Q1: Is the size distribution/segregation of EC (absorbing aerosol) well represented by the WRF-Chem model over Europe? What are the reasons for the uncertainties? (First publication)
- Q2: Is the chemical pathway of nitrate (scattering aerosol) well represented by the WRF-Chem model over Europe? What are the main reasons for the uncertainties? (Second publication)
- Q3: How can natural source particles (sea salt) influence the simulated anthropogenic nitrate particle mass size distribution? How wide can the influence of sea salt on nitrate particle mass size distribution be spread over Europe? (Second publication)

In general, these investigations will help to deepen the understanding on the importance of particle number/mass size distribution. EC and nitrate are the most important absorbing and scattering aerosols over Europe, respectively. The uncertainties of the modelled PSD of EC and its influence on EC transport simulation will be discussed. The influence of sea salt on nitrate particle mass size distribution will also be investigated. This work will be helpful to refine assessments of regional climate change over Europe in future modelling studies.

## Introduction

The present thesis is structured as following. The models and observational datasets are described in Chapter-2. The results are presented in Chapter-3, which is the cumulative part of my thesis including Chen et al. (2016a and 2016b). The summary and conclusion comprising the answers of the above formulated scientific questions are given in Chapter-4. The outlook will discuss the implications of this work for future measurement and modelling studies.

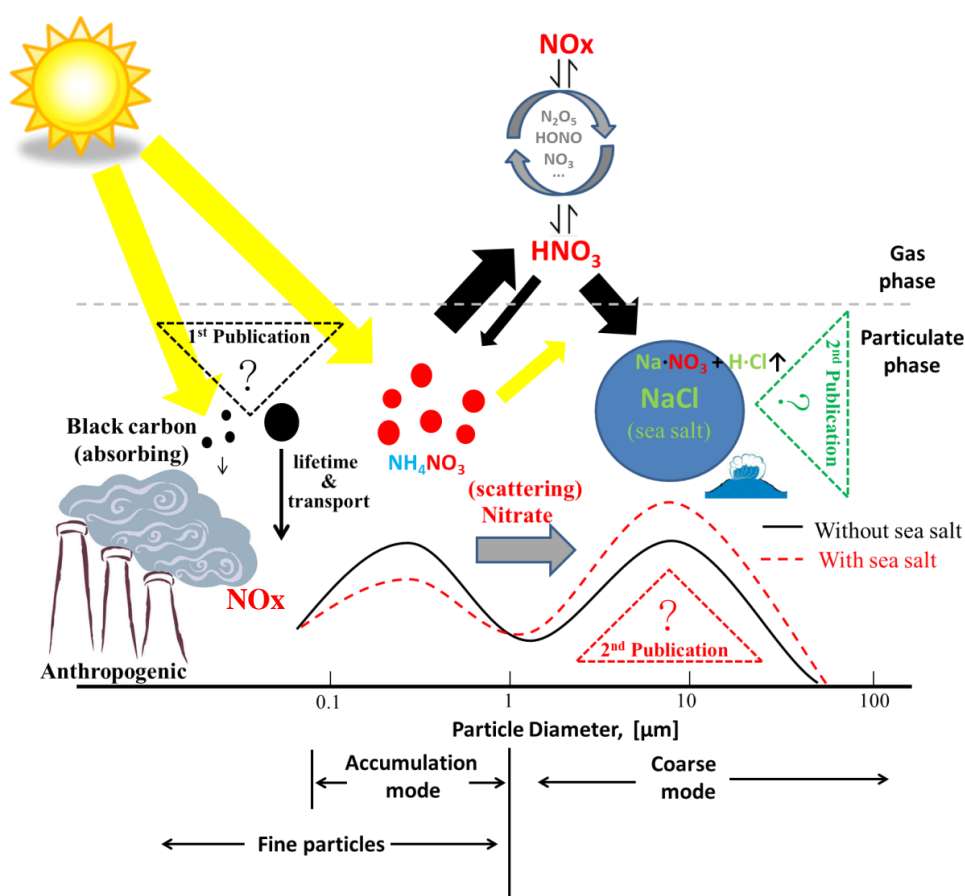


**Figure 3.** Schematic diagram of the scientific questions.



## **2. Methodology**

In this study, 3-D simulations with a widely used fully online-coupled mesoscale model WRF-Chem (V3.5.1) were performed for Europe by using a high resolution ( $7 \times 7$  km) anthropogenic emission inventory during the HOPE-Melpitz campaign (September 10-20<sup>th</sup>, 2013). The HOPE-Melpitz campaign, the GUAN network over Germany, and the other open accessed datasets were adopted to validate the simulations, including meteorological conditions, microphysical and chemical properties of size-resolved particles. In this section, the WRF-Chem model and the used measurements for validation will be described.

### **2.1. WRF-Chem model**

#### **2.1.1. General description**

An adequate modelling of dynamics requires a fully online-coupling between the chemical transport model (Chem) and the meteorological model (WRF). Online-coupling means that meteorological field and chemical compositions and reactions can influence each other. For example, aerosol particles can directly and indirectly influence the radiative transfer and cloud formation in the atmosphere. Clouds, in turn, may reduce aerosol concentrations by e.g. wet scavenging processes (Chapman et al., 2009).

The Weather Research and Forecast model (WRF), is a massive parallelized state-of-the-art numerical model designed for meteorological research. It is suitable for a broad spectrum of applications in simulating atmospheric phenomena of horizontal extents ranging from hundreds of meters to thousands of kilometers (Grell et al., 2005). In WRF, the compressible and non-hydrostatic Euler equations can be integrated with 2 dynamical solvers: (1) ARW (Advanced Research WRF, used in the present thesis), which was developed at NCAR (National Center of Atmospheric Research, Boulder, Colorado, USA); and (2) NMM (Non-hydrostatic Mesoscale Model) which was developed at NCEP (National Center for Environmental Prediction, Camp Springs, Maryland, USA). All equations are transformed to the terrain following hydrostatic pressure as the vertical coordinate and are horizontally discretized on an arakawa c-grid, which means that velocities are staggered about a half grid length to thermodynamic variables. WRF offers the opportunity to nest higher resolution domains into a coarser grid. The boundary conditions of the inner grid are taken from the coarse grid. There are two possibilities for nesting: (1) one-way nesting, which means no feedback of the inner grid to the coarse grid; (2) two-way

## Methodology

---

nesting with the feedback, which was applied in this study. WRF can account for a variety of microphysical settings, ranging from simple bulk schemes to more sophisticated schemes allowing for mixed phase cloud resolving simulations. Planetary boundary layer physics are suitable for turbulent kinetic energy prediction. The surface may consist of several layers allowing for a vegetation and soil moisture representation. Also snow cover and sea ice is included. The shortwave and longwave radiation field can be calculated for a broad spectral region, with respect to clouds, gases and aerosol (Skamarok et al., 2008). More details about WRF is given in <http://www.wrf-model.org/>.

The chemical transport model (Chem) is modular in design and provided with a rapidly expanding choice of gas-phase and aerosol chemical schemes for WRF-Chem. Aerosol modules include the GOCART (bulk mass approach, Chin et al., 2000), MADE-SORGAM (modal approach, Ackermann et al., 1998; Schell et al., 2001), MAM (modal approach, Liu et al., 2012), and MOSAIC (sectional approach, Zaveri et al., 2008) schemes. The gas-phase schemes include RADM2 (Stockwell et al., 1990, 59 species, 157 reactions), RACM (Stockwell et al., 1997, 73 species, 237 reactions), MOZART (Emmons et al., 2010, 85 species and 196 reactions), SAPRC99 (Carter, 2000, 79 species, 235 reactions) and CBMZ (Zaveri and Peters, 1999, 67 species, 164 reactions).

As described in the introduction, WRF-Chem has most widely been used for simulation of the Continental US and Asia. It is also steadily becoming more widely used in Europe (Archer-Nicholls et al., 2014): from regional air quality studies (Solazzo et al., 2012a and 2012b; Tuccella et al., 2012), to the impact of emissions from mega-cities (Hodnebrog et al., 2011), the impact of biomass burning and biogenic emissions on ozone levels (Hodnebrog et al., 2012), the impact of the aerosol direct effect on air quality (Forkel et al., 2012), and the evaluation of emission inventories (Nordmann et al., 2014). More details and related studies of WRF-Chem can be found in <https://ruc.noaa.gov/wrf/wrf-chem/> and <https://www.acom.ucar.edu/wrf-chem>.

### 2.1.2. Model configuration

The simulations were performed for the HOPE (HD(CP)<sup>2</sup> Observational Prototype Experiment, <https://icdc.zmaw.de/hopm.html>, Macke et al., 2016) campaign at Melpitz (12.93° E, 51.53° N; 86 m a.s.l.) during September 10-20<sup>th</sup>, 2013. In my second publication, three nested domains with 39 vertical layers were set up for the simulated case. The outer domain (D01) covers the entirety of Europe, a part of the North Sea and North Africa with a spatial resolution of 54 km,

## Methodology

providing the boundary conditions for the inner domains (Fig. 4). The second domain (D02) was centered at Melpitz and covers part of the North Sea, most part of Europe with a spatial resolution of 18 km. The innermost domain (D03) was also centered at Melpitz and had a spatial resolution of 6 km. And an extra high resolution domain (D04) was centered at Melpitz with a spatial resolution of 2 km, in order to evaluate the EC point sources in my first publication. Final (FNL) Operational Global Analysis (<http://rda.ucar.edu/datasets/ds083.2/>) and NCEP sea surface temperature (SST) datasets (<http://polar.ncep.noaa.gov/sst>), with a spatial resolution of 1 degree and a temporal resolution of 6 h, were utilized to drive and force the model meteorological field. The spin-up time of the simulations was 2 days. The chemical initial and boundary conditions were provided by the MOZART-4 global model with a spatial resolution of  $1.9^{\circ} \times 2.5^{\circ}$  and a temporal resolution of 6 h (<http://www.acom.ucar.edu/wrf-chem/mozart.shtml>). More details about the setups and the parameterizations are given in Table 1.

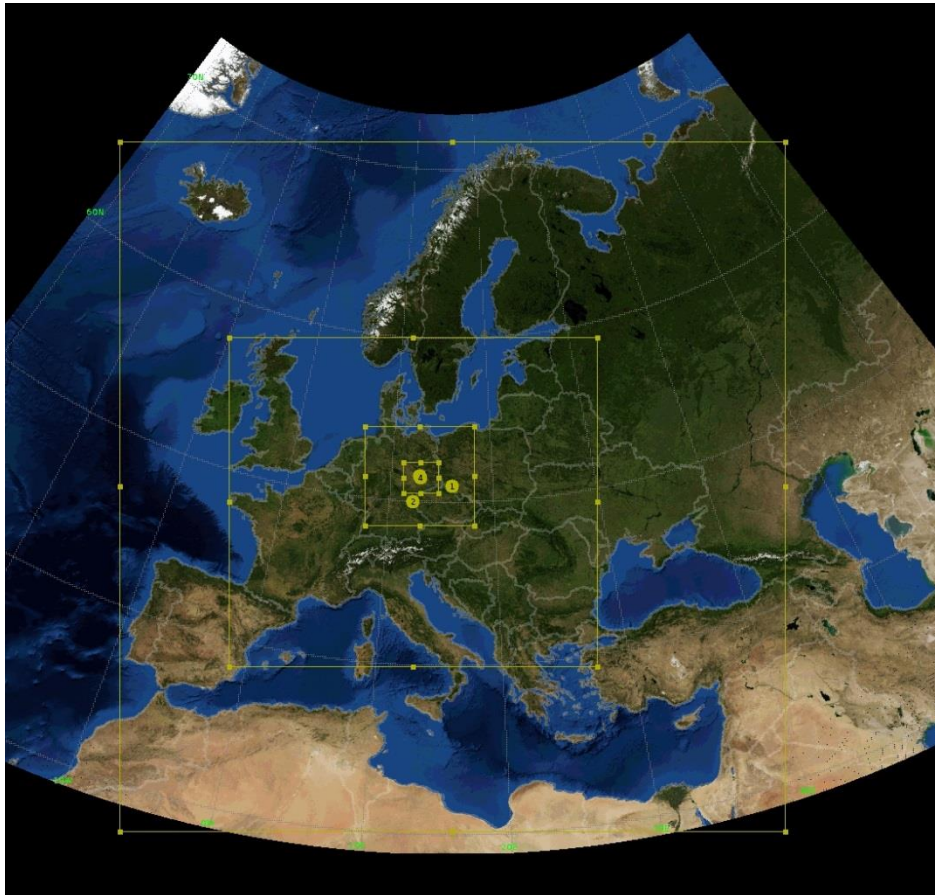


**Figure 4.** Setup of domains in WRF-Chem.

## Methodology

**Table 1.** Configurations of WRF-Chem.

Physics	WRF options
Micro physics	(Lin, 1983) scheme
Boundary layer	YSU (Hong, 2006)
Surface	Rapid Update Cycle (RUC) land surface model
Shortwave radiation	Goddard shortwave (Chou, 1998)
Longwave radiation	New Goddard scheme
Cumulus	Grell 3D
Urban	3-category UCM
Chemistry and Aerosol	Chem options
Aerosol module	MOSAIC with 8 bins
Gas-phase mechanism	CBMZ
Photolytic rate	Fast-J photolysis scheme
Sea salt emission	Gong (2003) scheme

In order to represent the properties of size-resolved particles, the fully online-coupled sectional aerosol module MOSAIC was used in this study. In MOSAIC, there are eight isogradient (in logarithmic scale) discrete size bins (from about 39 nm to 10  $\mu\text{m}$ ) of dry particles. Particles are assumed to be internally mixed in each bin (Zaveri et al., 2008).

In MOSAIC, sulfate, methane sulfonate, nitrate, chloride, carbonate, ammonium, sodium, calcium, EC, OC and other inorganic material are all treated in each bin. Both particle mass concentrations and particle number concentrations are simulated. Since the segregation of particles in the size bins is based on the dry diameter, there will be no transfer of particles between the bins due to the uptake or loss of water (Zaveri et al., 2008). However, particle growth or shrink due to chemical processes (e.g., chemical reaction, uptake/release of trace gases) and physical processes (e.g., coagulation) will result in the transfer of particles between the bins (Chapman et al., 2009). The formation of secondary organic aerosols is not included in the chosen MOSAIC version, but the nucleation of sulfuric acid and water vapor is considered (Zaveri et al., 2008; Fast et al., 2006). The heterogeneous reaction of nitric acid on the surface of sea salt with the production of sodium nitrate is considered in MOSAIC. For the deliquescent aerosol particles at high RH, the ionization equilibrium and the Kelvin effect are also considered in MOSAIC. More detailed descriptions are given in Zaveri et al. (2008).

The Carbon-Bond Mechanism version Z (CBMZ, Zaveri and Peters, 1999; Fast et al., 2006) was coupled with MOSAIC and described gas-phase atmospheric chemistry in the present thesis. In CBMZ, organic compounds are categorized according to their internal bond types (Fast et al.,

## Methodology

---

2006; Zaveri and Peters, 1999). The rates for photolytic reactions are calculated with the Fast-J scheme (Barnard et al., 2004; Wild et al., 2000).

Dry and wet deposition of particles is treated in the WRF-Chem model (Binkowski and Shankar, 1995). The dry deposition of particles is calculated by a resistance approach, including sublayer resistance, aerodynamic resistance and surface resistance (Grell et al., 2005). The scavenging process of particles was calculated using look-up tables (Nordmann et al., 2014). It is worth mentioning that Saide et al. (2012) found that the WRF-Chem model might overestimate wet deposition of particles in the regions where drizzle re-evaporates and releases the particles back into the atmosphere. And the WRF-Chem model may tend to slightly overestimate the deposition of EC particles, due to the treatment of internally mixed (Nordmann et al., 2014).

The aerosol optical depth (AOD) is online calculated in WRF-Chem model by integrating extinction coefficients over all vertical layers, and details are given in Barnard et al. (2010). In general, an internal mixture of all chemical constituents is assumed. The bulk refractive indices for each particle size bin are obtained by a mixing rule based on volume weighted averaging. The aerosol particle optical properties, such as particle extinction and scattering cross sections and asymmetry factor, are calculated online by a Mie code according to Ghan et al. (2001). The aerosol optical properties are calculated at 4 wavelengths (0.3, 0.4, 0.6 and 1  $\mu\text{m}$ ) and are then passed to the radiative transfer model, which is called the Goddard short-wave scheme (Chou et al., 1998). In this model, aerosol optical properties are accounted for in 11 spectral bands between 0.18 and 10  $\mu\text{m}$  in the ultraviolet, visible and near infrared wavelength region. Since the optical properties are only calculated at 4 wavelengths, interpolation and extrapolation is used to calculate the optical properties at the aerosol influenced spectral bands. The Goddard short-wave scheme also accounts for ultraviolet absorption by ozone and scattering of visible light by gases and clouds. In the infrared spectral region, contributions to absorption come from water vapor, O<sub>2</sub>, CO<sub>2</sub> and clouds. The transmission and reflection functions for each atmospheric layer are then calculated and a 2 stream adding method is applied to derive the fluxes in the atmosphere and at the surface (Fast et al., 2006). The changes of radiation fluxes due to aerosol particles may have a feedback on the atmospheric physics and the dynamics module in the meteorology simulation (e.g., Zhang et al., 2010b).

### 2.1.3 Anthropogenic source emissions

The inventory of anthropogenic emissions (PM<sub>2.5</sub>, PM<sub>2.5-10</sub>, CO, NO<sub>x</sub>, SO<sub>2</sub>, NH<sub>3</sub> and non-methane volatile organic compounds - NMVOCs), as well as temporally resolved emission factors, was provided by TNO for the AQMEII project (Air Quality Model Evaluation International Initiative, Pouliot et al., 2012). The dataset consists of European anthropogenic emissions on  $1/8^\circ \times 1/16^\circ$  (lon-lat, about  $7 \times 7$  km) grid. The Selected Nomenclature of Air Pollution (SNAP) code was used to categorize different source types (e.g., energy transformation, industrial combustion, road transport, agriculture), with area and point emissions distinguished. This inventory provides similar total German emissions as European Monitoring and Evaluation Programme (EMEP) inventory (<http://www.ceip.at/>), as shown in Table 2. More details about the anthropogenic emission inventory are given in related literature (Pouliot et al., 2012; Wolke et al., 2012).

The anthropogenic emissions of EC and OC were taken from the Pan-European Carbonaceous aerosol inventory (Visschedijk and Denier van der Gon, 2008), which was developed in the framework of the European Integrated project on Aerosol, Cloud, Climate and Air Quality Interactions (EUCAARI; Kulmala et al., 2011). The EUCAARI inventory is also provided by TNO and has the same spatial resolution and SNAP code categorization as the AQMEII one. The comparison between EUCAARI and the Lamarque EC emission (Lamarque et al., 2010) was given in Nordmann et al. (2014), which shown that the EUCAARI emissions are around 30% higher in eastern European countries: Poland, Czech Republic and Belarus. In EUCAARI, the size-segregated EC emission rates in PM<sub>1</sub>, PM<sub>1-2.5</sub> and PM<sub>2.5-10</sub> are provided. Sources such as power plants are gridded as point sources, and emissions from e.g. traffic or population are gridded as line or area sources. However, the point sources of EC in Germany were excluded in the study of second publication, because my first publication reported the very high uncertainties in the EC point sources.

**Table 2.** Comparison between EMEP and TNO emission inventory of Germany.

[unit: Gg]	SO <sub>2</sub>	CO	NO <sub>x</sub>	NH <sub>3</sub>	PM <sub>10</sub>	NMVOCs
EMEP (Germany)	412.298	3082.25	1310.058	680.125	216.21	1130.452
TNO (Germany)	449.490	3099.76	1245.169	597.325	181.54	1029.718
(EMEP-TNO)/EMEP	-9%	-0.6%	5%	12.2%	16%	8.9%

### 2.1.4 Natural source emissions

The Fire INventory from NCAR (FINN; Wiedinmyer et al., 2011), with the spatial resolution of 1 km and the temporal resolution of 1 h, was also included. Biogenic emissions were presented by the Model of Emissions of Gases and Aerosols from Nature (MEGAN; Guenther et al., 2006). Dust emissions were not considered due to the large uncertainty of the dust emission scheme in WRF-Chem (Saide et al., 2012). Dust contributed less than 3% to the total particle mass concentration at Melpitz during the simulated period, according to filter-based measurements (quartz-filter type MK360, Munktell/Ahlstorn, Schweden) with high-volume sampler DIGITEL DHA-80 (Walter RiemerMesstechnik, Germany).

The parameterization scheme for SSA emission coupled in the WRF-Chem model according to the Gong (2003) scheme (GO03). GO03 was developed based on the semi-empirical formulation (Monahan et al., 1986) and field measurements (O'Dowd et al., 1997), including two drop types produced by bursting bubbles (jet drop and film drop). The SSA flux from the ocean to the atmosphere is described as a function of 10 m wind speed and particle radius. Because the Monahan et al. (1986) scheme strongly overestimated the measurements of O'Dowd et al. (1997), Gong (2003) introduced an adjustable parameter to improve the results. In order to quantify the influence of SSA on the nitrate particles formation in this study (second publication), sensitivity studies were implemented with only 5% of SSA emission (R-CASE) and compared with the full (100 %) SSA emission case (F-CASE).

## 2.2 HOPE-Melpitz campaign

The HOPE campaign was designed to provide a critical evaluation of model simulations and further to provide information about land-surface-atmospheric boundary layer exchange, microphysical properties, cloud and precipitation processes (Macke et al. 2016). The HOPE campaign was executed as a major 2-month field experiment in Jülich, Germany, performed in April and May 2013, followed by a smaller campaign in Melpitz (HOPE-Melpitz campaign), Germany in September 2013. The Melpitz site is the TROPOS (Leibniz Institute for Tropospheric Research) research station for the continuous physical and chemical in-situ aerosol particle characterization of the regional background of central Europe (Spindler et al., 2010, 2012; Poulain et al., 2011; Brüggemann and Spindler, 1999; Birmili et al., 2001). The topography around Melpitz is rather flat over an area of several hundred square kilometers,

## Methodology

---

ranging 100-250 m a.s.l. Melpitz is part of the EMEP and provides a comprehensive set of in-situ observed chemical, microphysical and optical aerosol properties. In the present thesis, the measurements of particle number size distribution (PNSD), particle compositions and meteorological conditions from the HOPE-Melpitz campaign were used.

The instruments that measure aerosol particle microphysical properties were operated under dry condition, as recommended by WMO-GAW (World Meteorological Organization – Global Atmospheric Watch) and ACTRIS (Aerosols, Clouds, and Trace gases Research InfraStructure Network; Wiedensohler et al., 2012). A Dual Mobility Particle Size Spectrometer (TROPOS-type dual-SMPS, Birmili et al., 1999) combined with an Aerodynamic Particle Size Spectrometer (TSI APS Model 3321) were employed to measure the PNSD ranging from 5 nm to 10  $\mu\text{m}$  in diameter. Detailed information is given by Heintzenberg et al. (1998). A Multi-angle Absorption Photometers (MAAP Model 5012, Thermo, Inc., Waltham, MA USA) were employed to determine the particle light absorption coefficient for dry particles (Birmili et al., 2016). The MAAP were measured with a 10  $\mu\text{m}$  cut-off inlet, and the corrected mass absorption cross-section ( $\text{MAC} = 5 \text{ m}^2/\text{g}$ ) was used to derive the BC mass concentration at Melpitz (Genberg et al., 2013). The PNSD and BC mass concentration are made publicly available within the framework of the German Ultrafine Aerosol Network (GUAN; Birmili et al., 2016), which will be detailed described in the following section.

For chemical properties of particles, a Monitor for AeRosols and Gases in ambient Air (MARGA) system (Schaap et al., 2011; Thomas et al., 2009; ten Brink et al., 2007) continuously monitoring particle and gases in ambient air (Metrohm Applikon, Schiedam, The Netherlands), was operated downstream of a  $\text{PM}_{10}$  inlet. This instrument provided 1-hour data of secondary inorganic aerosols ( $\text{NH}_4^+$ ,  $\text{NO}_3^-$ ,  $\text{SO}_4^{2-}$ ,  $\text{Cl}^-$ ,  $\text{Ca}^{2+}$ ,  $\text{Mg}^{2+}$  and  $\text{K}^+$ ) and gaseous counterparts ( $\text{NH}_3$ ,  $\text{HNO}_3$ ,  $\text{HNO}_2$ ,  $\text{SO}_2$ ,  $\text{HCl}$ ). A high volume samplers DIGITEL DHA-80 (Walter RiemerMesstechnik, Germany), with sampling flow of about  $30 \text{ m}^3\text{h}^{-1}$ , were used to collect 24-hour  $\text{PM}_{10}$  and  $\text{PM}_1$  filter samples simultaneously (Spindler et al., 2013).

The near-ground meteorological variables (temperature, relative humidity, wind speed and direction) were simultaneously measured. Additional radiosounding measurements were performed at Melpitz on the days September 11–14<sup>th</sup>, 17<sup>th</sup> and 19<sup>th</sup>, 2013.



## 2.3 GUAN network over Germany

GUAN is a cooperative observation network over Germany, aiming to improve the scientific understanding of aerosol related effects in the troposphere (Birmili et al., 2016). The core activity of GUAN is to continuously collect the tropospheric BC mass concentrations and PNSD at 17 observation sites in Germany (Fig. 5). These sites cover various environmental settings including rural background, urban background, urban traffic and Alpine mountains. The measurements at Melpitz, Leipzig-TROPOS, Bösel, Hohenpeißenberg and Zugspitze were adopted to validate the model results in the present thesis, more details given in my first and second publications. The quality of the measurement data is assured by laboratory inter-comparisons as well as on-site comparisons with reference instruments. All data can be obtained online through the GUAN database (<https://doi.org/10.5072/guan>). More information about GUAN is given in Birmili et al. (2016).

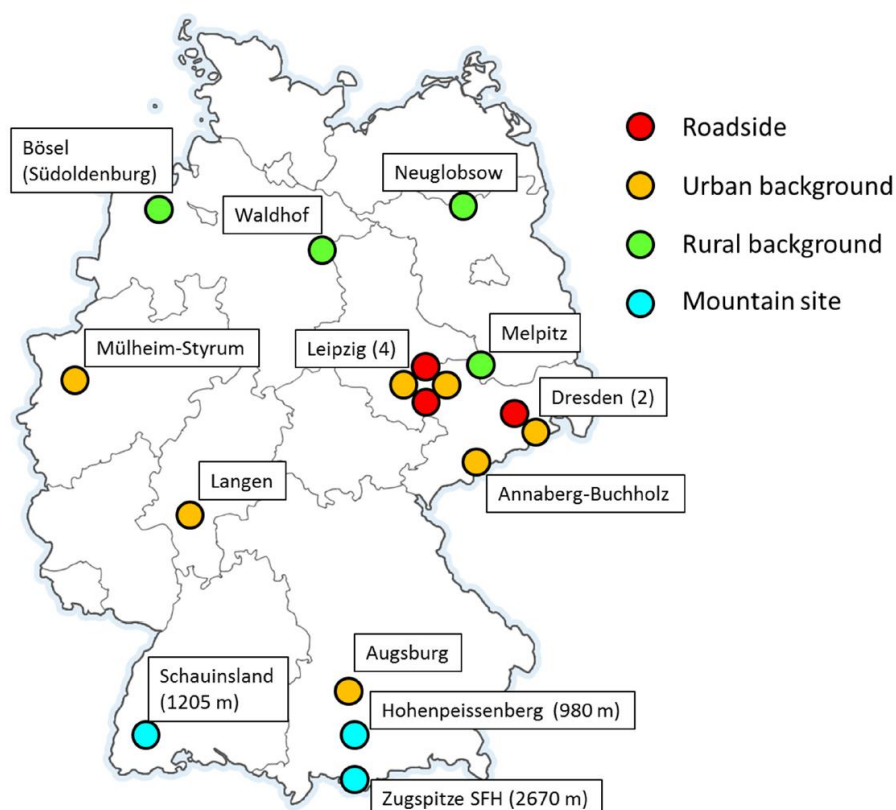


**Figure 5.** Observation sites of the GUAN network. Source: Birmili et al. (2016)

### 2.4 Other datasets

In addition to the measurements of the HOPE-Melpitz campaign and the GUAN network, other open accessed datasets over Europe were also used in the present thesis. The radiosounding for the stations all-over Europe (<http://www.weather.uwyo.edu/upperair/sounding.html>) were used for evaluating the modelled vertical structure of the atmosphere. The 24-hour filter-based measurements with PM<sub>10</sub> inlets (EMEP, 2014) at 3 coastal EMEP station (Bilthoven, Vredepeel, and Kollumerwaard, <http://ebas.nilu.no/>) were used to validate the modelled sea salt mass concentration. The AErosol RObotic NETwork (AERONET) dataset over Europe was utilized to validate the modelled AOD. The AERONET AOD was derived from sun photometer measurements of the direct (collimated) solar radiation. The level 2.0 AOD data, with pre and post field calibrated, automatically cloud cleared and manually inspected, were used in this study. The AOD at 500 nm wavelength and the Angstrom index are directly available in AERONET dataset, and AOD at 550 nm wavelength was derived. More detailed information is given in <http://aeronet.gsfc.nasa.gov/>.

## 3. Results and Discussion

### 3.1 First publication

#### 3.1.1 Evaluation of the size segregation of elemental carbon (EC) emission in Europe: influence on the simulation of EC long-range transportation

The content of this chapter has already been published in the manuscript “Evaluation of the size segregation of elemental carbon (EC) emission in Europe: influence on the simulation of EC long-range transportation” by Ying Chen, Yafang Cheng, Stephan Nordmann, Wolfram Birmili, Hugo A. C. Denier van der Gon, Nan Ma, Ralf Wolke, Birgit Wehner, Jia Sun, Gerald Spindler, Qing Mu, Ulrich Pöschl, Hang Su, and Alfred Wiedensohler in the journal “Atmospheric Chemistry and Physics” in 2016, in Volume 16, pages 1823–1835, doi: 10.5194/acp-16-1823-2016.

Reprinted with permission by the authors from Atmospheric Chemistry and Physics, 2016, 16, 1823–1835, doi: 10.5194/acp-16-1823-2016.



## Evaluation of the size segregation of elemental carbon (EC) emission in Europe: influence on the simulation of EC long-range transportation

Ying Chen<sup>1,2</sup>, Ya-Fang Cheng<sup>2</sup>, Stephan Nordmann<sup>2,3</sup>, Wolfram Birmili<sup>1,3</sup>, Hugo A. C. Denier van der Gon<sup>4</sup>, Nan Ma<sup>1,2</sup>, Ralf Wolke<sup>1</sup>, Birgit Wehner<sup>1</sup>, Jia Sun<sup>1</sup>, Gerald Spindler<sup>1</sup>, Qing Mu<sup>2</sup>, Ulrich Pöschl<sup>2</sup>, Hang Su<sup>2</sup>, and Alfred Wiedensohler<sup>1</sup>

<sup>1</sup>Leibniz-Institute for Tropospheric Research, Leipzig, Germany

<sup>2</sup>Multiphase Chemistry Department, Max Planck Institute for Chemistry, Mainz, Germany

<sup>3</sup>German Environment Agency, Dessau-Roßlau, Germany

<sup>4</sup>TNO, dept. Climate, Air, and sustainability, Utrecht, the Netherlands

Correspondence to: Ya-Fang Cheng (yafang.cheng@mpic.de) and Alfred Wiedensohler (ali@tropos.de)

Received: 25 September 2015 – Published in Atmos. Chem. Phys. Discuss.: 6 November 2015

Revised: 28 January 2016 – Accepted: 1 February 2016 – Published: 17 February 2016

**Abstract.** Elemental Carbon (EC) has a significant impact on human health and climate change. In order to evaluate the size segregation of EC emission in the EUCAARI inventory and investigate its influence on the simulation of EC long-range transportation in Europe, we used the fully coupled online Weather Research and Forecasting/Chemistry model (WRF-Chem) at a resolution of 2 km focusing on a region in Germany, in conjunction with a high-resolution EC emission inventory. The ground meteorology conditions, vertical structure and wind pattern were well reproduced by the model. The simulations of particle number and/or mass size distributions were evaluated with observations at the central European background site Melpitz. The fine mode particle concentration was reasonably well simulated, but the coarse mode was substantially overestimated by the model mainly due to the plume with high EC concentration in coarse mode emitted by a nearby point source. The comparisons between simulated EC and Multi-angle Absorption Photometers (MAAP) measurements at Melpitz, Leipzig-TROPOS and Bösel indicated that the coarse mode EC (EC<sub>c</sub>) emitted from the nearby point sources might be overestimated by a factor of 2–10. The fraction of EC<sub>c</sub> was overestimated in the emission inventory by about 10–30 % for Russia and 5–10 % for Eastern Europe (e.g., Poland and Belarus). This incorrect size-dependent EC emission results in a shorter atmospheric life time of EC particles and inhibits the long-range trans-

port of EC. A case study showed that this effect caused an underestimation of 20–40 % in the EC mass concentration in Germany under eastern wind pattern.

### 1 Introduction

Elemental carbon (EC) and black carbon (BC) are characterized by their strong radiation absorbing effect (Hansen et al., 2000; Jacobson et al., 2000; Cheng et al., 2008, 2009; Bond et al., 2013) and adverse health effects (Pope et al., 2009; Bond et al., 2013). For climate change, EC is the second strongest contributor to current global warming with a total radiative forcing of about  $+1.1 \text{ W m}^{-2}$ , just after the carbon dioxide (Bond et al., 2007; Ramanathan and Carmichael, 2008). Globally, biomass burning (40 %), fossil fuel combustion (40 %) and biofuels combustion (20 %) are the major source of EC emission (Ramanathan and Carmichael, 2008). The EC particles freshly emitted from incomplete combustion have sizes around 100 nm (Rose et al., 2006). The EC particles size segregation information is also very significant for climate, long-range transport and health effect. These fine mode (sub-micron) EC particles are much more important than the coarse mode, since fine particles have longer lifetime than coarse particles (Petzold and Kärcher, 2012; Croft et al., 2014). They have higher chances of accumulating in

the atmosphere and participate in long-range transportation (e.g. Himalayan and arctic region), and furthermore contributing to the global-scale climate forcing. Previous studies showed that EC long-range transport and deposition on ice could contribute to the glacier melting in Himalayan (Ming et al., 2008) and arctic regions (McConnell et al., 2007; Ramanathan and Carmichael, 2008). The EC deposition on snow and ice could change the surface albedo, absorbs solar radiation and causes positive climate forcing. Furthermore, regarding the effect on health, fine EC particles could translocate from lung to blood with the adsorbed toxic matters (e.g.: heavy metal) inducing many diseases (Pope et al., 2009; Meister et al., 2012). The definitions of EC and BC depend on how these species were measured. BC is used for an optical determination and EC for a thermographic measurement method (Nordmann et al., 2013; Vignati et al., 2010). However, the discrepancies between EC and BC are usually disregarded, and they are interchangeable in the modeling studies (Vignati et al., 2010). Nordmann et al. (2013) showed that the EC and BC were well correlated in the German Ultrafine Aerosol Network (GUAN) sites measurements. Nordmann et al. (2013) and Nordmann et al. (2014) indicated that EC in the model can be used as the best approximation of BC in modelling study.

The emission inventory is one of the key factors for the evaluation of the EC climate effect with model (Vignati et al., 2010). The IPCC (IPCC, 2013) reported BC radiative forcing of 0.4 (0.05–0.8), 0.2 and 0.04 (0.02–0.09)  $\text{W m}^{-2}$  from fossil fuel combustion, biomass burning and deposition on snow, respectively. The uncertainties in the evaluation of BC global and regional climate effect may be due to uncertainties in BC mass concentrations, which are derived from BC emission and removal processes (Koch et al., 2009). Emissions of carbonaceous aerosols are notoriously uncertain (Denier van der Gon et al., 2015). The European Environment Agency report (EEA, 2013) indicated that it was almost impossible to evaluate overall uncertainty at EU level. The uncertainty for EC emissions is at least 50% on global scales, and a factor of 2 to 5 on regional scale (Ramanathan and Carmichael, 2008). The uncertainty is originated not only from an instrument measurement uncertainty but also the conditions under which the emission factor measurements take place (Denier van der Gon et al., 2015). Global emission inventories of EC have been published (e.g.: Bond et al., 2004; Lamarque et al., 2010) without size segregation information. An emission inventory for UNECE-Europe of EC (EUCAARI 42-Pan-European Carbonaceous aerosol inventory) has been published with a  $1/8^\circ \times 1/16^\circ$  high resolution and separated size mode ( $\text{PM}_{10}$ ,  $\text{PM}_{1-2.5}$  and  $\text{PM}_{2.5-10}$ ) (Visschedijk and Denier van der Gon, 2008). UNECE-Europe includes the EU28 countries and Albania, Armenia, Azerbaijan, Belarus, Bosnia Herzegovina, Georgia, Moldova, Macedonia, Norway, Russia Federation, Serbia and Montenegro, Switzerland, Turkey and Ukraine (Denier van der Gon et al., 2015). The EUCAARI inventory consists of anthropogenic

emissions by country for the 10 Source Nomenclature for Air Pollution (SNAP) sectors: energy transformation, small combustion sources, industrial combustion, industrial processes, extraction of fossil fuels, solvent and product use, road transport, non-road transport, waste handling, and agriculture (Visschedijk and Denier van der Gon, 2008).

Numerous works have evaluated the performance of EC emission and transport models for Europe. Koch et al. (2009) evaluated 17 global models and found out that 13 of 17 models over-estimate EC in Europe. Stern et al. (2008) compared five models result with northern Germany observations, and none of the models could reproduce the high EC concentration at the central Europe background station Melpitz. Genberg et al. (2013) pointed out that the EMEP MSC-W model underestimates the EC concentration at Melpitz may because the low model resolution can not represent local effects (like point source). Nordmann et al. (2014) pointed out that the EUCAARI inventory may underestimate the Eastern European EC emission by a factor of about 2, but not considering the size segregation uncertainty of EC emission and its influence on transportation.

In this work, a high-resolution WRF-Chem simulation was set up in conjunction with the EUCAARI EC inventory, focusing on the central Europe region. The modelling result was evaluated by the aerosol and EC/BC in situ measurements from GUAN and HOPE-Melpitz Campaign. The EC emission fraction for coarse ( $\text{PM}_{2.5-10}$ ) mode of the EUCAARI inventory was evaluated. A case study of the high polluted episode in April 2009 (Nordmann et al., 2014) was re-simulated for validating the influence of size segregation in EC transportation.

## 2 Data and method

The fully coupled “online” Weather Research and Forecasting/Chemistry model (WRF-Chem V3.5.1) is a state-of-the-art regional air quality model (Grell et al., 2005). It is suitable for a broad spectrum of atmospheric research with horizontal extents ranging from hundreds of meters to thousands of kilometers. Trace gases, aerosols, and interactive processes with meteorology are simulated with several treatments in the model (Grell et al., 2005). The following is a brief summary of the primary WRF-Chem modules relevant to the current study.

In this study, the Carbon-Bond Mechanism version Z (CBMZ, Zaveri and Peters, 1999; Fast et al., 2006) was used for gas-phase atmospheric chemistry. 67 prognostic species and 164 reactions are included in CBMZ mechanism with a lumped structure approach, which classifies organic compounds according to their internal bond types. Fast-J scheme (Wild et al., 2000; Barnard et al., 2004) was used for calculating the rates for photolytic reactions within CBMZ.

The sectional approach Model for Simulating Aerosol Interactions and Chemistry (MOSAIC; Zaveri et al., 2008) was



**Table 1.** Sectional approach for aerosols: particle dry-diameter ranges used in this study.

	Bin 01	Bin 02	Bin 03	Bin 04	Bin 05	Bin 06	Bin 07	Bin 08
Minimum diameter ( $\mu\text{m}$ )	0.0390625	0.078125	0.15625	0.3125	0.625	1.25	2.5	5.0
Maximum diameter ( $\mu\text{m}$ )	0.078125	0.15625	0.3125	0.625	1.25	2.5	5.0	10.0

applied to better represent the size segregated aerosol properties. In MOSAIC, dry aerosol particles with eight discrete size bins were selected with upper and lower bin diameters defined as shown in Table 1; and particles are assumed to be inter-mixed in each bin (Zaveri et al., 2008). MOSAIC treats the following chemical species: sulfate, methane sulfonate, nitrate, chloride, carbonate, ammonium, sodium, calcium, elemental carbon (EC), organic carbon (OC) and other inorganic mass. Both particle mass and particle number are simulated for each bin. Water uptake or loss will not transfer particles between bins, since bins are based on dry particle diameters (Zaveri et al., 2008). However, particle growth or reduction due to chemical processes (e.g., uptake or release of trace gases, etc.) and physical processes (e.g., coagulation, etc.) will transfer particles between bins (Chapman et al., 2009). In addition, particle coagulation and nucleation processes of sulfuric acid and water vapor are included (Fast et al., 2006; Zaveri et al., 2008). But the formation mechanism of Secondary Organic Aerosol (SOA) is not included in this version (Zaveri et al., 2008).

In WRF-Chem, dry (Binkowski and Shankar, 1995) and wet (Easter et al., 2004) deposition processes of aerosol particles are considered. The dry deposition of aerosol in the lowest model layer is derived from the deposition velocities, which is dependant on the sublayer resistance, aerodynamic resistance and surface resistance (Grell et al., 2005). The scavenging of cloud-phase and below-cloud aerosol by interception and impaction processes is calculated by look-up tables. It is worth mentioning that the particles are treated internally mixed in each bin; therefore the hygroscopicity of EC contained particles tends to be slightly overestimated in the model. Furthermore, the model tends to overestimate the removal rate of EC, especially for the wet deposition processes (Nordmann et al., 2014). In addition, Saide et al. (2012) pointed out that the irreversible removal of aerosol by rain in WRF-Chem might overestimate the wet deposition. However, it was mostly dominated by dry conditions before 16 September 2013 in this simulation.

As shown in Fig. 1, the simulation consists of four nested domains with 39 vertical layers. The spatial resolutions of domains (D01–D04) are 54, 18, 6, and 2 km respectively. The outer domain (D01) covers Europe and the inner domain (D04) focuses on Saxony in Germany, centered at Melpitz (12.93° E, 51.53° N). The time period from 10 to 20 September 2013 was simulated, with 2 days spin-up. The model meteorology fields were driven and forced by Final Analysis (FNL) Operational Global Analysis data (

**Figure 1.** EUCARRI (resolution 7 km) EC emission ( $\text{kg m}^{-2} \text{ year}^{-1}$ ). The 4 nested model domains (D01–D04) are indicated in the picture. Melpitz and Bösel (Boesel) are marked by black stars.

<http://rda.ucar.edu/datasets/ds083.2/>) and sea surface temperature (SST) data set (<http://polar.ncep.noaa.gov/sst/oper/Welcome.html>) from NCEP (National Center for Environmental Prediction), with 1° spatial and 6 h temporal resolution. The chemical initial and boundary conditions were driven and forced by MOZART-4 global model results (<http://www.acd.ucar.edu/wrf-chem/mozart.shtml>) with 1.9° × 2.5° spatial and 6 h temporal resolution. The physical and chemical schemes used for the simulation are summarized in Table 2. The aerosol-cloud-radiation interaction is turned on.

## 2.1 Emissions

The anthropogenic emissions were taken from the Pan-European Carbonaceous aerosol inventory (Visschedijk and Denier van der Gon, 2008) for EC and OC, which was developed in the framework of the European Integrated project on Aerosol Cloud Climate and Air Quality interactions (EUCAARI, Kulmala et al., 2011) for the year 2005. It is available on a spatial resolution of  $1/8^\circ \times 1/16^\circ$  longitude–latitude grid, corresponding to around 7 km (Fig. 1). The EC emissions in different size modes ( $\text{PM}_{10}$ ,  $\text{PM}_{1-2.5}$  and  $\text{PM}_{2.5-10}$ ) are provided; more details about the emissions in each mode and the gridding method were given in Denier van der Gon et al. (2010). The emissions are assumed to be equally distributed over the whole year in this study. A diurnal cycle of the emissions was applied with two maxima, around 07:00 and 18:00 local time. The emissions were al-

located in the first six layers (from surface to about 550 meters) of the model depending on the emission types, such as area emission, small and large point sources. Nordmann et al. (2014) reported that the EC emissions of EUCAARI inventory are around 30 % higher than the Lamarque inventory (Bond et al., 2007; Junker and Liousse, 2008; Lamarque et al., 2010) in Eastern European countries (Poland, Czech Republic and Belarus).

The EMEP inventory for 2013 (<http://www.ceip.at>, Mareckova et al., 2013), with  $0.5^\circ \times 0.5^\circ$  spatial resolution, was applied in the model for the other anthropogenic emissions, such as PM, SO<sub>2</sub>, NO<sub>x</sub>, CO, NH<sub>3</sub>, NH<sub>4</sub> and volatile organic compounds (VOC). The emissions of VOCs from EMEP were allocated to compounds used in CBMZ chemical mechanism of WRF-Chem.

In this study, biogenic emissions are taken from the Model of Emissions of Gases and Aerosols from Nature (MEGAN, Guenther et al., 2006). The Fire INventory from NCAR (FINN, Wiedinmyer et al., 2011), with 1 km spatial and 1 hour temporal resolution, was used in this study. The previous studies reported that the dust emission scheme (Saide et al., 2012) and the sea-salt emission scheme (Saide et al., 2012; Zhang et al., 2013) in WRF-Chem have large uncertainties. However, based on the filter measurements with high volume sampler DIGITEL DHA-80 (Walter Riemer Messtechnik, Germany) at Melpitz, dust and sea-salt contributed less than 3 % of aerosol mass in the simulation period. Therefore, the online sea-salt and dust emissions were switched off.

## 2.2 Observations

The experimental data used in this paper were drawn from two major sources: first, the HOPE-Melpitz Campaign of the HD(CP)<sup>2</sup> Observational Prototype Experiment (<http://hdcp2.zmaw.de>) and second, the German Ultrafine Aerosol Network (GUAN) (Birmili et al., 2009, 2015). The meteorological variables (e.g. temperature, relative humidity, wind speed, wind direction), gaseous pollutants (e.g. O<sub>3</sub>, NO<sub>x</sub>, SO<sub>2</sub>) were simultaneously measured. In addition, the radio-sounding data for the stations all-over Europe (<http://www.weather.uwyo.edu/upperair/sounding.html>) were used for evaluating the modeled atmosphere vertical structure.

The regional background site Melpitz (12.93° E, 51.53° N) is representative for a larger rural area in Saxony Germany, detailed description was given in (Brüggemann and Spindler, 1999; Spindler et al., 2010, 2012; Poulain et al., 2011). A Twin Differential Mobility Particle Sizer (TDMPS, TROPOS, Leipzig, Germany; Birmili et al., 1999) was used to measure the Particle Number Size Distribution (PNSD) with an electrical mobility diameter between 5 and 800 nm. An Aerodynamic Particle Sizer (APS Model 3320, TSI, Inc., Shoreview, MN USA) was employed to measure the PNSD with aerodynamic diameter from 0.5 to 10 µm. All of them were operated under dry conditions. All the particles were

**Table 2.** Configurations of WRF-Chem.

Physics	WRF option
Micro physics	Lin et al. (1983) scheme
Surface	Rapid Update Cycle (RUC) land surface model
Boundary layer	YSU (Hong et al., 2006)
Cumulus	Grell 3D
Urban	3-category UCM
Shortwave radiation	Goddard shortwave (Chou et al., 1998)
Longwave radiation	New Goddard scheme
Chemistry and Aerosol	Chem option
Gas-phase mechanism	CBMZ
Aerosol module	MOSAIC with 8 bins
Photolytic rate	Fast-J photolysis scheme

assumed as spherical (shape factor = 1), with a density of 1.8 g cm<sup>-3</sup> for the sub-micrometer particles and 1.5 g cm<sup>-3</sup> for the super-micrometer particles (Heintzenberg et al., 1998). The mobility diameter can be calculated from the aerodynamic diameter and Particle Mass Size Distribution (PMSD) can be calculated from PNSD, as in Heintzenberg et al. (1998). Then PNSD and PMSD in the diameter range of 5–10 000 nm can be derived from TDMPS (5–638 nm) and APS (638–10 000 nm) measurements. A high-volume sampler DIGITEL DHA-80 (Walter Riemer Messtechnik, Germany), with sampling flux of about 30 m<sup>3</sup> h<sup>-1</sup>, was used for parallel continuous daily samples of PM<sub>10</sub>, detailed information was given in Spindler et al. (2013). Additional radio-sounding measurements were performed in Melpitz on the days 11–14, 17 and 19 September 2013.

At Melpitz, Bösel (7.94° E, 53.0° N) and Leipzig-TROPOS (12.43° E 51.35° N), Multi-angle Absorption Photometers (MAAP Model 5012, Thermo, Inc., Waltham, MA USA) were employed to determine the particle light absorption coefficient for dry particles (Birmili et al., 2015). All these stations are defined as rural or urban background station. The MAAPs were measured with 10 µm cut-off inlet and the corrected mass absorption cross-section (MAC) of 5 m<sup>2</sup> g<sup>-1</sup> was used to derive the BC mass concentration for Melpitz (Genberg et al., 2013), and the manual suggested MAC of 6.6 m<sup>2</sup> g<sup>-1</sup> was used for Bösel and Leipzig-TROPOS. Since EC and absorption-related BC were highly correlated in GUAN observation sites (Nordmann et al., 2013), we used the MAAP measured BC as the best approximation of EC (Nordmann et al., 2014) in this study.

## 3 Result and discussion

### 3.1 Meteorology conditions

The WRF performance on simulating the meteorological fields was evaluated with the Melpitz ground measurements data and radio-sounding measurements over the whole of Europe. The wind pattern in the simulated time period was dominated by westerly winds in Melpitz (Fig. 2d). It was mostly



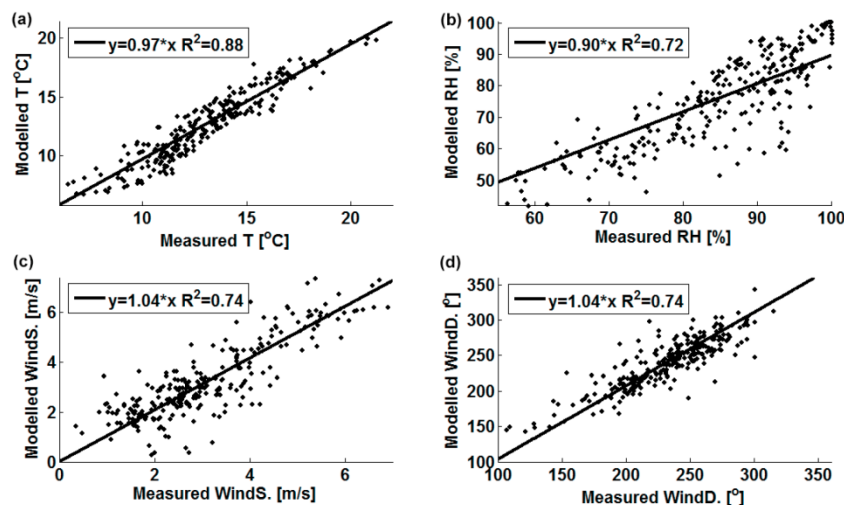


**Figure 2.** Comparison of meteorological variables between Melpitz ground-based measurements and WRF-Chem D04 result. (a) Temperature; (b) relative humidity; (c) wind speed; (d) wind direction.

dominated by dry conditions between 13 and 15 September in Melpitz. The air mass of northern Germany changed from continental to maritime after 15 September. The maritime air mass from the North Sea was relatively clean, with less anthropogenic pollutants. In 15–16 September, the concentration of primary gaseous pollutant NO was significantly lower at Melpitz than 13–14 September (Fig. S1 in the Supplement), and also the PM<sub>10</sub>, PM<sub>2.5</sub> and PM<sub>1</sub> mass concentrations were reduced by more than 50 %.

As shown in Fig. 2, the variances of temperature, relative humidity, wind speed and wind direction were validated with the ground measurements, with a correlation coefficient ( $R^2$ ) of 0.88, 0.72, 0.74, and 0.74 respectively. The peaks in NO concentration can be reproduced by the model, although overestimated in the peaks (Fig. S1). The transport process and emission location were also supposed to be well described in the model, because NO has a very short lifetime and therefore a good indicator of nearby sources. These results show that the WRF model can well reproduce the near surface meteorological condition and transport processes at Melpitz.

The vertical gradient of the potential temperature is an important indicator for the stability of atmosphere. Figure S2 shows a  $R^2$  map of comparison between radio-sounding observed and simulated vertical potential temperature in planetary boundary layer (PBL, under 3 km). The  $R^2$  values were higher than 0.8 for all the stations over Europe, especially for Melpitz region the  $R^2$  was higher than 0.9. The comparison at the Melpitz site is shown in Table 3, together with some profile examples in Fig. S3. The meteorological vertical structure was well captured by the model, with  $R^2$  value of 0.98, 0.84, 0.93 and 0.70 for the potential temperature, water vapor mixing ratio, wind speed and wind direction respectively. The results indicate that WRF well simulated the

**Table 3.** Comparison result for meteorological variables between Melpitz radio-sounding measurements and WRF-Chem model.

	Slope	$R^2$	Data point Number
Potential temperature	0.99	0.98	586
Water vapor mixing ratio	0.81	0.84	586
Wind speed	0.90	0.93	586
Wind direction	1.02	0.70	586

meteorological vertical structure and wind pattern, especially in central Europe (Melpitz region with 2 km resolution).

### 3.2 Particle size distribution

The modeled particle number size distribution (PNSD) and particle mass size distribution (PMSD) for Melpitz were compared with the measurements, shown in Fig. 3. For the fine mode (PM<sub>1</sub>, or sub-micron particles) aerosol the agreement is acceptable, but the model significantly overestimated the coarse mode (PM<sub>2.5–10</sub>) mass/number. The meteorology condition was well reproduced by the model. The transportation process was also supposed to be well simulated. It indicates that there may be some unrealistic sources of particles larger than 2.5  $\mu\text{m}$  included in the model, which leads to the overestimation of coarse mode. The detailed discussion about the unrealistic sources will be given in Sect. 3.3.

We found out that EC had a very high contribution of modeled coarse mode aerosol mass when the EC plumes hit Melpitz (Figs. 4a and 5a). In order to investigate the reasons of the EC plumes and its influence on coarse mode overestimation, a more detailed case study for the plume episode in the morning of 13 September will be given in Sect. 3.3.



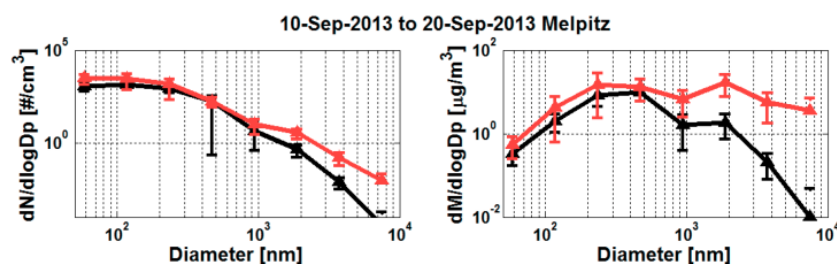


**Figure 3.** Comparison of Particle Number Size Distribution (PNSD, left) and Particle Mass Size Distribution (PMSD, right) between WRF-Chem model and Melpitz measurements. Model results indicated by the red lines and measurements by the black lines. The size distributions are averaged in the period 10–20 September 2013, the error bar indicates the upper and lower limits.

### 3.3 Elemental carbon point source size segregation and evaluation

In order to evaluate the EC emission in central Europe and investigate local effect of point source, MAAP measurements of three background sites (Melpitz, Leipzig-TROPOS and Bösel) were compared with modeled results (Fig. 4). In Leipzig-TROPOS, the relatively high EC concentration in the morning and night but low concentration at the noontime could have resulted from the development of planet boundary layer and traffic rush hours. According to modeled transportations, Melpitz and Bösel were influenced by the point source plume, but Leipzig-TROPOS was not (see Figs. 5b and S4). Here we use MAAP instead of DIGITEL measurement to compare with the model output, because only MAAP data are available for all those three sites and the higher temporal resolution of the MAAP is better for investigating the point source plume influence.

The model substantially overestimated the EC concentration in Melpitz especially for high episode peaks (Fig. 4a), during which the modeled EC concentration in  $PM_{10}$  can reach up to about 3–4 times higher than that in  $PM_{2.5}$ . While outside the peaks, EC concentration in  $PM_{10}$  and  $PM_{2.5}$  were very close to each other. Comparing with MAAP measurement, EC in  $PM_{10}$  was on average overestimated by a factor of 2.8 at Melpitz, and by a factor up to 6–10 for the peak periods. This overestimation of EC was due to the plume from a point source emission of type SNAP-5 (extraction and distribution fossil fuels, nomenclature described in Visschedijk and Denier van der Gon, 2008; Pouliot et al., 2012) located between Leipzig and Melpitz. Figure 5 is an example snapshot showing the EC plume passing through Melpitz at 05:00 a.m. on 13 September 2013. Plumes from the same sources also similarly influenced other peak periods to a different extent. When the plume hit Melpitz, the overestimation of EC concentration was substantial even when the uncertainties in the modeled transportation within  $12 \times 12 \text{ km}^2$  was accounted for (shaded area in Fig. 4a), and EC contributed 30–67% of coarse mode aerosol mass. At the same time, Leipzig was not influenced by point source plume, because of the pre-

vailing westerly wind in domain D04 (Fig. 5b). The comparison at the Leipzig-TROPOS site was thus much better (Fig. 4b). There, EC was only slightly overestimated by less than 40%, which may be due to the seasonal variability and/or decreasing emissions ( $\sim 25\%$  from 2010 to 2013, based on long-term MAAP measurements in Leipzig-TROPOS and DIGITEL measurements in Melpitz) in the context of “low emission zones” ([http://gis.uba.de/website/umweltzonen/umweltzonen\\_en.php](http://gis.uba.de/website/umweltzonen/umweltzonen_en.php)) implemented in several cities of the region (Leipzig and Halle/Saale) and the rest of Germany (Cyrys et al., 2014). The different behaviors of model at these two sites indicate that the coarse mode EC emission in the point sources near Melpitz can be significantly overestimated.

This EC plume effect was not only found in Melpitz. As shown in Fig. S4, Bösel was also influenced by a nearby EC point source in the morning of 13 and 14 September 2013 (also Fig. 4c). The EC concentration was overestimated and had a high coarse mode fraction, similar to Melpitz. However, the overestimation of EC was not as significant as for Melpitz, with  $\sim 87\%$  on average and about 200–400% during the peak periods. The fraction of EC in coarse mode was also not as high as in Melpitz. One reason could be the lower intensity of the point source nearby Bösel than the one near Melpitz (Fig. S4). Another reason may be the artificial dilution of local emissions by the coarser modelling resolution (Genberg et al., 2013), because we only have the highest resolution of 2 km covering the regions around Melpitz (D04), but 6 km resolution for Bösel (D03).

These results imply that the EC point sources in Germany can be overestimated by a factor of 2–10 in the EUCARI emission inventory, especially for the coarse mode EC emission in the large point sources. To further evaluate the coarse mode EC emission ( $EC_c$ , EC in  $PM_{2.5-10}$ ) over the whole of Europe, we first checked the emission fraction of  $EC_c$  to the total EC in EUCARI inventory. As shown in Fig. 6a, this fraction is generally lower than 10% over large regions in Western Europe. For almost all of the point sources, the  $EC_c$  emission fractions are higher than 30% (Fig. 6b), within which there are 3 and 10 point sources surrounding the Melpitz and Bösel regions, respectively, with  $EC_c$  emis-

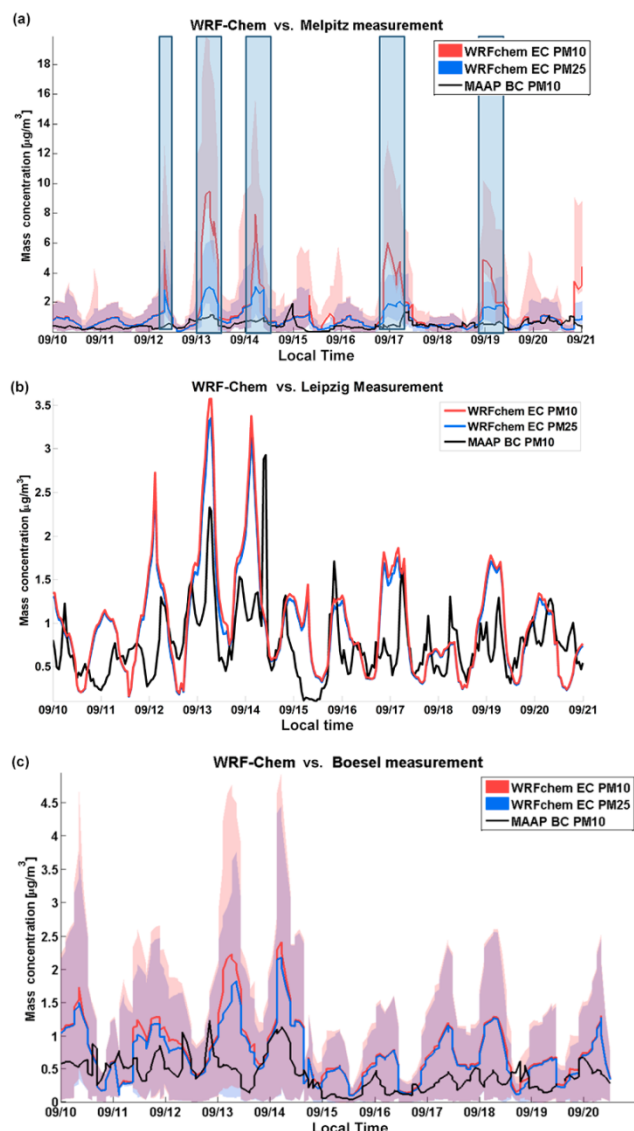


**Figure 4.** The comparison of EC/BC concentration between model and MAAP measurements. Red line: EC concentration in  $PM_{10}$  of model result; blue line: EC concentration in  $PM_{2.5}$  of model result; black line: BC concentration in  $PM_{10}$  of MAAP measurement, used as the best approximation of EC. The shaded areas indicate the model uncertainty defined by the maxima (upper limit of the shade) and minima (lower limit of the shade) values within 12 km distance from Melpitz/Bösel. The blue rectangles mark the EC plume episodes at Melpitz. (a) Melpitz: modelling result derived from D04 simulation with 2 km resolution; (b) Leipzig-TROPOS: modelling result derived from D04 simulation with 2 km resolution; (c) Bösel: modelling result derived from D03 simulation with 6 km resolution.

sion fractions even higher than 80 % (Table S1 and Fig. 6b). It is worth mentioning that these point sources with high ECc emission fractions also have a very high total EC emission rate. For example, the point source, influencing Melpitz in the morning of 13 September, is the largest point source for

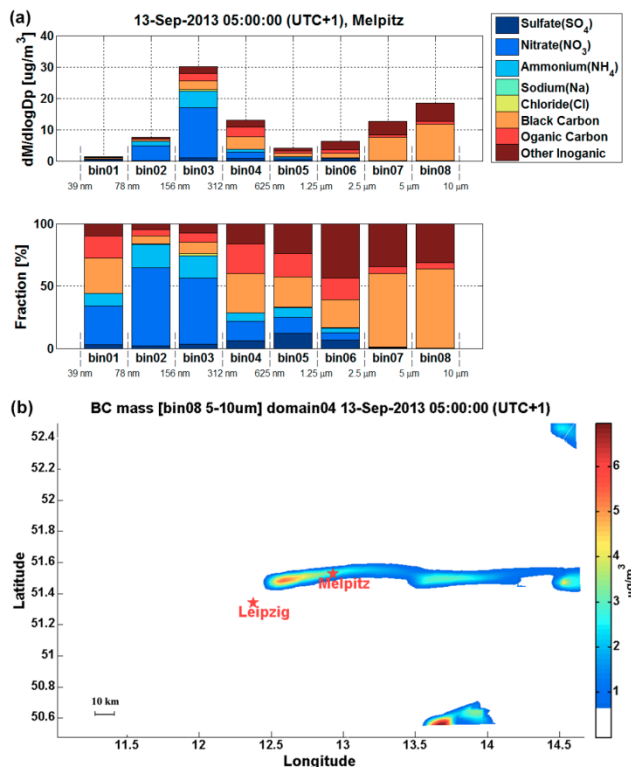


**Figure 5.** The model result: (a) aerosol chemistry compounds for each bins of Melpitz; (b) horizontal distribution of EC in bin08 [5–10  $\mu\text{m}$ ] at 05:00 (UTC + 1) of 13 September 2013.

SNAP-5 in Germany with a share of about 20 % in the total EC point emission. EC emissions from the SNAP-5 point sources originate from coal-mining, storage and handling (Visschedijk and Denier van der Gon, 2008; Pouliot et al., 2012; Denier van der Gon et al., 2015), for which a relatively high fraction in coarse mode emission is expected. Therefore, the emission fraction of ECc may be true. But, the total EC emission rate might be too high due to the overestimation of EC scaling factor out of all emitted compounds. But it is hard to quantify it due to the fact that few data are available for the storage and handling of coal, and about chemical composition and size distribution of the emission in SNAP-5 type of emissions.

Note that the dry and wet deposition processes also contribute to the uncertainty of the modeling results. The dominant removal process for EC is wet deposition (Genberg et al., 2013); Croft et al. (2005) estimated that about 75 % of the EC is removed by wet deposition and 25 % by dry deposition, based on global model runs. And the wet deposition of EC may be overestimated in the WRF-Chem model due to the irreversible removal process (Yang et al., 2011; Saide et al., 2012) and the internal mixture of EC (Nordmann et al., 2014). It indicates that the overestimation of EC should result from the emission source instead of the deposition process, although the uncertainty of deposition would influence the



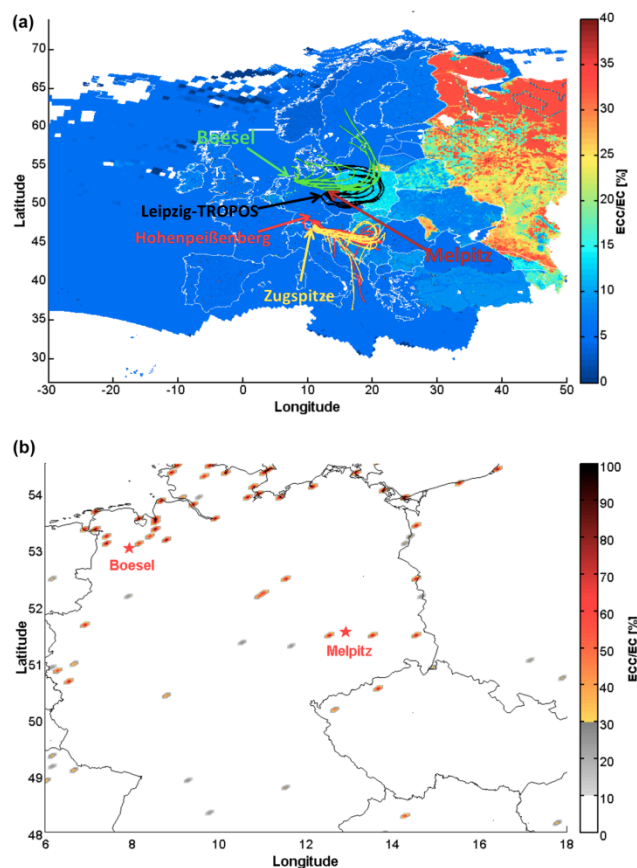


**Figure 6.** EUCAARI EC emission coarse mode fraction (ECc). (a) ECc result of total emission, including area and point sources. The location of Bösel, Leipzig-TROPOS, Melpitz, Hohenpeißenberg and Zugspitze are marked on the map. The colored lines indicated the 3-day back trajectories for each site (without Melpitz), in the period from 1 April 2009 to 4 April 2009 with 6 h interval. (b) ECc result of point source emissions.

emission evaluation results. More measurements and modeling studies are still needed for the quantified evaluation of the deposition processes uncertainty.

### 3.4 Influence on elemental carbon transportation

EC is in general mostly emitted in the fine mode, especially for the area emissions (Echalar et al., 1998; Hitzenberger and Tohno, 2001; Kuenen et al., 2014), although the SNAP-5 point sources may be an exception. The major SNAP-5 point sources giving coarse EC are coal mines and originate from storage and handling – dust being released due to loading and unloading, driving on the premises etc. Based on the EUCAARI inventory, the average ECc emission fraction for Western Europe is around 5 %, also about 5 % in Germany of year 2009 TNO-MACC\_II inventory (Kuenen et al., 2014). This is consistent with previous knowledge. But on the contrast to the generally low ECc emission fraction, this fraction is relatively high in Eastern Europe (e.g. Poland, Slovakia

and Belarus), about 15–20 %, and about 35 % in Poland of TNO-MACC\_II inventory (Kuenen et al., 2014). For Russia (including Kaliningrad in the north of Poland) and Moldova the fraction can reach up to 20–40 %, and about 17 % in Russia of TNO-MACC\_II inventory (Kuenen et al., 2014). As shown in the long-term (2003–2011) filter measurement study at Melpitz (Spindler et al., 2013), in the eastern wind dominated period when the air mass came from Eastern Europe and Russia, the EC coarse mode mass fraction was only in the range of 4–15 % ( $\sim 10$  % in average). Assuming that EC particles would not change the size during transportation, EUCAARI inventory may overestimate the fraction of ECc by about 5–10 % for Eastern Europe and 10–30 % for Russia.

The life-time for fine mode particles is about 5–7 days, but only 1–2 days for the coarse mode aerosol (Jaenicke, 1980; Petzold and Kärcher, 2012; Croft et al., 2014). Therefore, the fine mode EC particles have more time to accumulate in the atmosphere. To evaluate the influence of this high coarse mode EC emission fraction in Eastern Europe on EC's long-range transportation, we constructed the following concept model. In a steady state, where sources are continuous and there is a quasi-equilibrium between sources and sinks such that the EC concentration is constant in time. For the same emission rate of EC, the equilibrium mass concentration of fine mode will be 2–3 times higher than coarse mode as described in Eq. (1) (Croft et al., 2014).

$$\frac{dC(t)}{dt} = S(t) - \frac{C(t)}{\tau(t)}, \quad (1)$$

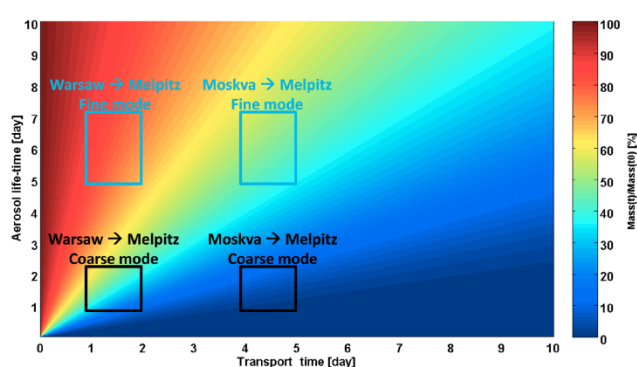
where  $C(t)$  is the EC concentration at time  $t$ ,  $S(t)$  is the source rate, and  $\tau(t)$  is the removal timescale. In the steady state, a quasi-equilibrium between sources and sinks,  $\tau(t)$  is defined as lifetime (Croft et al., 2014). Then the deposition rate (sink rate), with unit of percentage per second, is proportional to  $1/\tau(t)$  for stationary concentrations. The deposition rate of EC in coarse mode is 2–3 times higher than in fine mode.

On the other hand, longer lifetime makes fine mode EC particles have more opportunity to be transported from Eastern Europe to Melpitz. In the following scenario, the particles were emitted instantly into the air mass, which was assumed to be transported by an eastern wind pattern with  $5 \text{ m s}^{-1}$  speed. It will take about 4–5 days from Moskva to Melpitz, and 1–2 days from Warsaw, Poland. During the transport, only the deposition process was active, without subsequent emission. About 30–55 and 65–85 % of fine mode EC can be transported to Melpitz from Moskva and Warsaw, Poland respectively, but just 5–20 and 10–60 % for the coarse mode EC can make the same way (Fig. 7).

The overestimation of ECc emission fraction in EUCAARI inventory resulted in less EC transported from the Eastern Europe and Russia to Melpitz. This may be one reason for the underestimation of the EC mass concentration in the other studies under eastern wind pattern. For instance, Genberg et al. (2013) and Nordmann et al. (2014) reported

**Table 4.** Comparison between the adjusted EC coarse emission simulation and original one.

Sites	Adjusted EC coarse fraction			Original (Nordmann et al., 2014)			Air mass
	MB	MNB	$R^2$	MB	MNB	$R^2$	
Bösel	0.12	0.13	0.81	−0.31	−0.21	0.61	East
Leipzig-TROPOS	−1.01	−0.47	0.69	−1.57	−0.7	0.35	East
Hohenpeißenberg	−0.52	−0.64	0.43	−0.59	−0.72	0.66	Southeast
Zugspitze	−0.22	−0.56	0.72	−0.26	−0.46	0.79	Southeast

**Figure 7.** Aerosol mass residential rate with relationship of transport time and lifetime. The color indicates the percentage of aerosol mass that can be transported to Melpitz.

an underestimation of EC in Europe with the simulation of EUCAARI inventory.

Nordmann et al. (2014) reported an underestimation about 50 % of EC mass concentration in Germany during March–April 2009, especially for the period when air mass approached the observation sites from eastern directions. And they suspected that the EC emission in Eastern Europe may be underestimated by a factor of 2 to 5. In order to investigate the possible influence of the overestimated ECc emission fraction in Eastern Europe in this case, we re-simulated the same time period as in Nordmann et al. (2014) with the adjusted EC emission inventory. The ECc emission fraction was adjusted to 5 % (the average value for Western Europe, longitude < 15° E) if it is higher than 5 % in Eastern Europe (longitude > 15° E). The new simulation and the results of Nordmann et al. (2014) are shown in Table 4. The air mass back trajectories of the high EC concentration period (1 to 4 April 2009, Nordmann et al., 2014) are shown in Fig. 6a. The back trajectories were calculated based on the GDAS (with 0.5° resolution) data set with the Hysplit model ([http://www.arl.noaa.gov/HYSPLIT\\_info.php](http://www.arl.noaa.gov/HYSPLIT_info.php)). The underestimation for EC was significantly improved at Bösel and Leipzig-TROPOS. For Bösel, the mean normalized bias (MNB) increased from −21 to 13 % and  $R^2$  from 0.61 to 0.81; for Leipzig-TROPOS, the MNB increased from −70 to −47 % and  $R^2$  from 0.35 to 0.69. The results of Hohenpeißenberg

and Zugspitze were not significantly changed, with less than 10 % differences in MNB. This is because the air masses of Bösel and Leipzig-TROPOS originated from Eastern Europe passing through Poland, where the ECc emission fraction in EUCAARI inventory is high. But it was not the case for southeastern Europe, where the air masses of Hohenpeißenberg and Zugspitze originated from (Fig. 6a). Thus, it indicates that the Nordmann et al. (2014)'s conclusion of underestimation of EC emission in Eastern Europe for 2009 is generally correct, especially for southeastern Europe (e.g.: Austria, Slovenia, Croatia etc.). However, the overestimation of ECc emission fraction in Eastern Europe (e.g.: Poland, Belarus, Russia etc.) could be another reason for the underestimation of modeled EC mass concentration in the eastern wind pattern. It contributed about 20–40 % underestimation of the EC mass concentration in Germany. This is consistent with the result of concept model, which showed the adjustment of ECc emission fraction in Warsaw Poland would make about 25–55 % difference of EC transported to Melpitz.

#### 4 Conclusions

A WRF-Chem simulation was performed for the period between 10 and 20 September 2013, with an inner most domain of 2 km resolution for the Melpitz region in eastern Germany. The high-resolution EUCAARI inventory of EC emission was applied in the model. The measurements of HOPE-Melpitz Campaign and GUAN network project were used for modelling results validation.

The comparison of particle number/mass size distributions showed that the coarse mode particle concentration was substantially overestimated by the model. However, the meteorology and transport process were well simulated, because of the good agreement with the ground-based and radiosounding meteorological measurements. These results indicated that the overestimation of the coarse mode particle should mostly come from the uncertainty of emission inventories. The comparisons of EC mass concentrations at the Melpitz, Leipzig-TROPOS and Bösel sites indicated that the EC point sources may be overestimated by a factor of 2–10, which made a remarkable unrealistic plume in Melpitz.

The coarse mode EC emission fraction was substantially overestimated in Eastern Europe (e.g.: Poland, Belarus etc.) and Russia by EUCAARI inventory, with about 10–30 % for Russia and 5–10 % for the Eastern European countries. A concept model and a case study were designed to interpret the influence of this overestimation on EC long-range transportation. Due to the overestimation of ECc emission fraction, EC mass transported from Moskva to Melpitz would decrease by about 25–35 % of ECc mass concentration, and decrease by about 25–55 % from Warsaw to Melpitz. This is because the coarse mode particle has a shorter life-time and therefore less opportunity for being long-range transported and accumulated in the atmosphere. The March–April 2009 case (Nordmann et al., 2014) was re-simulated with adjusted ECc emission fraction in Eastern Europe in order to validate the influence on transportation. The result showed that the overestimation of ECc emission fraction in Eastern Europe was one reason of the underestimation of EC in Germany, when the air masses came from eastern direction. It contributed to an underestimation of about 20–40 %.

Will the health and climatic effects of atmospheric EC particles be local, regional or global? This is to some extent determined by the transportation of EC, which is largely influenced by its size distribution. The size segregation information of EC particles should be carefully considered in the model validation and climate change evaluation studies. Unfortunately, the size segregation information is not included in most of the current global EC emission inventories, and the size segregation in EUCAARI inventory only covers Europe and is still with high uncertainty. More EC particle size distribution measurements (e.g.: online analysis of SP2, offline analysis of Berner/MOUDI samples, etc.) and long-term model simulation studies are needed to further improve the EC emission inventories.

**The Supplement related to this article is available online at doi:10.5194/acp-16-1823-2016-supplement.**

**Acknowledgements.** Continuous aerosol measurements at Melpitz were supported by the German Federal Environment Ministry (BMU) grants F&E 370343200 (German title: “Erfassung der Zahl feiner und ultrafeiner Partikel in der Außenluft”) and F&E 371143232 (German title: “Trendanalysen gesundheitsgefährdender Fein- und Ultrafeinstaubfraktionen unter Nutzung der im German Ultrafine Aerosol Network (GUAN) ermittelten Immissionsdaten durch Fortführung und Interpretation der Messreihen”). The black carbon data used for this paper can be accessed through the German Ultrafine Aerosol Network’s data dissemination page: doi:10.5072/guan. The HOPE campaign was funded by the German Research Ministry under the project number 01LK1212 C. The work of Y. F. Cheng and H. Su was supported by the Max Planck Society (MPG) and National Natural Science Foundation of China (41330635). We would also like to thank Markus Hermann and Sascha Pfeifer for useful suggestions.

Edited by: V.-M. Kerminen

## References

- Barnard, J. C., Chapman, E. G., Fast, J. D., Schemmler, J. R., Slusser, J. R., and Shetter, R. E.: An evaluation of the FAST-J Photolysis Algorithm for predicting nitrogen dioxide photolysis rates under clear and cloudy sky conditions, *Atmos. Environ.*, 38, 3393–3403, 2004.
- Binkowski, F. S. and Shankar, U.: The Regional Particulate Matter Model: 1. Model description and preliminary results, *J. Geophys. Res.*, 100, 26191–26209, doi:10.1029/95JD02093, 1995.
- Birmili, W., Stratmann, F., and Wiedensohler, A.: Design of a DMA-based size spectrometer for a large particle size range and stable operation, *J. Aerosol Sci.*, 30, 549–533, 1999.
- Birmili, W., Weinhold, K., Nordmann, S., Wiedensohler, A., Spindler, G., Müller, K., Herrmann, H., Gnauk, T., Pitz, M., Cyrys, J., Flentje, H., Nickel, C., Kuhlbusch, T., Löschau, G., Haase, D., Meinhardt, F., Schwerin, A., Ries, L., and Wirtz, K.: Atmospheric aerosol measurements in the German Ultrafine Aerosol Network (GUAN) – Part – soot and particle number size distributions, *Gefahrst. Reinhalt. L.*, 69, 137–145, 2009.
- Birmili, W., Weinhold, K., Merkel, M., Rasch, F., Sonntag, A., Wiedensohler, A., Bastian, S., Schladitz, A., Löschau, G., Cyrys, J., Pitz, M., Gu, J., Kusch, T., Flentje, H., Quass, U., Kaminski, H., Kuhlbusch, T. A. J., Meinhardt, F., Schwerin, A., Bath, O., Ries, L., Wirtz, K., and Fiebig, M.: Long-term observations of tropospheric particle number size distributions and equivalent black carbon mass concentrations in the German Ultrafine Aerosol Network (GUAN), *Earth Syst. Sci. Data Discuss.*, 8, 935–993, doi:10.5194/essdd-8-935-2015, 2015.
- Bond, T. C., Streets, D. G., Yarber, K. F., Nelson, S. M., Woo, J., and Klimont, Z.: A technology-based global inventory of black and organic carbon emissions from combustion, *J. Geophys. Res.*, 109, D14203, doi:10.1029/2003JD003697, 2004.
- Bond, T. C., Bhardwaj, E., Dong, R., Jogani, R., Jung, S., Roden, C., Streets, D. G., and Trautmann, N. M.: Historical emissions of black and organic carbon aerosol from energy-related combustion, 1850–2000, *Global Biogeochem. Cy.*, 21, GB2018, doi:10.1029/2006GB002840, 2007.
- Bond, T. C., Doherty, S. J., Fahey, D. W., Forster, P. M., Bernsten, T., DeAngelo, B. J., Flanner, M. G., Ghan, S., Kärcher, B., Koch, D., Kinne, S., Kondo, Y., Quinn, P. K., Sarofim, M. C., Schultz, M. G., Schulz, M., Venkataraman, C., Zhang, H., Zhang, S., Bellouin, N., Guttikunda, S. K., Hopke, P. K., Jacobson, M. Z., Kaiser, J. W., Klimont, Z., Lohmann, U., Schwarz, J. P., Shindell, D., Storelvmo, T., Warren, S. G., and Zender, C. S.: Bounding the role of black carbon in the climate system: a scientific assessment, *J. Geophys. Res.-Atmos.*, 118, 5380–5552, doi:10.1002/jgrd.50171, 2013.
- Brüggemann, E. and Spindler, G.: Wet and dry deposition of sulphur at the site Melpitz in East Germany, *Water Air Soil Poll.*, 109, 81–99, 1999.
- Chapman, E. G., Gustafson Jr., W. L., Easter, R. C., Barnard, J. C., Ghan, S. J., Pekour, M. S., and Fast, J. D.: Coupling aerosol-cloud-radiative processes in the WRF-Chem model: Investigat-

- ing the radiative impact of elevated point sources, *Atmos. Chem. Phys.*, 9, 945–964, doi:10.5194/acp-9-945-2009, 2009.
- Cheng, Y. F., Wiedensohler, A., Eichler, H., Su, H., Gnauk, T., Brüggemann, E., Herrmann, H., Heintzenberg, J., Slanina, J., Tuch, T., Hu, M., and Zhang, Y. H.: Aerosol optical properties and related chemical apportionment at Xinken in Pearl River Delta of China, *Atmos. Environ.*, 42, 6351–6372, doi:10.1016/j.atmosenv.2008.02.034, 2008.
- Cheng, Y. F., Berghof, M., Garland, R. M., Wiedensohler, A., Wehner, B., Müller, T., Su, H., Zhang, Y. H., Achtert, P., Nowak, A., Pöschl, U., Zhu, T., Hu, M., and Zeng, L. M.: Influence of soot mixing state on aerosol light absorption and single scattering albedo during air mass aging at a polluted regional site in northeastern China, *J. Geophys. Res.*, 114, doi:10.1029/2008jd010883, 2009.
- Chou, M., Suarez, M., Ho, C., Yan, M., and Lee, K.: Parameterizations for Cloud Overlapping and Shortwave Single-Scattering Properties for Use in General Circulation and Cloud Ensemble Models, *J. Climate*, 11, 202–214, 1998.
- Croft, B., Lohmann, U., and von Salzen, K.: Black carbon ageing in the Canadian Centre for Climate modelling and analysis atmospheric general circulation model, *Atmos. Chem. Phys.*, 5, 1931–1949, doi:10.5194/acp-5-1931-2005, 2005.
- Croft, B., Pierce, J. R., and Martin, R. V.: Interpreting aerosol lifetimes using the GEOS-Chem model and constraints from radionuclide measurements, *Atmos. Chem. Phys.*, 14, 4313–4325, doi:10.5194/acp-14-4313-2014, 2014.
- Cyrys, J., Peters, A., Soentgen, J., and Wichmann, H. E.: Low emission zones reduce PM<sub>10</sub> mass concentrations and diesel soot in German cities, *J. Air Waste Manage. Assoc.*, 64, 481–487, 2014.
- Denier van der Gon, H. A. C., Visschedijk, A., Van der Brugh, H., and Dröge, R.: A High Resolution European Emission Database for the Year 2005, a Contribution to the UBAPROJECT PAREST: Particle Reduction Strategies, TNO report TNO-034-UT-2010-01895\_RPTMI., published by the German Federal Environment Agency (Umweltbundesamt) as Texte 41/2013, Utrecht, available at: <https://www.umweltbundesamt.de/publikationen> (last access: 3 September 2015), 2010.
- Denier van der Gon, H. A. C., Bergström, R., Fountoukis, C., Johansson, C., Pandis, S. N., Simpson, D., and Visschedijk, A. J. H.: Particulate emissions from residential wood combustion in Europe – revised estimates and an evaluation, *Atmos. Chem. Phys.*, 15, 6503–6519, doi:10.5194/acp-15-6503-2015, 2015.
- Easter, R. C., Ghan, S. J., Zhang, Y., Saylor, R. D., Chapman, E. G., Laulainen, N. S., Abdul-Razzak, H., Leung, L. R., Bian, X., and Zaveri, R. A.: MIRAGE: model description and evaluation of aerosols and trace gases, *J. Geophys. Res.*, 109, D20210, doi:10.1029/2004JD004571, 2004.
- Echalar, F., Artaxo, P., Martins, J. V., Yamasoe, M., Gerab, F., Maenhaut, W., and Holben, B.: Long-term monitoring of atmospheric aerosols in the Amazon Basin: source identification and apportionment, *J. Geophys. Res.-Atmos.*, 103, 31849–31864, 1998.
- EEA (European Environment Agency): European Union Emission Inventory Report 1990–2011 Under the UNECE Convention on Long-range Transboundary Air Pollution (LRTAP), EEA Technical report No. 10/2013, Copenhagen, doi:10.2800/44480, 2013.
- Fast, J. D., Gustafson Jr., W. I., Easter, R. C., Zaveri, R. A., Barnard, J. C., Chapman, F. G., Grell, G. A., and Peckham, S. E.: Evolution of ozone, particulates, and aerosol direct radiative forcing in the vicinity of Houston using a fully coupled meteorology-chemistry-aerosol model, *J. Geophys. Res.*, 111, D21305, doi:10.1029/2005JD006721, 2006.
- Genberg, J., Denier van der Gon, H. A. C., Simpson, D., Swietlicki, E., Areskoug, H., Beddows, D., Ceburnis, D., Fiebig, M., Hansson, H. C., Harrison, R. M., Jennings, S. G., Saarikoski, S., Spindler, G., Visschedijk, A. J. H., Wiedensohler, A., Yttri, K. E., and Bergström, R.: Light-absorbing carbon in Europe – measurement and modelling, with a focus on residential wood combustion emissions, *Atmos. Chem. Phys.*, 13, 8719–8738, doi:10.5194/acp-13-8719-2013, 2013.
- Grell, G. A., Peckham, S. E., Schmitz, R., McKeen, S. A., Frost, G., Skamarock, W. C., and Eder, B.: Fully coupled “online” chemistry within the WRF model, *Atmos. Environ.*, 39, 6957–6975, 2005.
- Guenther, A., Karl, T., Harley, P., Wiedinmyer, C., Palmer, P. I., and Geron, C.: Estimates of global terrestrial isoprene emissions using MEGAN (Model of Emissions of Gases and Aerosols from Nature), *Atmos. Chem. Phys.*, 6, 3181–3210, doi:10.5194/acp-6-3181-2006, 2006.
- Hansen, J. E., Sato, M., Ruedy, R., Lacis, A., and Oinas, V.: Global warming in the twenty-first century: an alternative scenario, *P. Natl. Acad. Sci. USA*, 97, 9875–9880, 2000.
- Heintzenberg, J., Müller, K., Birmili, W., Spindler, G., and Wiedensohler, A.: Mass-related aerosol properties over the Leipzig Basin, *J. Geophys. Res.-Atmos.*, 103, 13125–13135, 1998.
- Hitznerberger, R. and Tohno, S.: Comparison of black carbon (BC) aerosols in two urban areas – concentrations and size distributions, *Atmos. Environ.*, 35, 2153–2167, 2001.
- IPCC: Climate Change 2013: The Physical Science Basis, Contribution of Working Group I to the Fifth Assessment Report of the Intergovernmental Panel on Climate Change, Report, Cambridge University Press, New York, 2013.
- Jacobson, M. Z.: A physically-based treatment of elemental carbon optics: implications for global direct forcing of aerosols, *Geophys. Res. Lett.*, 27, 217–220, doi:10.1029/1999GL010968, 2000.
- Jaenicke, R.: Atmospheric aerosols and global climate, *J. Aerosol Sci.*, 11, 577–588, 1980.
- Junker, C. and Liousse, C.: A global emission inventory of carbonaceous aerosol from historic records of fossil fuel and biofuel consumption for the period 1860–1997, *Atmos. Chem. Phys.*, 8, 1195–1207, doi:10.5194/acp-8-1195-2008, 2008.
- Koch, D., Schulz, M., Kinne, S., McNaughton, C., Spackman, J. R., Balkanski, Y., Bauer, S., Bernsten, T., Bond, T. C., Boucher, O., Chin, M., Clarke, A., De Luca, N., Dentener, F., Diehl, T., Dubovik, O., Easter, R., Fahey, D. W., Feichter, J., Fillmore, D., Freitag, S., Ghan, S., Ginoux, P., Gong, S., Horowitz, L., Iversen, T., Kirkevåg, A., Klimont, Z., Kondo, Y., Krol, M., Liu, X., Miller, R., Montanaro, V., Moteki, N., Myhre, G., Penner, J. E., Perlwitz, J., Pitari, G., Reddy, S., Sahu, L., Sakamoto, H., Schuster, G., Schwarz, J. P., Seland, Ø., Stier, P., Takegawa, N., Takemura, T., Textor, C., van Aardenne, J. A., and Zhao, Y.: Evaluation of black carbon estimations in global aerosol models, *Atmos. Chem. Phys.*, 9, 9001–9026, doi:10.5194/acp-9-9001-2009, 2009.
- Kuenen, J. J. P., Visschedijk, A. J. H., Jozwicka, M., and Denier van der Gon, H. A. C.: TNO-MACC-II emission inventory; a multi-



- year (2003–2009) consistent high-resolution European emission inventory for air quality modelling, *Atmos. Chem. Phys.*, 14, 10963–10976, doi:10.5194/acp-14-10963-2014, 2014.
- Kulmala, M., Asmi, A., Lappalainen, H. K., Baltensperger, U., Brenguier, J.-L., Facchini, M. C., Hansson, H.-C., Hov, Ø., O'Dowd, C. D., Pöschl, U., Wiedensohler, A., Boers, R., Boucher, O., de Leeuw, G., Denier van der Gon, H. A. C., Feichter, J., Krejci, R., Laj, P., Lihavainen, H., Lohmann, U., McFiggans, G., Mentel, T., Pilinis, C., Riipinen, I., Schulz, M., Stohl, A., Swietlicki, E., Vignati, E., Alves, C., Amann, M., Ammann, M., Arabas, S., Artaxo, P., Baars, H., Beddows, D. C. S., Bergström, R., Beukes, J. P., Bilde, M., Burkhardt, J. F., Canonaco, F., Clegg, S. L., Coe, H., Crumeyrolle, S., D'Anna, B., Decesari, S., Gilardoni, S., Fischer, M., Fjaeraa, A. M., Fountoukis, C., George, C., Gomes, L., Halloran, P., Hamburger, T., Harrison, R. M., Herrmann, H., Hoffmann, T., Hoose, C., Hu, M., Hyvärinen, A., Hörrak, U., Iinuma, Y., Iversen, T., Josipovic, M., Kanakidou, M., Kiendler-Scharr, A., Kirkevåg, A., Kiss, G., Klimont, Z., Kolmonen, P., Komppula, M., Kristjánsson, J.-E., Laakso, L., Laaksonen, A., Labonnote, L., Lanz, V. A., Lehtinen, K. E. J., Rizzo, L. V., Makkonen, R., Manninen, H. E., McMeeking, G., Merikanto, J., Minikin, A., Mirme, S., Morgan, W. T., Nemitz, E., O'Donnell, D., Panwar, T. S., Pawlowska, H., Petzold, A., Pienaar, J. J., Pio, C., Plass-Dümler, C., Prévôt, A. S. H., Pryor, S., Reddington, C. I., Roberts, G., Rosenfeld, D., Schwarz, J., Seland, Ø., Sellegri, K., Shen, X. J., Shiraiwa, M., Siebert, H., Sierau, B., Simpson, D., Sun, J. Y., Topping, D., Tunved, P., Vaattovaara, P., Vakkari, V., Veefkind, J. P., Visschedijk, A., Vuollekoski, H., Vuolo, R., Wehner, B., Wildt, J., Woodward, S., Worsnop, D. R., van Zadelhoff, G.-J., Zardini, A. A., Zhang, K., van Zyl, P. G., Kerminen, V.-M., S Carslaw, K., and Pandis, S. N.: General overview: European Integrated project on Aerosol Cloud Climate and Air Quality interactions (EUCAARI) – integrating aerosol research from nano to global scales, *Atmos. Chem. Phys.*, 11, 13061–13143, doi:10.5194/acp-11-13061-2011, 2011.
- Lamarque, J.-F., Bond, T. C., Eyring, V., Granier, C., Heil, A., Klimont, Z., Lee, D., Lioussé, C., Mieville, A., Owen, B., Schultz, M. G., Shindell, D., Smith, S. J., Stehfest, E., Van Aardenne, J., Cooper, O. R., Kainuma, M., Mahowald, N., McConnell, J. R., Naik, V., Riahi, K., and van Vuuren, D. P.: Historical (1850–2000) gridded anthropogenic and biomass burning emissions of reactive gases and aerosols: methodology and application, *Atmos. Chem. Phys.*, 10, 7017–7039, doi:10.5194/acp-10-7017-2010, 2010.
- Marčeková, K., Wankmüller, R., Moosmann, L., and Pinterits, M.: Inventory Review 2013: Review of Emission Data reported under the LRTAP Convention and NEC Directive. Stage 1 and 2 review, Status of Gridded Data and LPS Data, STATUS Report 1/2013, Umweltbundesamt GmbH, Vienna, Austria, 2013.
- McConnell, J. R., Edwards, R., Kok, G. L., Flanner, M. G., Zender, C. S., Saltzman, E. S., Banta, J. R., Pasteris, D. R., Carter, M. M., and Kahl, J. D. W.: 20th-century industrial black carbon emissions altered arctic climate forcing, *Science*, 317, 1381–1384, 2007.
- Meister, K., Johansson, C., and Forsberg, B.: Estimated short-term effects of coarse particles on daily mortality in Stockholm, Sweden, *Environ. Health Persp.*, 120, 431–436, 2012.
- Ming, J., Cachier, H., Xiao, C., Qin, D., Kang, S., Hou, S., and Xu, J.: Black carbon record based on a shallow Himalayan ice core and its climatic implications, *Atmos. Chem. Phys.*, 8, 1343–1352, doi:10.5194/acp-8-1343-2008, 2008.
- Nordmann, S., Birmili, W., Weinhold, K., Müller, K., Spindler, G., and Wiedensohler, A.: Measurements of the mass absorption cross section of atmospheric soot particles using Raman spectroscopy, *J. Geophys. Res.-Atmos.*, 118, 12075–12085, doi:10.1002/2013JD002021, 2013.
- Nordmann, S., Cheng, Y. F., Carmichael, G. R., Yu, M., Denier van der Gon, H. A. C., Zhang, Q., Saide, P. E., Pöschl, U., Su, H., Birmili, W., and Wiedensohler, A.: Atmospheric black carbon and warming effects influenced by the source and absorption enhancement in central Europe, *Atmos. Chem. Phys.*, 14, 12683–12699, doi:10.5194/acp-14-12683-2014, 2014.
- Petzold, A. and Kärcher, B.: Aerosols in the Atmosphere, in: *Atmospheric Physics*, edited by: Schumann, U., Research Topics in Aerospace, Springer Berlin Heidelberg, 37–53, doi:10.1007/978-3-642-30183-4\_3, 2012.
- Pouliot, G., Pierce, T., van der Gon, H., Schaap, M., Moran, M., and Nopmongkol, U.: Comparing emission inventories and model-ready emission datasets between Europe and North America for the AQMEII project, *Atmos. Environ.*, 53, 4–14, 2012.
- Pope, C. A., Ezzati, M., and Dockery, D. W.: Fine-particulate air pollution and life expectancy in the united states, *N. Engl. J. Med.*, 360, 376–386, 2009.
- Poulain, L., Spindler, G., Birmili, W., Plass-Dümler, C., Wiedensohler, A., and Herrmann, H.: Seasonal and diurnal variations of particulate nitrate and organic matter at the IfT research station Melpitz, *Atmos. Chem. Phys.*, 11, 12579–12599, doi:10.5194/acp-11-12579-2011, 2011.
- Ramanathan, V. and Carmichael, G.: Global and regional climate changes due to black carbon, *Nat. Geosci.*, 1, 221–227, 2008.
- Rose, D., Wehner, B., Ketzel, M., Engler, C., Voigtländer, J., Tuch, T., and Wiedensohler, A.: Atmospheric number size distributions of soot particles and estimation of emission factors, *Atmos. Chem. Phys.*, 6, 1021–1031, doi:10.5194/acp-6-1021-2006, 2006.
- Saide, P. E., Spak, S. N., Carmichael, G. R., Mena-Carrasco, M. A., Yang, Q., Howell, S., Leon, D. C., Snider, J. R., Bandy, A. R., Collett, J. L., Benedict, K. B., de Szoce, S. P., Hawkins, L. N., Allen, G., Crawford, I., Crosier, J., and Springston, S. R.: Evaluating WRFChem aerosol indirect effects in Southeast Pacific marine stratocumulus during VOCALSREx, *Atmos. Chem. Phys.*, 12, 3045–3064, doi:10.5194/acp-12-3045-2012, 2012.
- Spindler, G., Brüggemann, E., Gnauk, T., Gruner, A., Müller, K., and Herrmann, H.: A four-year size-segregated characterization study of particles  $PM_{10}$ ,  $PM_{2.5}$  and  $PM_1$  depending on air mass origin at Melpitz, *Atmos. Environ.*, 44, 164–173, 2010.
- Spindler, G., Gnauk, T., Gruner, A., Iinuma, Y., Müller, K., Scheinhardt, S., and Herrmann, H.: Size-segregated characterization of  $PM_{10}$  at the EMEP site Melpitz (Germany) using a five-stage impactor: a 6 year study, *J. Atmos. Chem.*, 69, 127–157, 2012.
- Spindler, G., Gruner, A., Müller, K., Schlimper, S., and Herrmann, H.: Long-term sizesegregated particle ( $PM_{10}$ ,  $PM_{2.5}$ ,  $PM_1$ ) characterization study at Melpitz – influence of air mass inflow, weather conditions and season, *J. Atmos. Chem.*, 70, 165–195, doi:10.1007/s10874-013-9263-8, 2013.

- Stern, R., Builtjes, P., Schaap, M., Timmermans, R., Vautard, R., Hodzic, A., Memmesheimer, M., Feldmann, H., Renner, E., Wolke, R., and Kerschbaumer: a model inter-comparison study focussing on episodes with elevated PM<sub>10</sub> concentrations, *Atmos. Environ.*, 42, 4567–4588, doi:10.1016/j.atmosenv.2008.01.068, 2008.
- Vignati, E., Karl, M., Krol, M., Wilson, J., Stier, P., and Cavalli, F.: Sources of uncertainties in modelling black carbon at the global scale, *Atmos. Chem. Phys.*, 10, 2595–2611, doi:10.5194/acp-10-2595-2010, 2010.
- Visschedijk, A. and Denier van der Gon, H.: EUCAARI Deliverable: Pan-European Carbonaceous Aerosol Inventory, Report, TNO Built Environment and Geosciences, D42, Utrecht, the Netherlands, 2008.
- Wiedinmyer, C., Akagi, S. K., Yokelson, R. J., Emmons, L. K., Al-Saadi, J. A., Orlando, J. J., and Soja, A. J.: The Fire INventory from NCAR (FINN): a high resolution global model to estimate the emissions from open burning, *Geosci. Model Dev.*, 4, 625–641, doi:10.5194/gmd-4-625-2011, 2011.
- Wild, O., Zhu, X., and Prather, M. J.: Fast-J: accurate simulation of in- and below-cloud photolysis in tropospheric chemical models, *J. Atmos. Chem.*, 37, 245–282, 2000.
- Yang, Q., W. I. Gustafson Jr., Fast, J. D., Wang, H., Easter, R. C., Morrison, H., Lee, Y.-N., Chapman, E. G., Spak, S. N., and Mena-Carrasco, M. A.: Assessing regional scale predictions of aerosols, marine stratocumulus, and their interactions during VOCALS-REx using WRF-Chem, *Atmos. Chem. Phys.*, 11, 11951–11975, doi:10.5194/acp-11-11951-2011, 2011.
- Zhang, Y., Sartelet, K., Zhu, S., Wang, W., Wu, S.-Y., Zhang, X., Wang, K., Tran, P., Seigncur, C., and Wang, Z.-F.: Application of WRF/Chem-MADRID and WRF/Polyphemus in Europe – Part 2: Evaluation of chemical concentrations and sensitivity simulations, *Atmos. Chem. Phys.*, 13, 6845–6875, doi:10.5194/acp-13-6845-2013, 2013.
- Zaveri, R. A. and Peters, L. K.: A new lumped structure photochemical mechanism for largescale applications, *J. Geophys. Res.*, 104, 30387–30415, 1999.
- Zaveri, R. A., Easter, R. C., Fast, J. D., and Peters, L. K.: Model for Simulating Aerosol Interactions and Chemistry (MOSAIC), *J. Geophys. Res.*, 113, D13204, doi:10.1029/2007JD008782, 2008.



### 3.1.2 Supporting information

Supplement of Atmos. Chem. Phys., 16, 1823–1835, 2016  
<http://www.atmos-chem-phys.net/16/1823/2016/>  
doi:10.5194/acp-16-1823-2016-supplement  
© Author(s) 2016. CC Attribution 3.0 License.



Atmospheric  
Chemistry  
and Physics  
Open Access  
EGU

*Supplement of*

### **Evaluation of the size segregation of elemental carbon (EC) emission in Europe: influence on the simulation of EC long-range transportation**

**Y. Chen et al.**

*Correspondence to:* Ya-Fang Cheng (yafang.cheng@mpic.de) and Alfred Wiedensohler (ali@tropos.de)

The copyright of individual parts of the supplement might differ from the CC-BY 3.0 licence.

## Results and Discussion

**Table S1.** Point source number for the different ECc emission fraction level in the different regions.

Point source ECc emission fraction  unit: [%]	Number of point sources in each region		
	Germany and nearby region: 54.5°N 6°E 18°E 48°N	Melpitz region: 52°N 12°E 15°E 51°N	Bösel region: 54°N 7°E 9°E 53°N
90-100	22	0	8
80-90	15	3	2
60-80	5	0	2
30-60	18	0	0

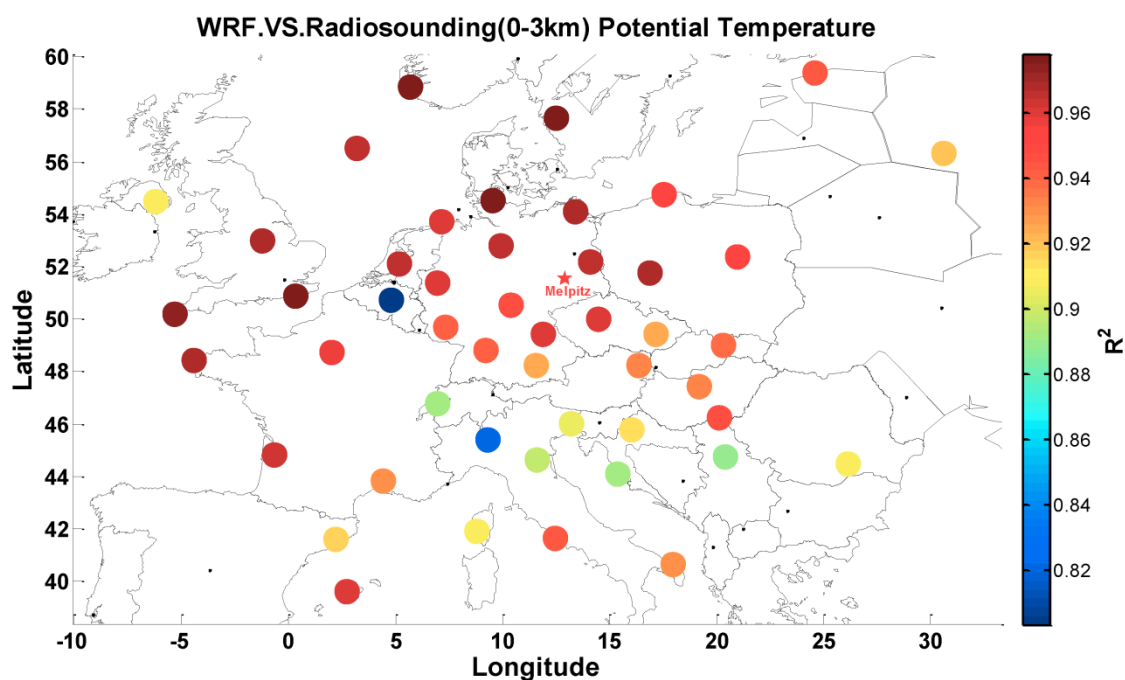


**Figure S2.** Correlation coefficient ( $R^2$ ) map of the potential temperature under 3 km between WRF-Chem model and radio-sounding measurements. Melpitz is marked as red star.

## Results and Discussion

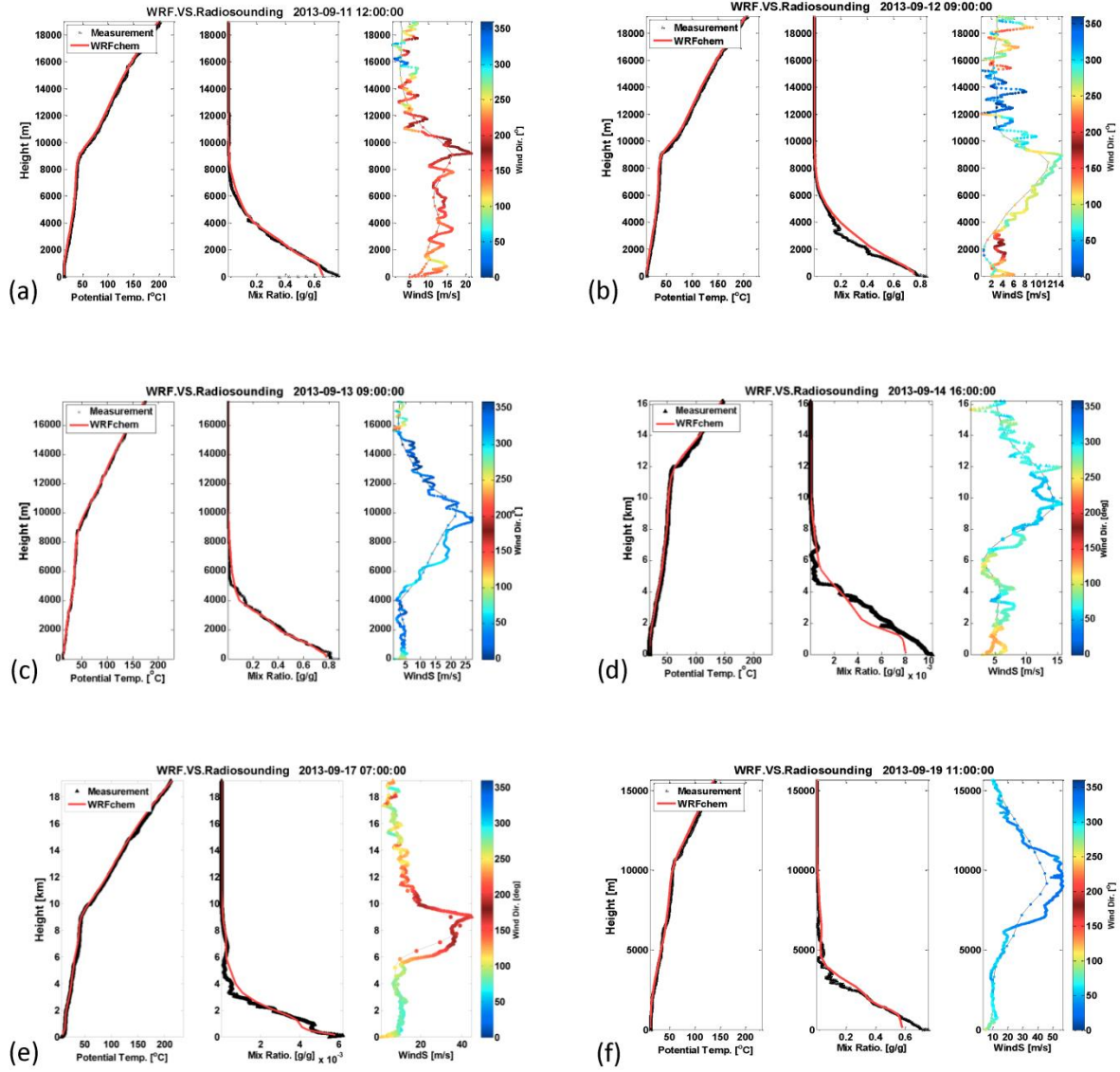


**Figure S3.** Some examples for meteorological variables comparison between Melpitz radio-sounding and WRF-Chem. (a) 2013-09-11 12:00; (b) 2013-09-12 09:00; (c) 2013-09-13 09:00; (d) 2013-09-14 16:00; (e) 2013-09-17 07:00; (f) 2013-09-19 11:00.

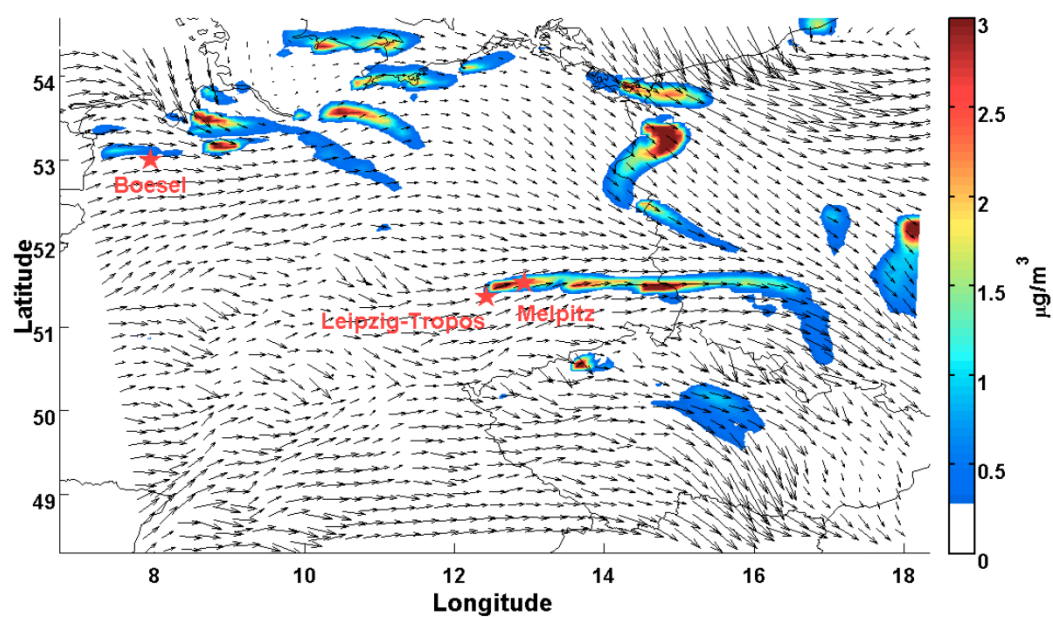


**Figure S4.** The model result of horizontal distribution for EC in bin08 [5-10  $\mu\text{m}$ ], at 08:00 13 September 2013. Melpitz, Leipzig-TROPOS and Bösel are marked by red stars.

### 3.2 Second publication

#### 3.2.1 Sea salt emission, transport and influence on size-segregated nitrate simulation: a case study in northwestern Europe by WRF-Chem

The content of this chapter has already been published in the manuscript “Sea salt emission, transport and influence on size-segregated nitrate simulation: a case study in northwestern Europe by WRF-Chem” by Ying Chen, Yafang Cheng, Nan Ma, Ralf Wolke, Stephan Nordmann, Stephanie Schüttauf, Liang Ran, Birgit Wehner, Wolfram Birmili, Hugo A. C. Denier van der Gon, Qing Mu, Stefan Barthel, Gerald Spindler, Bastian Stieger, Konrad Müller, Guang-Jie Zheng, Ulrich Pöschl, Hang Su, and Alfred Wiedensohler in the journal “Atmospheric Chemistry and Physics” in 2016, in Volume 16, pages 12081-12097, doi: 10.5194/acp-16-12081-2016.

Reprinted with permission by the authors from Atmospheric Chemistry and Physics, 2016, 16, 12081-12097, doi: 10.5194/acp-16-12081-2016.



## Sea salt emission, transport and influence on size-segregated nitrate simulation: a case study in northwestern Europe by WRF-Chem

Ying Chen<sup>1,2</sup>, Yafang Cheng<sup>2</sup>, Nan Ma<sup>1,2</sup>, Ralf Wolke<sup>1</sup>, Stephan Nordmann<sup>3</sup>, Stephanie Schüttauf<sup>1</sup>, Liang Ran<sup>4</sup>, Birgit Wehner<sup>1</sup>, Wolfram Birmili<sup>1,3</sup>, Hugo A. C. Denier van der Gon<sup>5</sup>, Qing Mu<sup>2</sup>, Stefan Barthel<sup>1</sup>, Gerald Spindler<sup>1</sup>, Bastian Stieger<sup>1</sup>, Konrad Müller<sup>1</sup>, Guang-Jie Zheng<sup>6</sup>, Ulrich Pöschl<sup>2</sup>, Hang Su<sup>2</sup>, and Alfred Wiedensohler<sup>1</sup>

<sup>1</sup>Leibniz Institute for Tropospheric Research, 04318 Leipzig, Germany

<sup>2</sup>Multiphase Chemistry Department, Max Planck Institute for Chemistry, 55128 Mainz, Germany

<sup>3</sup>German Environment Agency, 06844 Dessau-Roßlau, Germany

<sup>4</sup>Key Laboratory of Middle Atmosphere and Global Environment Observation, Institute of Atmospheric Physics, Chinese Academy of Sciences, Beijing, 100029, China

<sup>5</sup>Dept. of Climate, Air and Sustainability, TNO, Princetonlaan 6, 3584 CB Utrecht, the Netherlands

<sup>6</sup>State Key Joint Laboratory of Environment Simulation and Pollution Control, School of Environment, Tsinghua University, Beijing 100084, China

Correspondence to: Yafang Cheng (yafang.cheng@mpic.de) and Ying Chen (chen@tropos.de)

Received: 8 April 2016 – Published in Atmos. Chem. Phys. Discuss.: 11 May 2016

Revised: 14 September 2016 – Accepted: 17 September 2016 – Published: 27 September 2016

**Abstract.** Sea salt aerosol (SSA) is one of the major components of primary aerosols and has significant impact on the formation of secondary inorganic particles mass on a global scale. In this study, the fully online coupled WRF-Chem model was utilized to evaluate the SSA emission scheme and its influence on the nitrate simulation in a case study in Europe during 10–20 September 2013. Meteorological conditions near the surface, wind pattern and thermal stratification structure were well reproduced by the model. Nonetheless, the coarse-mode ( $PM_{1-10}$ ) particle mass concentration was substantially overestimated due to the overestimation of SSA and nitrate. Compared to filter measurements at four EMEP stations (coastal stations: Bilthoven, Kollumerwaard and Vredepeel; inland station: Melpitz), the model overestimated SSA concentrations by a factor of 8–20. We found that this overestimation was mainly caused by overestimated SSA emissions over the North Sea during 16–20 September. Over the coastal regions, SSA was injected into the continental free troposphere through an “aloft bridge” (about 500 to 1000 m above the ground), a result of the different thermodynamic properties and planetary boundary layer (PBL) structure between continental and marine regions. The injected SSA was further transported inland and mixed downward to the surface through downdraft and PBL

turbulence. This process extended the influence of SSA to a larger downwind region, leading, for example, to an overestimation of SSA at Melpitz, Germany, by a factor of  $\sim 20$ . As a result, the nitrate partitioning fraction (ratio between particulate nitrate and the summation of particulate nitrate and gas-phase nitric acid) increased by about 20 % for the coarse-mode nitrate due to the overestimation of SSA at Melpitz. However, no significant difference in the partitioning fraction for the fine-mode nitrate was found. About 140 % overestimation of the coarse-mode nitrate resulted from the influence of SSA at Melpitz. In contrast, the overestimation of SSA inhibited the nitrate particle formation in the fine mode by about 20 % because of the increased consumption of precursor by coarse-mode nitrate formation.

### 1 Introduction

Atmospheric aerosols play an important role in climate change (IPCC, 2013). Further, they have an adverse effect on human health (Pope et al., 2009). Aerosol particles are either emitted directly as a so-called “primary aerosol” or generated by atmospheric secondary processes (“secondary particles”). Sea salt aerosol (SSA) is one major constituent

of primary natural aerosol particles on a global scale (Lewis and Schwartz, 2004), comparable with mineral dust particles in the Northern Hemisphere (IPCC, 2013; Mårtensson et al., 2010). SSA belongs to the naturally produced aerosol and is generated mainly by bursting bubbles during whitecap formation in the open ocean (Monahan et al., 1986). Waves breaking in the surf zone, where there are more whitecaps and stronger SSA emission due to increased ocean bottom and higher intensity of wave breaking, may affect SSA concentrations at areas within 25 km distance from the coastline and can dominate the SSA concentration at the coastal region (de Leeuw et al., 2000; Monahan, 1995; Woodcock et al., 1963).

SSA exerts an influence on the aerosol burden of other aerosols, which makes the intensity of SSA emission even more important. SSA can participate in heterogeneous reactions by interacting with trace gases, leading to the formation of particulate nitrate on SSA surface and increase nitrate particle mass concentration (Seinfeld and Pandis, 2006). Nitrate is one of the most important secondary inorganic aerosol and is the dominant aerosol component in western and central Europe (Schaap et al., 2011). SSA can also facilitate the formation of nitrate aerosol (Neumann et al., 2016a; Liu et al., 2015; Im, 2013; Athanasopoulou et al., 2008). However, these previous studies mainly focused on the influence of SSA on bulk nitrate mass concentration and did not address its influence on size-segregated nitrate particles. In this study, we quantified the SSA influence on both fine-mode and coarse-mode nitrate particles formation, respectively, and the effect could be different for the different size mode, resulting from the heterogeneous reaction on SSA surface with the formation of sodium nitrate. The timescale of this reaction is considered to be several hours (Meng and Seinfeld, 1996). Sodium nitrate is produced with a chloride displacement in the SSA (Schaap et al., 2011; Seinfeld and Pandis, 2006). Importantly, thermodynamically stable sodium nitrate will not return to the gas phase as the semivolatile ammonium nitrate does (Schaap et al., 2011). According to previous studies, sodium nitrate largely contributes to nitrates in northern and southern Europe (Pakkanen et al., 1999), whereas in western and central Europe ammonium nitrate dominates (Schaap et al., 2002; ten Brink et al., 1997). The reason is enhanced ammonia emission from husbandry and agricultural sources in central and western Europe (Backes et al., 2016a, b).

Coarse sea salt particles have a short lifetime (Grythe et al., 2014), usually depositing close to their source. SSA emitted near the shore will therefore deposit mainly in coastal regions. Its influence on nitrate particle formation is thus expected to be of less importance over central Europe, where nitrate concentrations are high due to land-based sources (Xu and Penner, 2012). However, local circulations can change the vertical distributions of aerosol particles and make the long-range transport of SSA possible by lifting up aerosol from the planetary boundary layer (PBL) into the free troposphere (Chen et al., 2009; Dacre et al., 2007; Lu and Turco,

1994, 1995). The development of PBL or downdraft over the continent could drag the lifted particles downward, back to the surface, later on (Chen et al., 2009). These mechanisms facilitate the long-range transportation of SSA and thereby expand their influences from coast to a broader region.

SSA contributes to the global aerosol burden multiple times more than the anthropogenic aerosol (Grythe et al., 2014). Meanwhile, in terms of global mass concentration, SSA has the largest uncertainty among all aerosols (Grythe et al., 2014). There is still high uncertainty (Grythe et al., 2014; Neumann et al., 2016a, b) in the parameterization scheme (Gong, 2003; Monahan et al., 1986, i.e., GO03) of SSA emissions in the Weather Research and Forecasting/Chemistry model (WRF-Chem). Previous studies (Neumann et al., 2016a, b; Nordmann et al., 2014; Archer-Nicholls et al., 2014; Zhang et al., 2013; Saide et al., 2012, 2013; de Leeuw et al., 2011) showed that the parameterization of Gong (2003) may overestimate the emission of SSA. Saide et al. (2012) demonstrated that GO03 overestimated SSA by a factor of 10 for sub-micron particles and a factor of 2 for super-microns in the southeast Pacific Ocean. Jaeglé et al. (2011) found that GO03 overestimated the coarse-mode SSA mass concentrations by factors of 2–3 at high wind speeds over the cold waters of the South Pacific, North Pacific and North Atlantic oceans. Other studies also indicated an overestimation of SSA emissions in varying degrees (Zhang et al., 2013; de Leeuw et al., 2011; Yang et al., 2011; Neumann et al., 2016b).

The accuracy of an SSA emission scheme is critical for the evaluation of its climate effect (Soares et al., 2016) and its influence on nitrate particle formation. The heterogeneous reaction could amplify the uncertainty of total aerosol burden due to the influence of SSA on secondary aerosol formation (e.g., nitrate; Seinfeld and Pandis, 2006) and, therefore, SSA has an indirect effect on the total aerosol burden. The participation of gaseous pollutants (e.g.,  $\text{NO}_x$ ) is needed for this indirect effect. However,  $\text{NO}_x$  is abundant not only along the coast area but also in some inland regions (Fig. S1 in the Supplement). Therefore, the long-range transport mechanism, as mentioned above, extends the impact of SSA indirect effect on nitrate particle formation to a broader region.

In this study, the long-range transport mechanism and the influence of SSA on the size-resolved nitrate particle formation over the inland region were analyzed in detail in Europe. The model parameterization schemes and the observations are introduced in Sect. 2. The background meteorological conditions are described in Sect. 3.1. Basic physical and chemical properties obtained from model simulations are evaluated in Sect. 3.2. The long-range transport mechanism of SSA and evaluation of SSA emission are shown in Sect. 3.3. In Sect. 3.4, the influence of SSA on the size-segregated nitrate particle simulation is quantitatively analyzed.



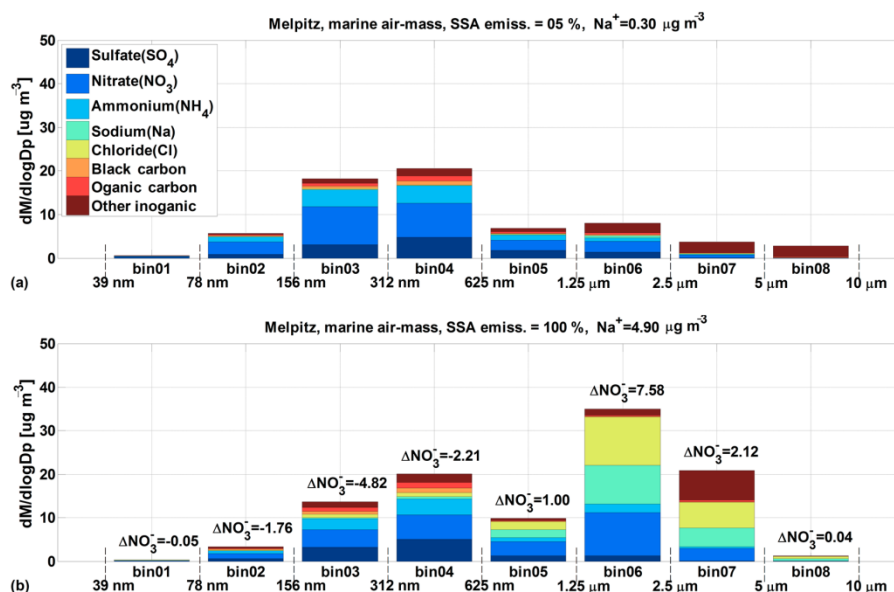


**Figure 1.** WRF-Chem simulation results of particle mass size distribution (PMSD) for each chemical compounds, averaged during marine period at Melpitz: (a) result of the R-CASE; (b) result of the F-CASE. The difference of nitrate PMSD between the R-CASE and the F-CASE for each bin is marked.

## 2 Data and methods

### 2.1 WRF-Chem model v3.5.1

The WRF-Chem model is a fully “online” coupled regional meteorology and air quality model system. It is designed for a broad spectrum of atmospheric research, ranging from several hundred meters to thousands of kilometers in horizontal extent. In addition to the meteorology, aerosols, trace gases and interactive processes are simulated in the model (Grell et al., 2005). The gas-phase atmospheric chemistry was presented by the Carbon-Bond Mechanism version Z (CBMZ), which is coupled with the MOdel for Simulating Aerosol Interactions and Chemistry (MOSAIC; Zaveri et al., 2008).

In order to represent the properties of size-resolved aerosol particles, the fully coupled sectional aerosol module MOSAIC was chosen in this study. In MOSAIC, there are eight discrete size bins (from about 39 nm to 10  $\mu\text{m}$ ; see Fig. 1) of dry particles. Particles are assumed to be internally mixed in each bin (Zaveri et al., 2008). The fine-mode ( $\text{PM}_{10}$ ) and coarse-mode ( $\text{PM}_{1-10}$ ) particle mass concentration can be derived from this eight size bins. The size range of the fifth bin is from 625 to 1250 nm. Assuming that particle mass size distribution was constant in the fifth bin, we divided the particle mass in this size bin into 60 % to the fine-mode ( $\text{PM}_{10}$ , diameter smaller than 1  $\mu\text{m}$ ) and the rest 40 % to the coarse-mode ( $\text{PM}_{1-10}$ , diameter ranging from 1 to 10  $\mu\text{m}$ ). In MOSAIC, sulfate, methane sulfonate, nitrate, chloride, carbonate, ammonium, sodium, calcium, elemental carbon (EC), other inorganic material and organic carbon (OC) are all treated in each bin. Both particle mass concentrations and

particle number concentrations are simulated. Since the segregation of particles in the size bin is based on the dry diameter, there will be no transfer of particles between the bins due to the uptake or loss of water (Zaveri et al., 2008). However, particle growth or shrink due to chemical processes (e.g., chemical reaction, uptake/release of trace gases) and/or physical processes (e.g., coagulation) will result in the transfer of particles between the bins (Chapman et al., 2009). The formation of secondary organic aerosols is not included in the chosen MOSAIC version, but the nucleation of sulfuric acid and water vapor is considered (Zaveri et al., 2008; Fast et al., 2006). The heterogeneous reaction of nitric acid on SSA surface with the production of sodium nitrate is considered in MOSAIC. For the deliquescent aerosol particles at high relative humidity, the ionization equilibrium and the Kelvin effect are also taken into consideration in MOSAIC. More detailed descriptions are given in Zaveri et al. (2008).

In CBMZ, 67 prognostic species and 164 reactions are included with a lumped structure approach (Fast et al., 2006; Zaveri and Peters, 1999). Organic compounds are categorized according to their internal bond types. The rates for photolytic reactions are calculated with the Fast-J scheme (Barnard et al., 2004; Wild et al., 2000).

Dry and wet deposition of particles is treated in the WRF-Chem model (Binkowski and Shankar, 1995). The dry deposition of particles is calculated by a resistance approach, including sublayer resistance, aerodynamic resistance and surface resistance (Grell et al., 2005). The scavenging process of particles was calculated using look-up tables (Nordmann et al., 2014). It is worth mentioning that Saide et al. (2012) found that the WRF-Chem model might overesti-



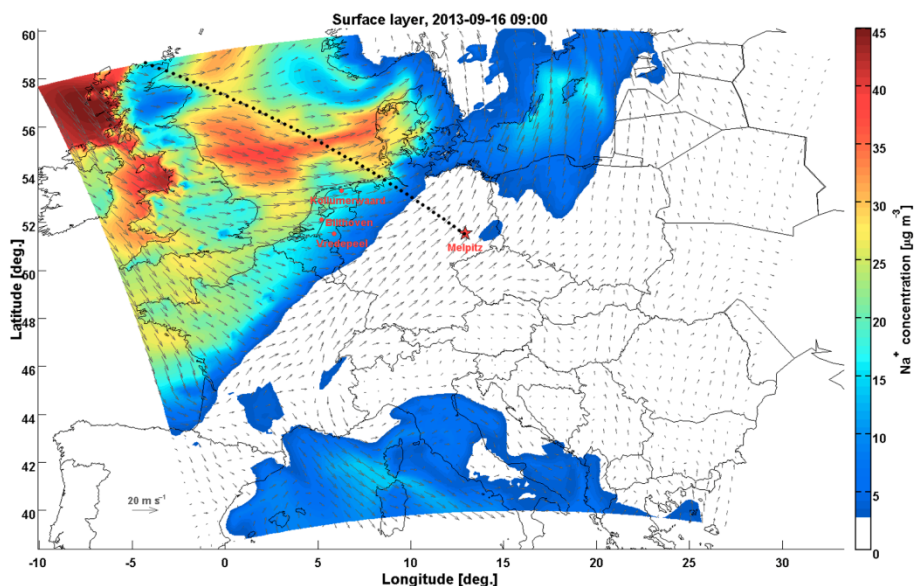


**Figure 2.** The horizontal distribution of surface  $\text{Na}^+$  mass concentration in domain 02 (intermediate domain) at 16 September 2013, 09:00 LT. The grey arrows indicate the wind field. The locations of four EMEP stations (Melpitz, Bilthoven, Kollumerwaard and Vredepeel) are marked. The vertical cross section of dash black line is shown in Fig. 8.

mate wet deposition of particles in the regions where drizzle re-evaporates and releases the particles back into the atmosphere.

The aerosol optical depth (AOD) is online calculated in WRF-Chem model by integrating extinction coefficients over all vertical layers, and details are given in Barnard et al. (2010). In general, an internal mixture of all chemical constituents is assumed. The bulk refractive indices for each particle size bin are obtained by a mixing rule based on volume-weighted averaging. The aerosol particle optical properties, such as particle extinction and scattering cross sections and asymmetry factor, are calculated online by a Mie code described in Ghan et al. (2001).

The simulations were performed for the HOPE (HD(CP)<sup>2</sup> Observational Prototype Experiment, <https://icdc.zmaw.de/hopm.html>) campaign held at the observatory Melpitz (12.93° E, 51.53° N; 86 m a.s.l.) from 10 to 20 September 2013. Three nested domains with 39 vertical layers were set up for the simulated case. The outer domain covers the entirety of Europe, a part of the North Sea and North Africa with a spatial resolution of 54 km, providing the boundary conditions for the inner domains. The intermediate domain (D02, Fig. 2) was centered at Melpitz and covers part of the North Sea, central and southern Europe with a spatial resolution of 18 km. The innermost domain was also centered at Melpitz and had a spatial resolution of 6 km. The spin-up time of the model run was 2 days.

Final (FNL) Operational Global Analysis (<http://rda.ucar.edu/datasets/ds083.2/>) and NCEP sea surface temperature (SST) datasets (<http://polar.ncep.noaa.gov/sst/oper/Welcome.html>), with a spatial resolution of 1° and a tem-

poral resolution of 6 h, were utilized to drive and force the model meteorological field. The chemical initial and boundary conditions were provided by the MOZART-4 global model (<http://www.acom.ucar.edu/wrf-chem/mozart.shtml>) with a spatial resolution of  $1.9^\circ \times 2.5^\circ$  and a temporal resolution of 6 h. More details on simulation about setups and parameterizations are given in Table 1 and Chen et al. (2016).

## 2.2 Emissions

SSA is produced through the evaporation of sea sprays, which were ejected into the atmosphere from the sea surface (Lewis and Schwartz, 2004). Sea spray is emitted by bubble bursting, breaking waves or tearing of wave crests by winds. Strong winds exceeding  $10 \text{ m s}^{-1}$  are needed for the second process (Monahan et al., 1986). The parameterization scheme (GO03) for SSA emission coupled in the WRF-Chem model follows the Gong (2003) scheme. GO03 was developed based on the semi-empirical formulation (Monahan et al., 1986) and field measurements (O'Dowd et al., 1997), including two drop types produced by bursting bubbles (jet drop and film drop). The SSA flux from the ocean to the atmosphere is described as a function of 10 m wind speed and particle radius. Because the Monahan et al. (1986) scheme strongly overestimated the measurements of O'Dowd et al. (1997), Gong (2003) introduced an adjustable parameter to improve the results. He found that a value of 30 produced the best results. Therefore, this value was also used in WRF-Chem simulation; although Gantt et al. (2015) suggested that a value of 8 may be better for the adjustable parameter in some conditions. In order to quantify

Table 1. Configurations of WRF-Chem.

Physics	WRF options
Microphysics	Lin et al. (1983) scheme
Boundary layer	YSU (Hong et al., 2006)
Surface	Rapid Update Cycle (RUC) land surface model
Shortwave radiation	Goddard shortwave (Chou et al., 1998)
Longwave radiation	New Goddard scheme
Cumulus	Grell 3-D
Urban	Three-category UCM
Chemistry and aerosol	Chem options
Aerosol module	MOSAIC with eight bins
Gas-phase mechanism	CBMZ
Photolytic rate	Fast-J photolysis scheme
Sea salt emission	Gong (2003) scheme

the influence of SSA on the nitrate particles formation in this study, a sensitivity study was implemented with only 5 % of SSA emission (R-CASE) and compared with the full (100 %) SSA emission case (F-CASE).

The inventory of anthropogenic emissions ( $\text{PM}_{2.5}$ ,  $\text{PM}_{2.5-10}$ ,  $\text{CO}$ ,  $\text{NO}_x$ ,  $\text{SO}_2$ ,  $\text{NH}_3$  and non-methane volatile organic compounds), as well as temporally resolved emission factors, was provided by TNO for the AQMEII project (Pouliot et al., 2012). The dataset consists of European anthropogenic emissions on  $1/8^\circ \times 1/16^\circ$  long–lat grid for the whole year 2006. The Selected Nomenclature of Air Pollution (SNAP) code was used to categorize different source types (e.g., energy transformation, industrial combustion, road transport, agriculture), with area and point emissions distinguished. More details about the anthropogenic emission inventory are given in related literature (Pouliot et al., 2012; Wolke et al., 2012).

The anthropogenic emissions of EC and OC were taken from the Pan-European Carbonaceous aerosol inventory (Visschedijk and Denier van der Gon, 2008), which was developed in the framework of the European Integrated project on Aerosol Cloud Climate and Air Quality interactions (EU-CAARI; Kulmala et al., 2011). This inventory of EC/OC is also provided by TNO and has the same spatial resolution and SNAP code categorization as the AQMEII one. However, the point sources of EC in Germany were excluded due to their large uncertainties (Chen et al., 2016).

The Fire INventory from NCAR (FINN; Wiedinmyer et al., 2011), with the spatial resolution of 1 km and the temporal resolution of 1 h, was also included. Biogenic emissions were presented by the Model of Emissions of Gases and Aerosols from Nature (MEGAN; Guenther et al., 2006). Dust emissions were not considered due to the large uncertainty of the dust emission scheme in WRF-Chem (Saide et al., 2012). According to quartz-filter-based measurements (quartz-filter type MK360, Munktell/Ahlstorn, Schweden) with high-volume sampler DIGITEL DHA-80 (Walter

RiemerMesstechnik, Germany), dust contributed less than 3 % to the total particle mass concentration in Melpitz during the simulated period.

## 2.3 Observations

Measurements of the HOPE campaign and the European Monitoring and Evaluation Programme (EMEP, <http://www.emep.int>) were adopted to validate the model results. In addition, the modeled atmospheric vertical thermodynamic structures were validated by the radiosonde measurements all over Europe (<http://www.weather.uwyo.edu/upperair/sounding.html>). The Melpitz Observatory is representative of the regional background of central Europe (Spindler et al., 2010, 2012; Poulain et al., 2011; Brüggemann and Spindler, 1999; Birmili et al., 2001). The instruments that measure aerosol physical properties were operated under dry condition, as recommended by WMO-GAW (World Meteorological Organization – Global Atmospheric Watch) and ACTRIS (Aerosols, Clouds, and Trace gases Research InfraStructure Network; Wiedensohler et al., 2012). A dual mobility particle size spectrometer (TROPOS-type dual-SMPS; Birmili et al., 1999) combined with an Aerodynamic Particle Size Spectrometer (TSI APS, model 3321) were employed to measure the particle number size distribution (PNSD) ranging from 5 nm to 10  $\mu\text{m}$  in diameter. PNSDs are made publicly available within the framework of the German Ultrafine Aerosol Network (GUAN; Birmili et al., 2016). Detailed information is given by Chen et al. (2016) and Heintzenberg et al. (1998). A Monitor for Aerosols and Gases in ambient Air (MARGA) system (Schaap et al., 2011; Thomas et al., 2009; ten Brink et al., 2007), continuously monitoring aerosol and gases in ambient air (Metrohm Applikon, Schiedam, the Netherlands), was operated downstream of a  $\text{PM}_{10}$  inlet. This instrument provided 1 h data of secondary inorganic aerosols ( $\text{NH}_4^+$ ,  $\text{NO}_3^-$ ,  $\text{SO}_4^{2-}$ ,  $\text{Cl}^-$ ,  $\text{Ca}^{2+}$ ,  $\text{Mg}^{2+}$  and  $\text{K}^+$ ) and gaseous counterparts ( $\text{NH}_3$ ,

$\text{HNO}_3$ ,  $\text{HNO}_2$ ,  $\text{SO}_2$ ,  $\text{HCl}$ ). The high-volume samplers DIGITEL DHA-80 (Walter Riemer Messtechnik, Germany), with sampling flow of about  $30 \text{ m}^3 \text{ h}^{-1}$ , were used to collect 24 h  $\text{PM}_{10}$  and  $\text{PM}_1$  filter samples simultaneously (Spindler et al., 2013). Information on the coarse-mode ( $\text{PM}_{1-10}$ ) aerosol chemical compositions, such as nitrate and sodium, was obtained from the difference between the results of  $\text{PM}_{10}$  and  $\text{PM}_1$ . Additionally, 24 h filter sampler measurements with  $\text{PM}_{10}$  inlets (EMEP, 2014) at three coastal EMEP stations near the SSA transportation pathway (Bilthoven, Vredepeel and Kollumerwaard; see Fig. 2), which were collected every second day, were obtained from EBAS (<http://ebas.nilu.no/>).

The AERONET (AErosol RObotic NETwork; <http://aeronet.gsfc.nasa.gov/>) dataset over Europe was utilized to validate the AOD simulation. The AERONET AOD was derived from sun photometer measurements of the direct (collimated) solar radiation. The level 2.0 AOD data, with pre- and post-field calibrated, automatically cloud cleared and manually inspected, were used in this study. The AOD at 500 nm wavelength and the Ångström index are directly available in AERONET dataset, and AOD at 550 nm wavelength was derived. More detailed information is given in <http://aeronet.gsfc.nasa.gov/>.

## 2.4 Nitrate partitioning fraction

The participation of SSA changes the partitioning processes of nitrate. In order to quantify this effect, the nitrate partitioning fraction ( $\text{PF}_{\text{nitrate}}$ ) was analyzed for coarse-mode ( $\text{PM}_{1-10}$ ) and fine-mode ( $\text{PM}_1$ ) particles. The definition of  $\text{PF}_{\text{nitrate}}$  for coarse/fine mode is shown in Eq. (1).

$$\text{PF}_{\text{nitrate}}^{\text{coarse/fine}} = \frac{[\text{NO}_3^-]_{\text{coarse/fine}}}{[\text{NO}_3^-]_{\text{coarse/fine}} + [\text{HNO}_3]}, \quad (1)$$

where  $[\text{NO}_3^-]_{\text{coarse/fine}}$  is the coarse/fine-mode particulate nitrate mass concentration and  $[\text{HNO}_3]$  is the nitric acid mass concentration.

## 3 Results and discussion

### 3.1 Meteorology

During the HOPE campaign, continental air masses prevailed over northern Germany before 15 September (Fig. S2). On 16 September, a low-pressure trough began to dominate the North Sea, while a high-pressure ridge dominated over the continent. A frontal system was clearly formed along the coast of the North Sea as could be seen in Fig. S3, accompanied by sharp wind shear and also high convective available potential energy. Evidently, strong vertical mixing occurred in the coastal region, which lifted SSA upward.

Meteorology simulated by WRF with hourly output frequency was evaluated with the near-ground measurements at Melpitz and radiosounding measurements all over Europe.

Both surface meteorology and the vertical structure of meteorological parameters were well captured by the model. Simulated surface temperature, relative humidity, wind speed and wind direction were in good agreement with Melpitz near-ground hourly measurements (Fig. S4), with correlation coefficients ( $R$ ) of 0.94, 0.85, 0.86 and 0.86, respectively, and with mean bias (MB)  $0.38^\circ\text{C}$ , 9.1 %,  $-0.18 \text{ m s}^{-1}$  and  $10.62^\circ$ , respectively. The vertical gradient of potential temperature is an important indicator to measure the stability of the atmosphere. Figure 3 shows the maps of  $R$  values and normalized mean bias (NMB; Balzarini et al., 2015) for potential temperature and wind speed between the simulated and measured vertical profile in PBL (0–3 km). High values of  $R$  and low absolute values of NMB for potential temperature vertical profile were found at all stations, especially near Melpitz, Germany ( $R > 0.85$  and the absolute NMB  $< 2\%$ ), and the coastal region of North Sea ( $R > 0.95$  and the absolute NMB  $< 2\%$ ). The vertical pattern of wind speed was also captured by the model, especially over the North Sea and coastal regions (see Fig. 3b and d). Generally, the  $R$  values were higher than 0.6. In particular, the  $R$  values were higher than 0.9 over the SSA emission source area (the North Sea) and coastal regions, and the absolute NMB values were lower than 5 % over Melpitz region and the coastal region of North Sea. Statistical results of comparisons between the simulation and Melpitz radiosounding measurements are shown in Table S1 in the Supplement. Several examples of vertical profiles are given in Chen et al. (2016). Simulated meteorological vertical structures were in good agreement with measurements in Melpitz. Corresponding, the averaged  $R$  values of vertical profiles were 0.99, 0.96, 0.84 and 0.92 for potential temperature, wind speed, wind direction and water vapor mixing ratio, respectively. Therefore, the WRF simulations reproduced the meteorological conditions well for both ground level and vertical structures.

### 3.2 Aerosol physical and chemical properties

The modeled PNSD and particle mass size distribution (PMSD) at Melpitz were compared with measurements (Fig. 4). Although the simulation of PNSD/PMSD for size bins 01–04 not exactly matched with the measurements, the agreement is in the reasonable range with a factor of  $\sim 2$  (Fig. 4). However, the model significantly overestimated the concentration for the size bins 05–08 (625–10 000 nm) in the F-CASE. Since the meteorology was well reproduced by the model, it can be assumed that the air movement was also reasonably simulated. Therefore, unrealistic high sources of coarse particles might be the cause for the overestimation, which would be discussed in following.

The chemical compositions in  $\text{PM}_{1-10}$  of the DIGITEL measurements and simulation results at Melpitz are displayed in Fig. 5. The simulated particles composition for each size bin is shown in Fig. 1. Sea salt ( $\text{Na}^+$ ) and nitrate mass concentrations in  $\text{PM}_{1-10}$  were overestimated by fac-

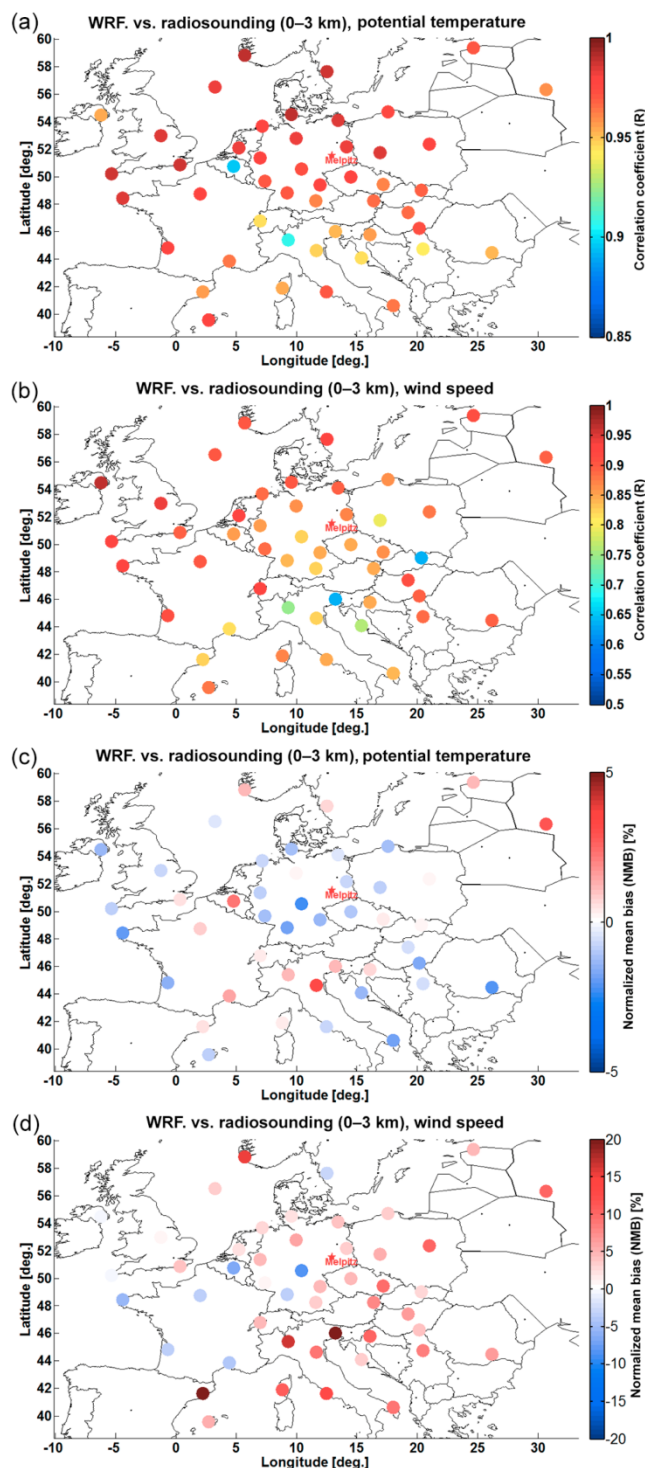


**Figure 3.** Comparison between WRF-Chem model and radiosounding measurements (0–3 km). Melpitz is marked as red star. (a)  $R$  map of potential temperature; (b)  $R$  map of wind speed; (c) NMB map of potential temperature; (d) NMB map of wind speed. Note that the panels have the different color-bar scale.

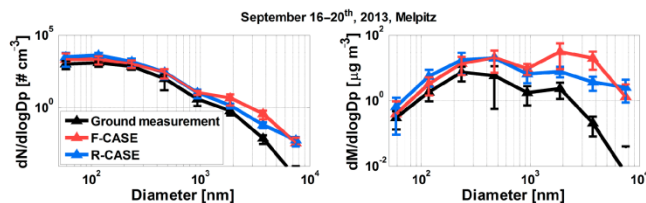


**Figure 4.** Comparison of particle number size distribution (PNSD, left) and particle mass size distribution (PMSD, right) between simulation results (F-CASE and R-CASE) and Melpitz measurements. The results are averaged during 16–20 September 2013; the error bars indicate the upper and lower limits.

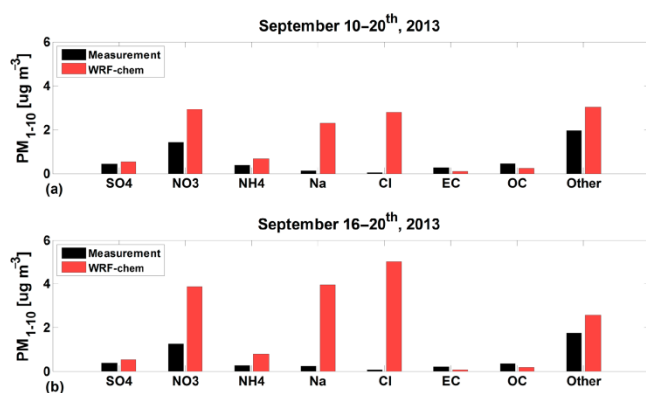


**Figure 5.** Comparison of coarse-mode aerosol ( $PM_{1-10}$ ) chemistry compounds between the F-CASE results and Melpitz measurements: (a) averaged during the HOPE campaign period of 10–20 September 2013; (b) averaged during the marine air mass period of 16–20 September 2013.

tors of  $\sim 18$  and  $\sim 2$ , respectively (see also Tables 2 and 3). Particularly, the overestimation factors could reach up to  $\sim 20$  and 3, respectively, for  $Na^+$  and nitrate mass concentration in the period influenced by marine air masses (starting from 16 September; see Fig. 5b). These results indicated that the overestimations in bins 05–08 were mainly caused by SSA and nitrate.

The column-accumulated aerosol property AOD was evaluated for the R-CASE (Fig. 6a) and the F-CASE (Fig. 6b). Since AERONET AOD data only can be measured during daytime under clear-sky condition, the corresponding simulation results were analyzed.

As shown in Fig. 6a, except the Modena station in Italy, in the R-CASE the spatial distribution of AOD over Europe can be captured by the model in general with correlation coefficient ( $R$ ) value 0.64: the highest AOD value (about 0.15–0.3) over inland region, relatively high value (about 0.07–0.15) over the coastal region of North Sea and Baltic Sea, relatively low value (about 0.03–0.1) over the southern Europe and extremely low value (about 0.01–0.03) over Alps region. And the R-CASE result showed a moderate AOD range (about 0.05–0.12) over the North Sea, which was comparable with



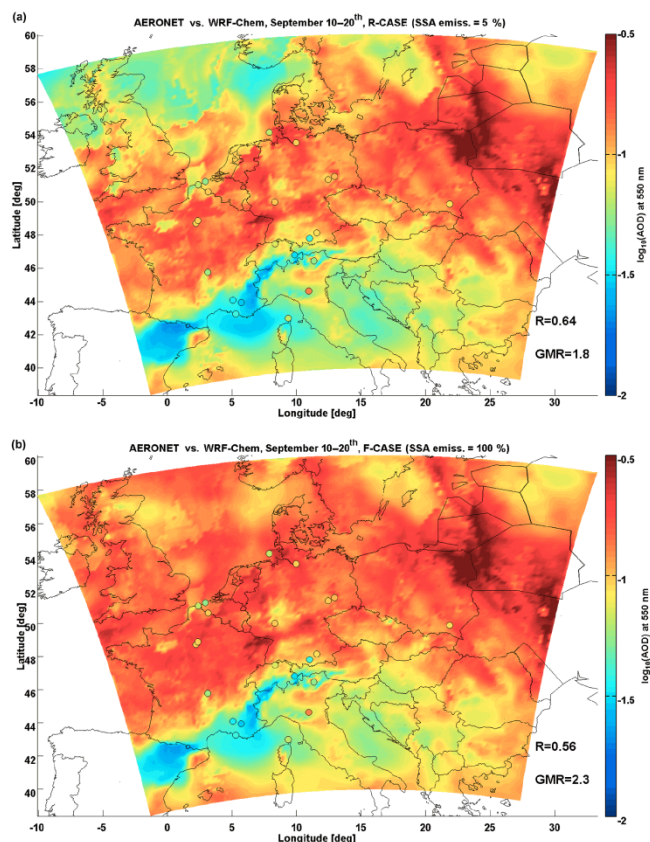


**Figure 6.** Comparisons of AOD at 550 nm wavelength between AERONET measurements and WRF-Chem results, averaged during 10–20 September. The correlation coefficient ( $R$ ) and geometric mean ratio (GMR) are shown in the figure. The plotted WRF-Chem AOD results are divided by 2 in order to see details with AERONET AOD in one color bar. (a) R-CASE result; (b) F-CASE result.

the southern European region (e.g., Italy and Greece). However, the R-CASE result overestimated the AOD in general with a geometric mean ratio (GMR) value 1.8, which could be resulting from the overestimation of nitrate particles. The nitrate particle mass concentrations in  $\text{PM}_{10}$  were overestimated by a factor of  $\sim 5$  in the R-CASE at Melpitz (see Table 2). Although some shortcomings can be identified, the overall performance of AOD simulation is satisfactory and in line with previous studies (e.g., Banzhaf et al., 2013; Li et al., 2013).

The spatial distribution of AOD was less matched between modeled result and AERONET AOD measurements in the F-CASE (Fig. 6b). The  $R$  value reduced to 0.56, with much higher overestimation of AOD and GMR increased to 2.3. The modeled AOD over the North Sea is significantly increased to an unreasonable value, which was comparable with the central Europe. This is because GO03 overestimated SSA emission over the North Sea. The detailed evaluation of SSA mass concentration is given in the next Sect. 3.3.

### 3.3 Sea salt emission and the transport

For the sea salt event studied here, the abrupt SSA emission event happened over the North Sea. And SSA mass concentration was overall overestimated in the coastal and continental regions during 16–20 September, as shown in Fig. 7. Here we used sodium ( $\text{Na}^+$ ) as an indicator of SSA (Neumann et al., 2016a; Gustafsson and Franzén, 2000), since chloride ( $\text{Cl}^-$ ) could be depleted due to nitrate partitioning (Schaap et al., 2011; Seinfeld and Pandis, 2006). Marine air masses first arrived at the three coastal stations (Bilthoven, Vredepeel and Kollumerwaard; see Fig. 2) and then went further inland along with the low-pressure trough system. The  $\text{Na}^+$  concentration peaked on 16 September for the coastal stations and about 1 day later for Melpitz (Fig. 7).

As shown in Fig. 7, the day-to-day temporal pattern of  $\text{Na}^+$  concentrations can be captured by the model, with the correlation coefficient ( $R$ ) of 0.95, 0.81, 0.92 and 0.89 for Melpitz, Bilthoven, Kollumerwaard and Vredepeel, respectively. The transport mechanism was well captured by the model in general. However, SSA mass concentrations were overestimated by about 20 times in Melpitz and around 9, 13 and 8 times, respectively, for the coastal stations of Bilthoven, Kollumerwaard and Vredepeel. This implies that GO03 might overestimate SSA emission by a factor of 8–20. The overestimation is consistent with previous modeling studies using WRF-Chem: in the southeastern Pacific ocean (Saide et al., 2012), in the coast region of California, USA (Saide et al., 2013), over Europe (Nordmann et al., 2014; Zhang et al., 2013; Tsyro et al., 2011; Manders et al., 2010) and over the cold waters of the South Pacific, North Pacific and North Atlantic oceans (Jaeglé et al., 2011). Similarly, Neumann et al. (2016b) found overestimations during winter and attributed the reason to the missing of SST influence in GO03. GO03 describes SSA emission as a function of wind speed at 10 m above the ground. The uncertainties of this scheme may be attributable to the lack of parameters, such as sea surface temperature (Neumann et al., 2016b; Soares et al., 2016; Grythe et al., 2014; Jaeglé et al., 2011; Sofiev et al., 2011), salinity (Soares et al., 2016; Neumann et al., 2016a; Sofiev et al., 2011) and wave data (Ovadnevaite et al., 2014; Jaeglé et al., 2011). The lack of proper droplet generation processes from GO03 might be another source of the uncertainties (Neumann et al., 2016a).

After been emitted over the North Sea, the SSA might experience chemical degradation (such as  $\text{Cl}^-$  depletion) and dry/wet deposition when transported over continental area. Generally, SSA is mostly in coarse mode with lifetime shorter than 2 days in the continental boundary layer and reaching about 1 week in free troposphere (Croft et al., 2014; Petzold and Kärcher, 2012; Jaenicke, 1980). According to the simulation results, the component of the 10 m wind vector that is directed from the coast to Melpitz shows a wind speed in the range of  $2\text{--}3\text{ m s}^{-1}$  (Fig. 2). It would therefore take about 1.5–2 days for SSA to be transported to Melpitz

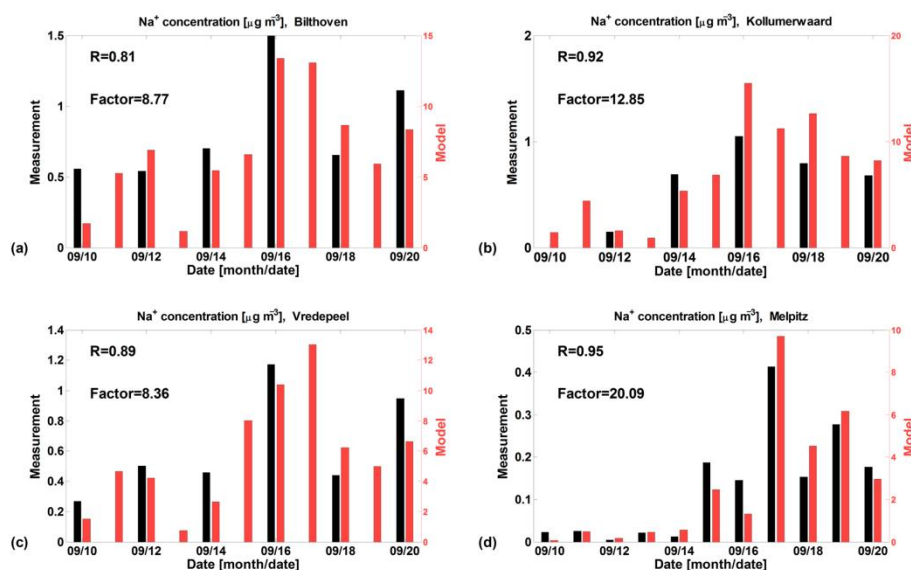


**Figure 7.** Comparison of  $\text{Na}^+$  mass concentration in  $\text{PM}_{10}$  between the filter sampler measurements (left y axis) in four EMEP stations and the F-CASE results (right y axis). (a) Bilthoven; (b) Kollumerwaard; (c) Vredepeel; (d) Melpitz. The locations of the stations are shown in Fig. 2.

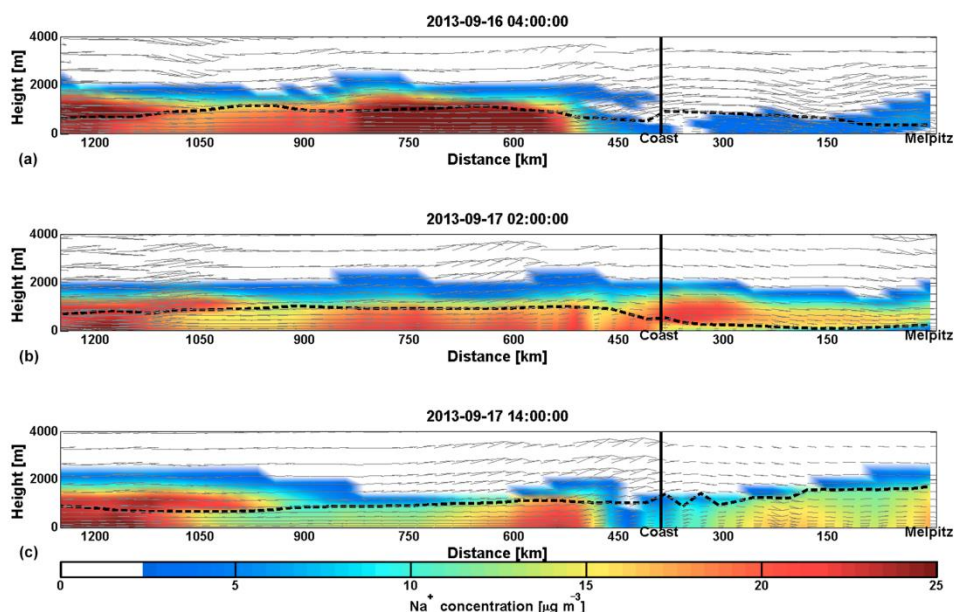


**Figure 8.** WRF-Chem result of the sea salt ( $\text{Na}^+$ ) concentration on the vertical cross section, which is shown by the black dash line in Fig. 2. The locations of Melpitz and coast (black line) are marked. The grey arrows indicate the wind field, and the black dash line indicates the planetary boundary layer (PBL) height. (a) 16 September 2013, 04:00 LT; (b) 17 September 2013, 02:00 LT; (c) 17 September 2013, 14:00 LT.

( $\sim 400$  km distant to the coast). The result (Fig. S5) from the Deposition-Lifetime Concept Model (Chen et al., 2016; Croft et al., 2014) indicates that on average only 10–35 % of the emitted SSA could be transported to Melpitz through the surface pathway, whereas, according to the observed SSA peaks (Fig. 7), about 30–40 % of the initial SSA mass at

coastal stations was actually transported to the inland station of Melpitz. The observed transport efficiency was about 1.6 times of the expected value. The transport mechanism of the SSA to the inland (Melpitz) will be discussed in the following with the aid of a model simulation, despite the overestimation in the WRF-Chem SSA emission scheme. As demon-

## Results and Discussion

12090

Y. Chen et al.: Influence of sea salt on size-segregated nitrate simulation

strated in Fig. 8, during nighttime the warmer sea surface resulted in a higher PBL (black dash lines in Fig. 8) above the sea than over the continent (Dacre et al., 2007; Lu and Turco, 1994, 1995). Due to the difference of thermodynamic structure between continental and marine area, there is often a sharp gradient of PBL height over the coastal region (Fig. 8), which could serve as an “aloft bridge” connecting the marine PBL and continental free troposphere (Dacre et al., 2007; Lu and Turco, 1994, 1995). In the early morning of 16 September, SSA was emitted into the surface layer of the North Sea and lifted upward by convective mixing and turbulence (Fig. 8a). According to the simulation result (Fig. 8), about 70 % of SSA penetrated the marine PBL and was injected into continent free troposphere through the “aloft bridge”. In the free troposphere, SSA has a much longer life time and faster transportation than in the PBL. Therefore, about 70–85 % of SSA (Fig. S5) could have been carried further towards the inland in free troposphere and arrive at the Melpitz region in the early morning of 17 September (Fig. 8b). Then the downward draft resulted from high-pressure ridge and the turbulent mixing after sunrise (Fig. 8b and c) brought the lofted SSA back into the surface layer. The  $\text{Na}^+$  mass concentration at Melpitz surface increased from  $\sim 7 \mu\text{g m}^{-3}$  (Fig. 8b) to  $\sim 15 \mu\text{g m}^{-3}$  (Fig. 8c). About 35 % of the lofted SSA contributed to the increase of the  $\text{Na}^+$  surface concentration. This result is in agreement with the previous study (Chen et al., 2009), which reported  $\sim 30$  % of elevated pollutants contributed to the increase of surface pollutants concentration in Beijing due to the turbulent mixing after sunrise.

### 3.4 Influence of sea salt on nitrate simulation

As discussed above, the overproduction of SSA by GO03 will lead to an 8–20 times overestimation of the primary sea salt mass concentration. However, its influence is not only on the aerosol burden of SSA itself but also on promoting the formation of secondary inorganic particle mass, such as nitrate (Neumann et al., 2016a; Seinfeld and Pandis, 2006). The gas-phase nitric acid ( $\text{HNO}_3$ ) can be produced with the oxidation of  $\text{NO}_x$ .  $\text{HNO}_3$  undergoes a partitioning process between gas phase and liquid particle phase via condensation. The condensed  $\text{HNO}_3$  deprotonates to  $\text{NO}_3^-$ . In MO-SAIC aerosol scheme (Zaveri et al., 2008), one partitioning process between gas phase and solid phase is the equilibrium reaction with ammonia ( $\text{NH}_3$ ) and the formation of ammonium nitrate. The other one is the irreversible process with SSA ( $\text{NaCl}$ ) and the formation of sodium nitrate with depletion of chloride. Ammonium nitrate is semivolatile and can turn back to the gas-phase precursors, while sodium nitrate is thermodynamically stable (Schaap et al., 2011). The presences of SSA might facilitate the condensation process of nitrate.

Overall, nitrate in the size range of  $\text{PM}_{10}$  was overestimated by the model, with an average factor of  $\sim 5$  (Table 2). Comparisons of nitrate and its precursors between the simu-

**Table 2.** Comparison of WRF-Chem results with Melpitz near-ground filter measurements. The factors (simulation/measurement) and correlation coefficient ( $R$ ) are shown for the F-CASE and the R-CASE, respectively.

	F-CASE factor	R-CASE factor	F-CASE $R$	R-CASE $R$
$\text{NO}_x$	0.98	0.98	0.73	0.73
Total ammonia	2.12	2.21	0.59	0.60
Nitrate in $\text{PM}_{10}$	5.09	4.97	0.76	0.72
Nitrate in $\text{PM}_{1-10}$	2.10	0.73	0.31	0.33

**Table 3.** Comparison of WRF-Chem modeled  $\text{Na}^+$  mass concentration results with four EMEP stations measurements. The factors (simulation/measurement) and correlation coefficient ( $R$ ) are shown for the F-CASE and the R-CASE, respectively.

	F-CASE factor	R-CASE factor	F-CASE $R$	R-CASE $R$
Melpitz ( $\text{PM}_{10}$ )	20.10	1.25	0.95	0.94
Melpitz ( $\text{PM}_{1-10}$ )	18.10	1.09	0.94	0.94
Bilthoven ( $\text{PM}_{10}$ )	8.77	0.54	0.81	0.81
Kollumerwaard ( $\text{PM}_{10}$ )	12.85	0.74	0.92	0.92
Vredepeel ( $\text{PM}_{10}$ )	8.36	0.53	0.89	0.89

lation results and the MARGA measurements at Melpitz are shown in Fig. 9. Assuming that the chemical mechanism is correctly described in the model, the same concentration of gaseous precursors ( $\text{NO}_x$  and ammonia) should produce the same concentration of nitrate in the model and observation. The location of the data dots (Fig. 9a) may be shifted due to the uncertainty of precursors emissions, but the nitrate mass concentration is always expected to be consistent with the observed concentration in Fig. 9b when they have the same mass concentration of precursors. However, even with the same mass concentrations of precursors, the simulated nitrate mass concentrations (Fig. 9a) were still significantly higher than the observed ones (Fig. 9b). This indicated that in addition to an overestimation caused by overestimated  $\text{NH}_3$  (see also Table 2), improper chemical pathway in the model also contributed to the nitrate overestimation.

In order to quantify the influence of  $\text{NaCl}$  on the nitrate particles formation, the comparisons between results of the F-CASE and the R-CASE are shown in Tables 2 and 3. The simulated  $\text{NO}_x$  concentrations were in good agreements with measurements, but total ammonia was overestimated by a factor of  $\sim 2$  in both cases (Table 2), which may stem from the uncertainty of ammonia emission inventory. The prediction of SSA ( $\text{Na}^+$ ) was significantly improved after reducing SSA emission, with a factor of 1.09 and  $R$  value of 0.94 for size range of 1–10  $\mu\text{m}$  at Melpitz (Table 3). Also, results at coastal stations were not overestimated in the R-CASE. However,  $\text{NO}_x$  and total ammonia concentration results of the R-CASE did not show significant changes (Table 2). The factor for nitrate between model and measurement at Melpitz



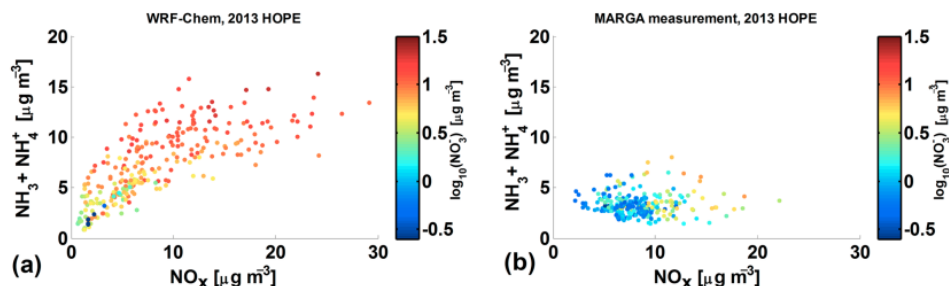


**Figure 9.** Relationship between nitrate, total ammonia and  $\text{NO}_x$  during 10–20 September 2013 at Melpitz. The color indicates the nitrate mass concentration in logarithmic scale. (a) WRF-Chem model results; (b) MARGA measurement results.

pitz dramatically decreased from 2.1 to 0.73 in coarse mode ( $\text{PM}_{1-10}$ , see Table 2), thus changing from overestimation to underestimation. Therefore, the difference of nitrate between the F-CASE and the R-CASE should mainly arise from the influence of the SSA concentrations.

The comparisons of the frequency distribution of  $\text{PF}_{\text{nitrate}}$  between the F-CASE and the R-CASE are shown in Fig. 10, respectively, for fine-mode ( $\text{PM}_1$ ) and coarse-mode ( $\text{PM}_{1-10}$ ) particles during the marine period ( $[\text{Na}^+] > 1.8 \mu\text{g m}^{-3}$  in the F-CASE, 105 time steps in total). Since the MARGA measurements were only available for the size range of  $\text{PM}_{10}$ ,  $\text{PF}_{\text{nitrate}}$  derived from MARGA observations should not be directly compared with the simulated one. Additionally, we need to keep in mind that high uncertainties exist in the  $\text{HNO}_3$  measurements due to its sticky property (Rumsey et al., 2014; Neuman et al., 1999), which brings further difficulty into the comparison between measurements and simulation. In this study, the R-CASE had a much more reasonable SSA prediction (within a factor of  $\sim 1$  at Melpitz) than the F-CASE; therefore, the simulated values of  $\text{PF}_{\text{nitrate}}$  from the R-CASE were used as the basic simulation. In 17 September at Melpitz, about 88 % SSA mass was concentrated in the coarse-mode particles in both simulation and filter measurement results. Since coarse particles have a higher dry deposition velocity than fine particle one, we can expect that the SSA emissions consisted of more than 88 % of coarse particles. The  $\text{PF}_{\text{nitrate}}$  results for coarse-mode particles should be more representative for the influence of SSA on particulate nitrate formation, also more sensitive to the change of the SSA emission. As shown in Fig. 10a and b, the median value of coarse-mode  $\text{PF}_{\text{nitrate}}$  in the R-CASE was about 0.75, with the distribution broadly spread in the range of  $\sim 0.2$  to 1, whereas in the F-CASE the median value increased to 0.96 with a much narrowed distribution. In this study, the ammonium mass concentration was quite similar in both R-CASE and F-CASE; SSA was highly overestimated by the model in the F-CASE and the overestimated amount was transported to the surface layer at Melpitz; and the coarse-mode nitrate partitioning fraction increased from 0.75 (R-CASE) to 0.96 (F-CASE). These indicated that the participation of SSA in the nitrate partitioning process facili-

tated the coarse-mode nitrate particle formation, which accumulated as the thermodynamic stable sodium nitrate. About 140 % overestimation of the coarse-mode nitrate was a result of this (Table 2).

For the fine-mode nitrate, the  $\text{PF}_{\text{nitrate}}$  of fine mode was insensitive to SSA emission (Fig. 10). Although the fine-mode  $\text{PF}_{\text{nitrate}}$  revealed no significant difference between the R-CASE and the F-CASE simulations (Fig. 10c and d), the fine-mode nitrate mass concentration was reduced by  $\sim 20\%$  in the F-CASE due to the consumption of precursor by the coarse-mode nitrate formation. Therefore nitrate particle mass moved from fine mode to coarse mode and the total nitrate mass concentrations in size range of  $\text{PM}_{10}$  were similar between the R-CASE and the F-CASE (Table 2).

In order to see the influence of SSA on nitrate PMSD in a clearer way, the simulated PMSD during marine period at Melpitz was shown in Fig. 1. It clearly shows that the nitrate PMSD decreased in the smaller size bins (bins 01–04) but increased in the larger size bins (bins 05–08). In the F-CASE (Fig. 1b) when the overestimated SSA participated in nitrate particle formation, nitrate particle moved from fine mode to coarse mode compared with the R-CASE (see also Fig. 4).

In general and as illustrated in Fig. 11, the overestimation of SSA emission scheme has a significant influence on the particulate nitrate simulation in both the coarse mode (directly) and the fine mode (indirectly). In this case study, the overestimation of SSA in the F-CASE made the coarse-mode nitrate partitioning fraction increased from 0.75 to 0.96. The increase of consumption of precursor in the coarse-mode nitrate particle formation might slow down the formation of nitrate particle in the fine mode. The PMSD was thus altered due to these influences.

## 4 Conclusions

In order to investigate atmospheric SSA emission and transport over central Europe and its influence on particulate nitrate prediction, the WRF-Chem model was used to simulate the aerosol physical and chemical aerosol properties during the HOPE campaign, 10–20 September 2013, at Melpitz. The



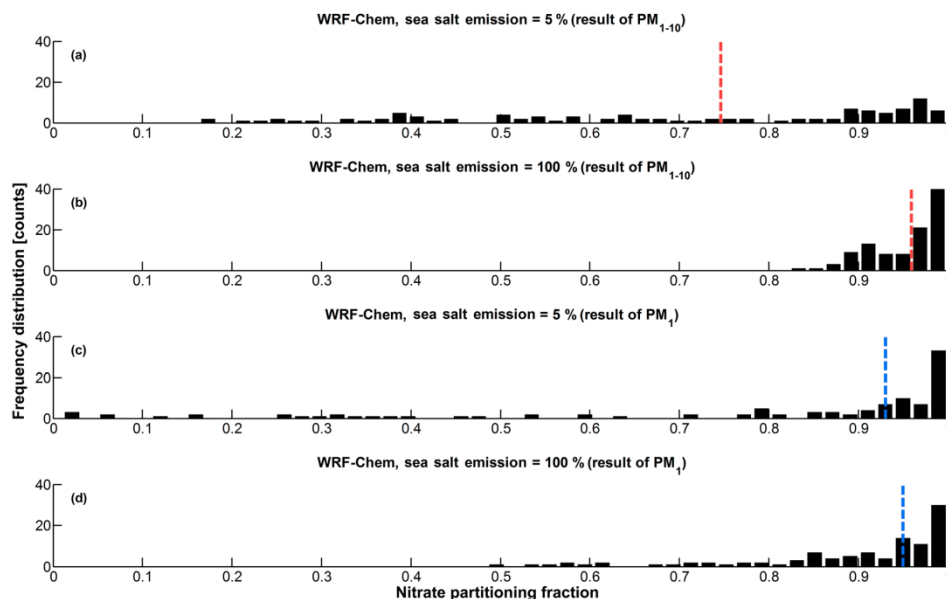


**Figure 10.** WRF-Chem results of the frequency distribution of PF<sub>nitrate</sub> at Melpitz. The results were analyzed during the marine period ( $[\text{Na}^+] > 1.8 \mu\text{g m}^{-3}$  in the F-CASE). The dash lines (coarse mode: red; fine mode: blue) indicate the median value (with 50 % probability in both sides). (a) R-CASE result of the size range  $\text{PM}_{1-10}$ ; (b) F-CASE result of the size range  $\text{PM}_{1-10}$ ; (c) R-CASE result of the size range  $\text{PM}_1$ ; (d) F-CASE result of the size range  $\text{PM}_1$ .

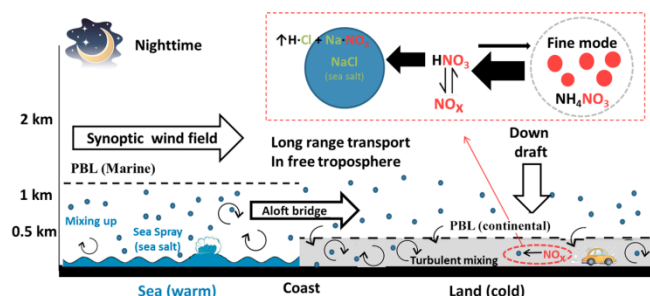


**Figure 11.** Schematic of sea salt transportation and its influence on nitrate particle formation.

simulated meteorological variables, vertical thermal stratification and near-ground level particle number size distribution were validated by observations. The ground meteorology and vertical thermal stratification were well captured by the model. Coarse-mode particles were, however, significantly overestimated both in number and mass due to an overestimate in SSA emissions caused by the current SSA emission scheme.

SSA mass concentrations were evaluated at four ground-based EMEP stations, including one continental inland station (Melpitz) and three coastal stations (Bilthoven, Kollumerwaard and Vredepeel). The day-to-day variations of SSA mass concentrations were well captured by the model despite an overestimation of SSA concentrations by a factor of 8–20 due to the shortcoming of the WRF-Chem SSA emis-

sion scheme. In addition to the wind speed at 10 m above the ground, more parameters, such as sea surface temperature, salinity and wave data, might be needed for consideration in the SSA emission scheme to reduce its overestimation. With reduction of SSA emission to 10 %, the simulated AOD results showed a better agreement with the AERONET AOD measurement over Europe. The correlation coefficient ( $R$ ) between AOD simulation and measurement increased from 0.56 to 0.64, and the GMR decreased from 2.3 to 1.8.

Transport of SSA from the North Sea into central Europe was analyzed in detail. Due to different nighttime PBL structure over the continental and marine region, an “aloft bridge” between the marine PBL and continental free troposphere was formed over the coastal area. The overestimated SSA released from the North Sea was mixed up and injected into the continental free troposphere and participated in the long-range transport because the lifetime of aerosols can be about 5 times longer in free troposphere than in the PBL. This injected SSA was transported over Melpitz and later on mixed downward to the surface by the downdraft and the turbulence of fully developed PBL on 17 September 2013. The overestimation of SSA emission, combined with the “aloft bridge” transport process, led the SSA overestimated by a factor of 20 at Melpitz.

The overestimation in SSA emissions did not only influence the release of primary SSA itself but also led to significant uncertainties in the particulate nitrate prediction. As described in Fig. 11, nitrate and precursors can be locked in the particulate phase as thermodynamically stable sodium ni-

trate, which is produced from the heterogeneous reaction on SSA surface. Since most of the SSA was emitted as coarse-mode particles, nitrate partitioning fraction of coarse mode was overestimated by  $\sim 20\%$  when the SSA mass concentration was highly overestimated. This contributed to an overestimation of the coarse-mode particulate nitrate by around 140%. Meanwhile, the nitrate partitioning fraction of fine mode was insensitive to the SSA emission. However, the increased consumption of the gas-phase precursor, caused by the coarse-mode nitrate formation with the participation of SSA, may reduce the formation of fine-mode nitrate.

In this work, the atmospheric transport of SSA from the North Sea to central Europe was demonstrated in detail. The emission of SSA was evaluated and the influence of SSA on particulate nitrate prediction was quantitatively analyzed. The overestimation of SSA emission will affect not only primary aerosol concentrations but also the formation of secondary inorganic particle mass like nitrates. It is anticipated to change heterogeneous reactions and the conversion pathways from gas-phase precursors to particulate phase. Such changes will also alter the physical and chemical aerosol properties, e.g., particle mass size distribution and hygroscopicity. A nitrate coating on a SSA surface may reduce the hygroscopicity of coarse-mode particles, and the re-distribution of nitrate from fine mode to coarse mode may increase its deposition rate. Furthermore, the direct and indirect radiative forcing evaluation will also be influenced, since the optical properties (e.g., single scattering albedo) are strongly related to the size of particles. All these influences are crucial for climate change evaluation. Due to the “aloft bridge” transport mechanism, as described in this paper, the influences of SSA are not only confined to the coastal region but also extended to a broader region reaching as far as 400 km from coast.

## 5 Data availability

The data shown in the graphs are available as part of the Supplement related to this article. In case further additional information is required about the published data, please contact the first author at chen@tropos.de.

**The Supplement related to this article is available online at doi:10.5194/acp-16-12081-2016-supplement.**

**Acknowledgements.** Continuous aerosol measurements at Melpitz were supported by the German Federal Environment Ministry (BMU) grant F&E 371143232 (German title: “Trendanalysen gesundheitsgefährdender Fein- und Ultrafeinstaubfraktionen unter Nutzung der im German Ultrafine Aerosol Network (GUAN) ermittelten Immissionsdaten durch Fortführung und Interpretation der Messreihen”), 2012–2014. Particle number size distributions

at Melpitz can be obtained online through the German Ultrafine Aerosol Network (<https://doi.org/10.5072/guan>). The HOPE campaign was funded by the German Research Ministry under the project number 01LK1212 C. We would also like to thank Albert Ansmann (TROPOS, Germany) for useful suggestions on AERONET AOD data.

Edited by: A. Laaksonen

Reviewed by: three anonymous referees

## References

- Archer-Nicholls, S., Lowe, D., Utembe, S., Allan, J., Zaveri, R. A., Fast, J. D., Hodnebrog, Ø., Denier van der Gon, H., and McFiggans, G.: Gaseous chemistry and aerosol mechanism developments for version 3.5.1 of the online regional model, WRF-Chem, *Geosci. Model Dev.*, 7, 2557–2579, doi:10.5194/gmd-7-2557-2014, 2014.
- Athanasopoulou, E., Tombrou, M., Pandis, S. N., and Russell, A. G.: The role of sea-salt emissions and heterogeneous chemistry in the air quality of polluted coastal areas, *Atmos. Chem. Phys.*, 8, 5755–5769, doi:10.5194/acp-8-5755-2008, 2008.
- Barnard, J. C., Chapman, E. G., Fast, J. D., Schmelzer, J. R., Slusser, J. R., and Shetter, R. E.: An evaluation of the FAST-J photolysis algorithm for predicting nitrogen dioxide photolysis rates under clear and cloudy sky conditions, *Atmos. Environ.*, 38, 3393–3403, doi:10.1016/j.atmosenv.2004.03.034, 2004.
- Barnard, J. C., Fast, J. D., Parcdes-Miranda, G., Arnott, W. P., and Laskin, A.: Technical Note: Evaluation of the WRF-Chem “Aerosol Chemical to Aerosol Optical Properties” Module using data from the MILAGRO campaign, *Atmos. Chem. Phys.*, 10, 7325–7340, doi:10.5194/acp-10-7325-2010, 2010.
- Backes, A., Aulinger, A., Bieser, J., Matthias, V., and Quante, M.: Ammonia emissions in Europe, part I: Development of a dynamical ammonia emission inventory, *Atmos. Environ.*, 131, 55–66, doi:10.1016/j.atmosenv.2016.01.041, 2016a.
- Backes, A. M., Aulinger, A., Bieser, J., Matthias, V., and Quante, M.: Ammonia emissions in Europe, part II: How ammonia emission abatement strategies affect secondary aerosols, *Atmos. Environ.*, 126, 153–161, doi:10.1016/j.atmosenv.2015.11.039, 2016b.
- Balzarini, A., Pirovano, G., Honzak, L., Žabkar, R., Curci, G., Forkel, R., Hirtl, M., San José, R., Tuccella, P., and Grell, G. A.: WRF-Chem model sensitivity to chemical mechanisms choice in reconstructing aerosol optical properties, *Atmos. Environ.*, 115, 604–619, doi:10.1016/j.atmosenv.2014.12.033, 2015.
- Banzhaf, S., Schaap, M., Wichink Kruit, R. J., Denier van der Gon, H. A. C., Stern, R., and Bultjes, P. J. H.: Impact of emission changes on secondary inorganic aerosol episodes across Germany, *Atmos. Chem. Phys.*, 13, 11675–11693, doi:10.5194/acp-13-11675-2013, 2013.
- Binkowski, F. S. and Shankar, U.: The Regional Particulate Matter Model: I. Model description and preliminary results, *J. Geophys. Res.-Atmos.*, 100, 26191–26209, doi:10.1029/95JD02093, 1995.
- Birmili, W., Stratmann, F., and Wiedensohler, A.: Design of a DMA-based size spectrometer for a large particle size range and stable operation, *J. Aerosol Sci.*, 30, 549–553, doi:10.1016/S0021-8502(98)00047-0, 1999.

- Birmili, W., Wiedensohler, A., Heintzenberg, J., and Lehmann, K.: Atmospheric particle number size distribution in central Europe: Statistical relations to air masses and meteorology, *J. Geophys. Res.*, 106, 32005–32018, 2001.
- Birmili, W., Weinhold, K., Rasch, F., Sonntag, A., Sun, J., Merkel, M., Wiedensohler, A., Bastian, S., Schladitz, A., Löschau, G., Cyrys, J., Pitz, M., Gu, J., Kusch, T., Flentje, H., Quass, U., Kaminski, H., Kuhlbusch, T. A. J., Meinhardt, F., Schwerin, A., Bath, O., Ries, L., Wirtz, K., and Fiebig, M.: Long-term observations of tropospheric particle number size distributions and equivalent black carbon mass concentrations in the German Ultrafine Aerosol Network (GUAN), *Earth Syst. Sci. Data*, 8, 355–382, doi:10.5194/essd-8-355-2016, 2016.
- Brüggemann, E. and Spindler, G.: Wet and dry deposition of sulphur at the site Melpitz in East Germany, *Water Air Soil Pollut.*, 109, 81–99, 1999.
- Chapman, E. G., Gustafson Jr., W. I., Easter, R. C., Barnard, J. C., Ghan, S. J., Pckour, M. S., and Fast, J. D.: Coupling aerosol-cloud-radiative processes in the WRF-Chem model: Investigating the radiative impact of elevated point sources, *Atmos. Chem. Phys.*, 9, 945–964, doi:10.5194/acp-9-945-2009, 2009.
- Chen, Y., Zhao, C., Zhang, Q., Deng, Z. Z., Huang, M. Y., and Ma, X. C.: Aircraft study of mountain chimney effect of Beijing, China, *J. Geophys. Res.-Atmos.*, 114, D08306, doi:10.1029/2008JD010610, 2009.
- Chen, Y., Cheng, Y.-F., Nordmann, S., Birmili, W., Denier van der Gon, H. A. C., Ma, N., Wolke, R., Wehner, B., Sun, J., Spindler, G., Mu, Q., Pöschl, U., Su, H., and Wiedensohler, A.: Evaluation of the size segregation of elemental carbon (EC) emission in Europe: influence on the simulation of EC long-range transportation, *Atmos. Chem. Phys.*, 16, 1823–1835, doi:10.5194/acp-16-1823-2016, 2016.
- Chou, M., Suarez, M., Ho, C., Yan, M., and Lee, K.: Parameterizations for Cloud Overlapping and Shortwave Single-Scattering Properties for Use in General Circulation and Cloud Ensemble Models, *J. Climate*, 11, 202–214, 1998.
- Croft, B., Pierce, J. R., and Martin, R. V.: Interpreting aerosol lifetimes using the GEOS-Chem model and constraints from radionuclide measurements, *Atmos. Chem. Phys.*, 14, 4313–4325, doi:10.5194/acp-14-4313-2014, 2014.
- Dacre, H. F., Gray, S. L., and Belcher, S. E.: A case study of boundary layer ventilation by convection and coastal processes, *J. Geophys. Res.-Atmos.*, 112, D17106, doi:10.1029/2006JD007984, 2007.
- de Leeuw, G., Neele, F. P., Hill, M., Smith, M. H., and Vignati, E.: Production of sea spray aerosol in the surf zone, *J. Geophys. Res.-Atmos.*, 105, 29397–29409, doi:10.1029/2000JD900549, 2000.
- de Leeuw, G., Andreas, E. L., Angelova, M. D., Fairall, C. W., Lewis, E. R., O'Dowd, C., Schulz, M., and Schwartz, S. E.: Production flux of sea spray aerosol, *Rev. Geophys.*, 49, RG2001, doi:10.1029/2010RG000349, 2011.
- EMEP: EMEP Manual for Sampling and Analysis, EMEP, available at: <http://www.nilu.no/projects/ccc/manual/index.html> (last access: 30 November 2015), 2014.
- Fast, J. D., Gustafson, W. I., Easter, R. C., Zaveri, R. A., Barnard, J. C., Chapman, E. G., Grell, G. A., and Peckham, S. E.: Evolution of ozone, particulates, and aerosol direct radiative forcing in the vicinity of Houston using a fully coupled meteorology-chemistry-aerosol model, *J. Geophys. Res.-Atmos.*, 111, D21305, doi:10.1029/2005JD006721, 2006.
- Gantt, B., Kelly, J. T., and Bash, J. O.: Updating sea spray aerosol emissions in the Community Multiscale Air Quality (CMAQ) model version 5.0.2, *Geosci. Model Dev.*, 8, 3733–3746, doi:10.5194/gmd-8-3733-2015, 2015.
- Ghan, S., Laulainen, N., Easter, R., Wagoner, R., Nemesure, S., Chapman, E., Zhang, Y., and Leung, R.: Evaluation of aerosol direct radiative forcing in MIRAGE, *J. Geophys. Res.*, 106, 5295–5316, 2001.
- Gong, S. L.: A parameterization of sea-salt aerosol source function for sub- and super-micron particles, *Global Biogeochem. Cy.*, 17, 1097, doi:10.1029/2003GB002079, 2003.
- Grell, G. A., Peckham, S. E., Schmitz, R., McKeen, S. A., Frost, G., Skamarock, W. C., and Eder, B.: Fully coupled “online” chemistry within the WRF model, *Atmos. Environ.*, 39, 6957–6975, doi:10.1016/j.atmosenv.2005.04.027, 2005.
- Grythe, H., Ström, J., Krejci, R., Quinn, P., and Stohl, A.: A review of sea-spray aerosol source functions using a large global set of sea salt aerosol concentration measurements, *Atmos. Chem. Phys.*, 14, 1277–1297, doi:10.5194/acp-14-1277-2014, 2014.
- Guenther, A., Karl, T., Harley, P., Wiedinmyer, C., Palmer, P. I., and Geron, C.: Estimates of global terrestrial isoprene emissions using MEGAN (Model of Emissions of Gases and Aerosols from Nature), *Atmos. Chem. Phys.*, 6, 3181–3210, doi:10.5194/acp-6-3181-2006, 2006.
- Gustafsson, M. E. R. and Franzén, L. G.: Inland transport of marine aerosols in southern Sweden, *Atmos. Environ.*, 34, 313–325, doi:10.1016/S1352-2310(99)00198-3, 2000.
- Heintzenberg, J., Müller, K., Birmili, W., Spindler, G., and Wiedensohler, A.: Mass-related aerosol properties over the Leipzig Basin, *J. Geophys. Res.-Atmos.*, 103, 13125–13135, doi:10.1029/98JD00922, 1998.
- Hong, S.-Y., Noh, Y., and Dudhia, J.: A new vertical diffusion package with an explicit treatment of entrainment processes, *Mon. Weather Rev.*, 134, 2318–2341, 2006.
- Im, U.: Impact of sea-salt emissions on the model performance and aerosol chemical composition and deposition in the East Mediterranean coastal regions, *Atmos. Environ.*, 75, 329–340, doi:10.1016/j.atmosenv.2013.04.034, 2013.
- IPCC: Intergovernmental Panel on Climate Change, *Climate Change 2013: The Physical Science Basis. Contribution of Working Group I to the Fifth Assessment Report of the Intergovernmental Panel on Climate Change*, Report, edited by: Stocker, T. F., Qin, D. H., Plattner, G. K., Tignor, M. M. B., Allen, S. K., Boschung, J., Nauels, A., Xia, Y., Bex, V., and Midgley, P. M., Cambridge University Press, New York, available at: <http://www.ipcc.ch/report/ar5/> (last access: 10 September 2016), 2013.
- Jaeglé, L., Quinn, P. K., Bates, T. S., Alexander, B., and Lin, J.-T.: Global distribution of sea salt aerosols: new constraints from in situ and remote sensing observations, *Atmos. Chem. Phys.*, 11, 3137–3157, doi:10.5194/acp-11-3137-2011, 2011.
- Jaenicke, R.: Atmospheric aerosols and global climate, *J. Aerosol Sci.*, 11, 577–588, 1980.
- Kulmala, M., Asmi, A., Lappalainen, H. K., Baltensperger, U., Brenguier, J.-L., Facchini, M. C., Hansson, H.-C., Hov, Ø., O'Dowd, C. D., Pöschl, U., Wiedensohler, A., Boers, R., Boucher, O., de Leeuw, G., Denier van der Gon, H. A. C., Fe-

- ichter, J., Krejci, R., Laj, P., Lihavainen, H., Lohmann, U., McFiggans, G., Mentel, T., Pilinis, C., Riipinen, I., Schulz, M., Stohl, A., Swietlicki, E., Vignati, E., Alves, C., Amann, M., Ammann, M., Arabas, S., Artaxo, P., Baars, H., Beddows, D. C. S., Bergström, R., Beukes, J. P., Bilde, M., Burkhardt, J. F., Canonaco, F., Clegg, S. L., Coe, H., Crumeyrolle, S., D'Anna, B., Decesari, S., Gilardoni, S., Fischer, M., Fjaeraa, A. M., Fountoukis, C., George, C., Gomes, L., Halloran, P., Hamburger, T., Harrison, R. M., Herrmann, H., Hoffmann, T., Hoose, C., Hu, M., Hyvärinen, A., Hörrak, U., Iinuma, Y., Iversen, T., Josipovic, M., Kanakidou, M., Kiendler-Scharr, A., Kirkevåg, A., Kiss, G., Klimont, Z., Kolmonen, P., Komppula, M., Kristjánsson, J.-E., Laakso, L., Laaksonen, A., Labonnote, L., Lanz, V. A., Lehtinen, K. E. J., Rizzo, L. V., Makkonen, R., Manninen, H. E., McMeeking, G., Merikanto, J., Minikin, A., Mirme, S., Morgan, W. T., Nemitz, E., O'Donnell, D., Panwar, T. S., Pawlowska, H., Petzold, A., Pienaar, J. J., Pio, C., Plass-Dümler, C., Prévôt, A. S. H., Pryor, S., Reddington, C. L., Roberts, G., Rosenfeld, D., Schwarz, J., Seland, Ø., Sellegri, K., Shen, X. J., Shiraiwa, M., Siebert, H., Sierau, B., Simpson, D., Sun, J. Y., Topping, D., Tunved, P., Vaattovaara, P., Vakkari, V., Veefkind, J. P., Visschedijk, A., Vuollekoski, H., Vuolo, R., Wehner, B., Wildt, J., Woodward, S., Worsnop, D. R., van Zadelhoff, G.-J., Zardini, A. A., Zhang, K., van Zyl, P. G., Kerminen, V.-M., Carslaw, K., and Pandis, S. N.: General overview: European Integrated project on Aerosol Cloud Climate and Air Quality interactions (EUCAARI) – integrating aerosol research from nano to global scales, *Atmos. Chem. Phys.*, 11, 13061–13143, doi:10.5194/acp-11-13061-2011, 2011.
- Lewis, E. R. and Schwartz, S. E.: Sea Salt Aerosol Production: Mechanisms, Methods, Measurements and Models – A Critical Review, AGU, Washington, DC, 152, 29711, doi:10.1029/GM152, 2004.
- Li, S., Garay, M. J., Chen, L., Rees, E., and Liu, Y.: Comparison of GEOS-Chem aerosol optical depth with AERONET and MISR data over the contiguous United States, *J. Geophys. Res.-Atmos.*, 118, 11228–11241, doi:10.1002/jgrd.50867, 2013.
- Liu, Y., Zhang, S., Fan, Q., Wu, D., Chan, P., Wang, X., Fan, S., Feng, Y., and Hong, Y.: Accessing the Impact of Sea-Salt Emissions on Aerosol Chemical Formation and Deposition over Pearl River Delta, China, *Aerosol Air Qual. Res.*, 15, 2232–2245, doi:10.4209/aaqr.2015.02.0127, 2015.
- Lin, Y., Farley, R., and Orville, H.: Bulk Parameterization of the Snow Field in a Cloud Model, *J. Clim. Appl. Meteorol.*, 22, 1065–1092, 1983.
- Lu, R. and Turco, R. P.: Air Pollutant Transport in a Coastal Environment. Part I: Two-Dimensional Simulations of Sea-Breeze and Mountain Effects, *J. Atmos. Sci.*, 51, 2285–2308, doi:10.1175/1520-0469(1994)051<2285:APTIAC>2.0.CO;2, 1994.
- Lu, R. and Turco, R. P.: Air pollutant transport in a coastal environment – II. Three-dimensional simulations over Los Angeles basin, *Atmos. Environ.*, 29, 1499–1518, doi:10.1016/1352-2310(95)00015-Q, 1995.
- Manders, A. M. M., Schaap, M., Querol, X., Albert, M. F. M. A., Vercouteren, J., Kuhlbusch, T. A. J., and Hoogerbrugge, R.: Sea salt concentrations across the European continent, *Atmos. Environ.*, 44, 2434–2442, doi:10.1016/j.atmosenv.2010.03.028, 2010.
- Mårtensson, E. M., Tunved, P., Korhonen, H., and Nilsson, E. D.: The role of sea-salt emissions in controlling the marine Aitken and accumulation mode aerosol: a model study, *Tellus B*, 62, 259–279, doi:10.3402/tellusb.v62i4.16552, 2010.
- Meng, Z. and Seinfeld, J. H.: Time scales to achieve atmospheric gas-aerosol equilibrium for volatile species, *Atmos. Environ.*, 30, 2889–2900, doi:10.1016/1352-2310(95)00493-9, 1996.
- Monahan, E. C.: Coastal Aerosol Workshop Proceedings, edited by: Goroch, A. K. and Geernaert, G. L., Rep. NRL/MR/7542-95-7219, 138 pp., Nav. Res. Lab., Monterey, Calif., 1995.
- Monahan, E. C., Spiel, D. E., and Davidson, K. L.: A model of marine aerosol generation via whitecaps and wave disruption, in: *Oceanic Whitecaps*, edited by: Monahan, E. and Niocaill, G. M., D. Reidel, Norwell, Mass, 167–174, 1986.
- Neuman, J. A., Huey, L. G., Ryerson, T. B., and Fahey, D. W.: Study of Inlet Materials for Sampling Atmospheric Nitric Acid, *Environ. Sci. Technol.*, 33, 1133–1136, doi:10.1021/es980767f, 1999.
- Neumann, D., Matthias, V., Bieser, J., Aulinger, A., and Quante, M.: Sensitivity of modeled atmospheric nitrogen species and nitrogen deposition to variations in sea salt emissions in the North Sea and Baltic Sea regions, *Atmos. Chem. Phys.*, 16, 2921–2942, doi:10.5194/acp-16-2921-2016, 2016a.
- Neumann, D., Matthias, V., Bieser, J., Aulinger, A., and Quante, M.: A comparison of sea salt emission parameterizations in north-western Europe using a chemistry transport model setup, *Atmos. Chem. Phys.*, 16, 9905–9933, doi:10.5194/acp-16-9905-2016, 2016b.
- Nordmann, S., Cheng, Y. F., Carmichael, G. R., Yu, M., Denier van der Gon, H. A. C., Zhang, Q., Saide, P. E., Pöschl, U., Su, H., Birmili, W., and Wiedensohler, A.: Atmospheric black carbon and warming effects influenced by the source and absorption enhancement in central Europe, *Atmos. Chem. Phys.*, 14, 12683–12699, doi:10.5194/acp-14-12683-2014, 2014.
- O'Dowd, C. D., Smith, M. H., Consterdine, I. E., and Lowe, J. A.: Marine aerosol, sea-salt, and the marine sulphur cycle: a short review, *Atmos. Environ.*, 31, 73–80, doi:10.1016/S1352-2310(96)00106-9, 1997.
- Ovadnevaite, J., Manders, A., de Leeuw, G., Ceburnis, D., Monahan, C., Partanen, A.-I., Korhonen, H., and O'Dowd, C. D.: A sea spray aerosol flux parameterization encapsulating wave state, *Atmos. Chem. Phys.*, 14, 1837–1852, doi:10.5194/acp-14-1837-2014, 2014.
- Pakkanen, T. A., Hillamo, R. E., Aurela, M., Andersen, H. V., Grundahl, L., Ferm, M., Persson, K., Karlsson, V., Reissell, A., Røysset, O., Fløisand, I., Oyola, P., and Ganko, T.: Nordic intercomparison for measurement of major atmospheric nitrogen species, *J. Aerosol Sci.*, 30, 247–263, doi:10.1016/S0021-8502(98)00039-1, 1999.
- Petzold, A. and Kärcher, B.: Aerosols in the Atmosphere, in: *Atmospheric Physics*, edited by: Schumann, U., Research Topics in Aerospace, Springer Berlin Heidelberg, 37–53, doi:10.1007/978-3-642-30183-4\_3, 2012.
- Pope, C. A., Ezzati, M., and Dockery, D. W.: Fine-particulate air pollution and life expectancy in the united states, *N. Engl. J. Med.*, 360, 376–386, 2009.
- Poulain, L., Spindler, G., Birmili, W., Plass-Dümler, C., Wiedensohler, A., and Herrmann, H.: Seasonal and diurnal variations of particulate nitrate and organic matter at the IfT re-

- search station Melpitz, *Atmos. Chem. Phys.*, 11, 12579–12599, doi:10.5194/acp-11-12579-2011, 2011.
- Pouliot, G., Pierce, T., Denier van der Gon, H., Schaap, M., Moran, M., and Nopmongkol, U.: Comparing emission inventories and model-ready emission datasets between Europe and North America for the AQMEII project, *Atmos. Environ.*, 53, 4–14, doi:10.1016/j.atmosenv.2011.12.041, 2012.
- Rumsey, I. C., Cowen, K. A., Walker, J. T., Kelly, T. J., Hanft, E. A., Mishoe, K., Rogers, C., Proost, R., Beachley, G. M., Lear, G., Frelink, T., and Otjes, R. P.: An assessment of the performance of the Monitor for Aerosols and Gases in ambient air (MARGA): a semi-continuous method for soluble compounds, *Atmos. Chem. Phys.*, 14, 5639–5658, doi:10.5194/acp-14-5639-2014, 2014.
- Saïde, P. E., Spak, S. N., Carmichael, G. R., Mena-Carrasco, M. A., Yang, Q., Howell, S., Leon, D. C., Snider, J. R., Bandy, A. R., Collett, J. L., Benedict, K. B., de Szoëke, S. P., Hawkins, L. N., Allen, G., Crawford, I., Crosier, J., and Springston, S. R.: Evaluating WRF-Chem aerosol indirect effects in Southeast Pacific marine stratocumulus during VOCALS-REx, *Atmos. Chem. Phys.*, 12, 3045–3064, doi:10.5194/acp-12-3045-2012, 2012.
- Saïde, P. E., Carmichael, G. R., Liu, Z., Schwartz, C. S., Lin, H. C., da Silva, A. M., and Hyer, E.: Aerosol optical depth assimilation for a size-resolved sectional model: impacts of observationally constrained, multi-wavelength and fine mode retrievals on regional scale analyses and forecasts, *Atmos. Chem. Phys.*, 13, 10425–10444, doi:10.5194/acp-13-10425-2013, 2013.
- Schaap, M., Müller, K., and ten Brink, H. M.: Constructing the European aerosol nitrate concentration field from quality analysed data, *Atmos. Environ.*, 36, 1323–1335, doi:10.1016/S1352-2310(01)00556-8, 2002.
- Schaap, M., Otjes, R. P., and Weijers, E. P.: Illustrating the benefit of using hourly monitoring data on secondary inorganic aerosol and its precursors for model evaluation, *Atmos. Chem. Phys.*, 11, 11041–11053, doi:10.5194/acp-11-11041-2011, 2011.
- Seinfeld, J. H. and Pandis, S. N.: *Atmospheric Chemistry and Physics – From Air Pollution to Climate Change*, John Wiley & Sons, New York, 2nd Edn., ISBN-13: 978-0-471-72018-8, 2006.
- Soares, J., Sofiev, M., Geels, C., Christensen, J. H., Andersson, C., Tsyro, S., and Langner, J.: Impact of climate change on the production and transport of sea salt aerosol on European seas, *Atmos. Chem. Phys. Discuss.*, doi:10.5194/acp-2015-1056, in review, 2016.
- Sofiev, M., Soares, J., Prank, M., de Leeuw, G., and Kukkonen, J.: A regional-to-global model of emission and transport of sea salt particles in the atmosphere, *J. Geophys. Res.-Atmos.*, 116, D21302, doi:10.1029/2010JD014713, 2011.
- Spindler, G., Brüggemann, E., Gnauk, T., Grüner, A., Müller, K., and Herrmann, H.: A four-year size-segregated characterization study of particles PM<sub>10</sub>, PM<sub>2.5</sub> and PM<sub>1</sub> depending on air mass origin at Melpitz, *Atmos. Environ.*, 44, 164–173, 2010.
- Spindler, G., Gnauk, T., Grüner, A., Iinuma, Y., Müller, K., Scheinhardt, S., and Herrmann, H.: Size-segregated characterization of PM<sub>10</sub> at the EMEP site Melpitz (Germany) using a five-stage impactor: a six year study, *J. Atmos. Chem.*, 69, 127–157, doi:10.1007/s10874-012-9233-6, 2012.
- Spindler, G., Grüner, A., Müller, K., Schlimper, S., and Herrmann, H.: Long-term size-segregated particle (PM<sub>10</sub>, PM<sub>2.5</sub>, PM<sub>1</sub>) characterization study at Melpitz – influence of air mass inflow, weather conditions and season, *J. Atmos. Chem.*, 70, 165–195, doi:10.1007/s10874-013-9263-8, 2013.
- ten Brink, H., Otjes, R., Jongejan, P., and Slanina, S.: An instrument for semi-continuous monitoring of the size-distribution of nitrate, ammonium, sulphate and chloride in aerosol, *Atmos. Environ.*, 41, 2768–2779, doi:10.1016/j.atmosenv.2006.11.041, 2007.
- ten Brink, H. M., Kruisz, C., Kos, G. P. A., and Berner, A.: Composition/size of the light-scattering aerosol in the Netherlands, *Atmos. Environ.*, 31, 3955–3962, doi:10.1016/S1352-2310(97)00232-X, 1997.
- Thomas, R. M., Trebs, I., Otjes, R., Jongejan, P. A. C., Brink, H. t., Phillips, G., Kortner, M., Meixner, F. X., and Nemitz, E.: An Automated Analyzer to Measure Surface-Atmosphere Exchange Fluxes of Water Soluble Inorganic Aerosol Compounds and Reactive Trace Gases, *Environ. Sci. Technol.*, 43, 1412–1418, doi:10.1021/es8019403, 2009.
- Tsyro, S., Aas, W., Soares, J., Sofiev, M., Berge, H., and Spindler, G.: Modelling of sea salt concentrations over Europe: key uncertainties and comparison with observations, *Atmos. Chem. Phys.*, 11, 10367–10388, doi:10.5194/acp-11-10367-2011, 2011.
- Visschedijk, A. and Denier van der Gon, H.: European Integrated project on Aerosol Cloud Climate and Air Quality interactions (EUCAARI, No036833-2) deliverable D42: Pan-European Carbonaceous aerosol inventory, Report, TNO Built Environment and Geosciences, D42, Utrecht, the Netherlands, 2008.
- Wiedensohler, A., Birmili, W., Nowak, A., Sonntag, A., Weinhold, K., Merkel, M., Wehner, B., Tuch, T., Pfeifer, S., Fiebig, M., Fjåraa, A. M., Asmi, E., Sellegri, K., Depuy, R., Venzac, H., Villani, P., Laj, P., Aalto, P., Ogren, J. A., Swietlicki, E., Williams, P., Roldin, P., Quincey, P., Hüglin, C., Fierz-Schmidhauser, R., Gysel, M., Weingartner, E., Riccobono, F., Santos, S., Gröning, C., Faloon, K., Beddows, D., Harrison, R., Monahan, C., Jennings, S. G., O'Dowd, C. D., Marinoni, A., Horn, H.-G., Keck, L., Jiang, J., Scheckman, J., McMurry, P. H., Deng, Z., Zhao, C. S., Moerman, M., Henzing, B., de Leeuw, G., Löschau, G., and Bastian, S.: Mobility particle size spectrometers: harmonization of technical standards and data structure to facilitate high quality long-term observations of atmospheric particle number size distributions, *Atmos. Meas. Tech.*, 5, 657–685, doi:10.5194/amt-5-657-2012, 2012.
- Wiedinmyer, C., Akagi, S. K., Yokelson, R. J., Emmons, L. K., Al-Saadi, J. A., Orlando, J. J., and Soja, A. J.: The Fire INventory from NCAR (FINN): a high resolution global model to estimate the emissions from open burning, *Geosci. Model Dev.*, 4, 625–641, doi:10.5194/gmd-4-625-2011, 2011.
- Wild, O., Zhu, X., and Prather, M. J.: Fast-J: Accurate Simulation of In- and Below-Cloud Photolysis in Tropospheric Chemical Models, *J. Atmos. Chem.*, 37, 245–282, 2000.
- Wolke, R., Schröder, W., Schrödner, R., and Renner, E.: Influence of grid resolution and meteorological forcing on simulated European air quality: A sensitivity study with the modeling system COSMO–MUSCAT, *Atmos. Environ.*, 53, 110–130, doi:10.1016/j.atmosenv.2012.02.085, 2012.
- Woodcock, A. H., Blanchard, D. C., and Rooth, C. G. H.: Salt-induced convection and clouds, *J. Atmos. Sci.*, 20, 159–169, 1963.
- Xu, L. and Penner, J. E.: Global simulations of nitrate and ammonium aerosols and their radiative effects, *Atmos. Chem. Phys.*, 12, 9479–9504, doi:10.5194/acp-12-9479-2012, 2012.

- Yang, Q., Gustafson Jr., W. I., Fast, J. D., Wang, H., Easter, R. C., Morrison, H., Lee, Y.-N., Chapman, E. G., Spak, S. N., and Mena-Carrasco, M. A.: Assessing regional scale predictions of aerosols, marine stratocumulus, and their interactions during VOCALS-REx using WRF-Chem, *Atmos. Chem. Phys.*, 11, 11951–11975, doi:10.5194/acp-11-11951-2011, 2011.
- Zaveri, R. A. and Peters, L. K.: A new lumped structure photochemical mechanism for large-scale applications, *J. Geophys. Res.*, 104, 30387–30415, 1999.
- Zaveri, R. A., Easter, R. C., Fast, J. D., and Peters, L. K.: Model for Simulating Aerosol Interactions and Chemistry (MOSAIC), *J. Geophys. Res.-Atmos.*, 113, D13204, doi:10.1029/2007JD008782, 2008.
- Zhang, Y., Sartelet, K., Zhu, S., Wang, W., Wu, S.-Y., Zhang, X., Wang, K., Tran, P., Seigneur, C., and Wang, Z.-F.: Application of WRF/Chem-MADRID and WRF/Polyphemus in Europe – Part 2: Evaluation of chemical concentrations and sensitivity simulations, *Atmos. Chem. Phys.*, 13, 6845–6875, doi:10.5194/acp-13-6845-2013, 2013.

### 3.2.2 Supporting information

Supplement of Atmos. Chem. Phys., 16, 12081–12097, 2016  
<http://www.atmos-chem-phys.net/16/12081/2016/>  
doi:10.5194/acp-16-12081-2016-supplement  
© Author(s) 2016. CC Attribution 3.0 License.



#### *Supplement of*

### **Sea salt emission, transport and influence on size-segregated nitrate simulation: a case study in northwestern Europe by WRF-Chem**

**Ying Chen et al.**

*Correspondence to:* Yafang Cheng (yafang.cheng@mpic.de) and Ying Chen (chen@tropos.de)

- [acp-16-12081-2016-supplement-title-page.pdf](#)
- [acp-2016-309-new supplement.pdf](#)
- [datasets of figures.zip](#)

The copyright of individual parts of the supplement might differ from the CC-BY 3.0 licence.



## Results and Discussion

**Table S1.** Comparisons for meteorological variables between Melpitz radio-sounding measurements and WRF-Chem model results

	<b>Slope</b>	<b>R</b>
<b>Potential Temperature</b>	0.99	0.99
<b>Wind Speed</b>	0.90	0.96
<b>Wind Direction</b>	1.02	0.84
<b>Water Vapor Mixing Ratio</b>	0.81	0.92

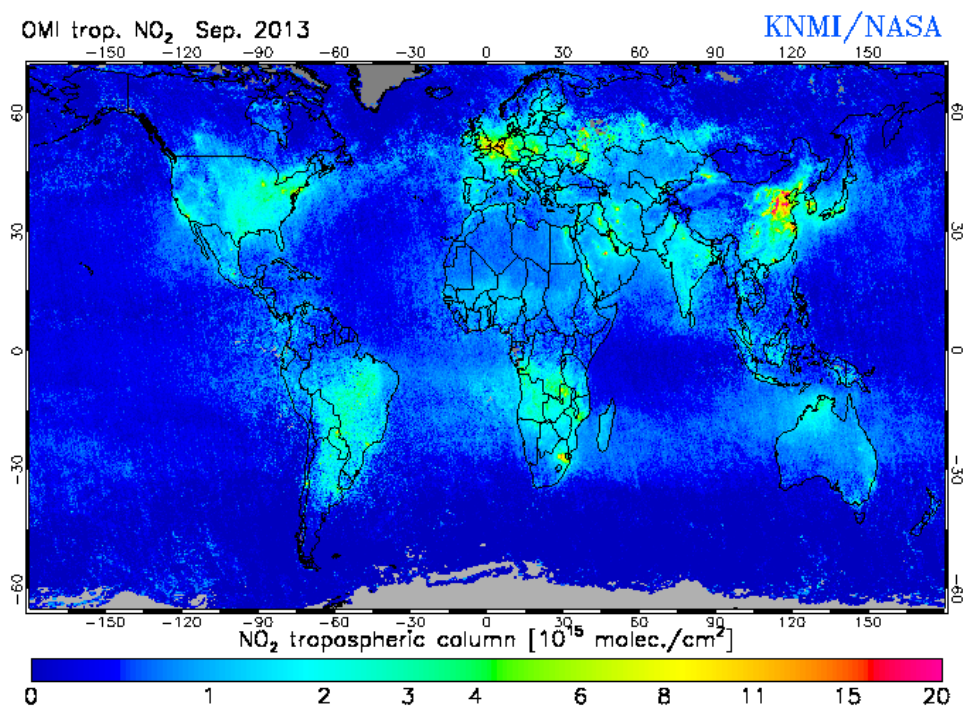


**Figure S1.** Global NO<sub>2</sub> tropospheric column concentration in September 2013 from OMI satellite.

Source: <http://www.temis.nl/airpollution/no2col/>, last access: November 04<sup>th</sup>, 2015



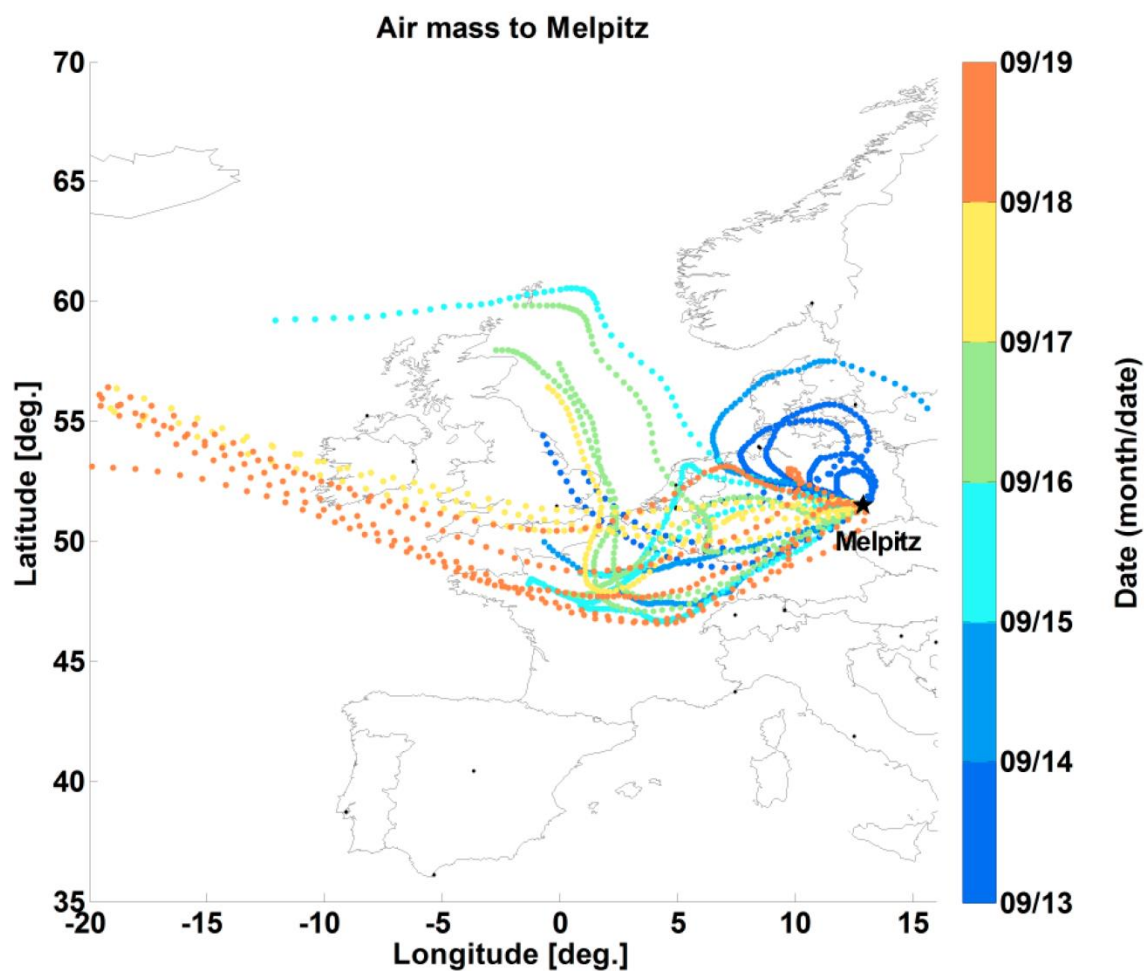
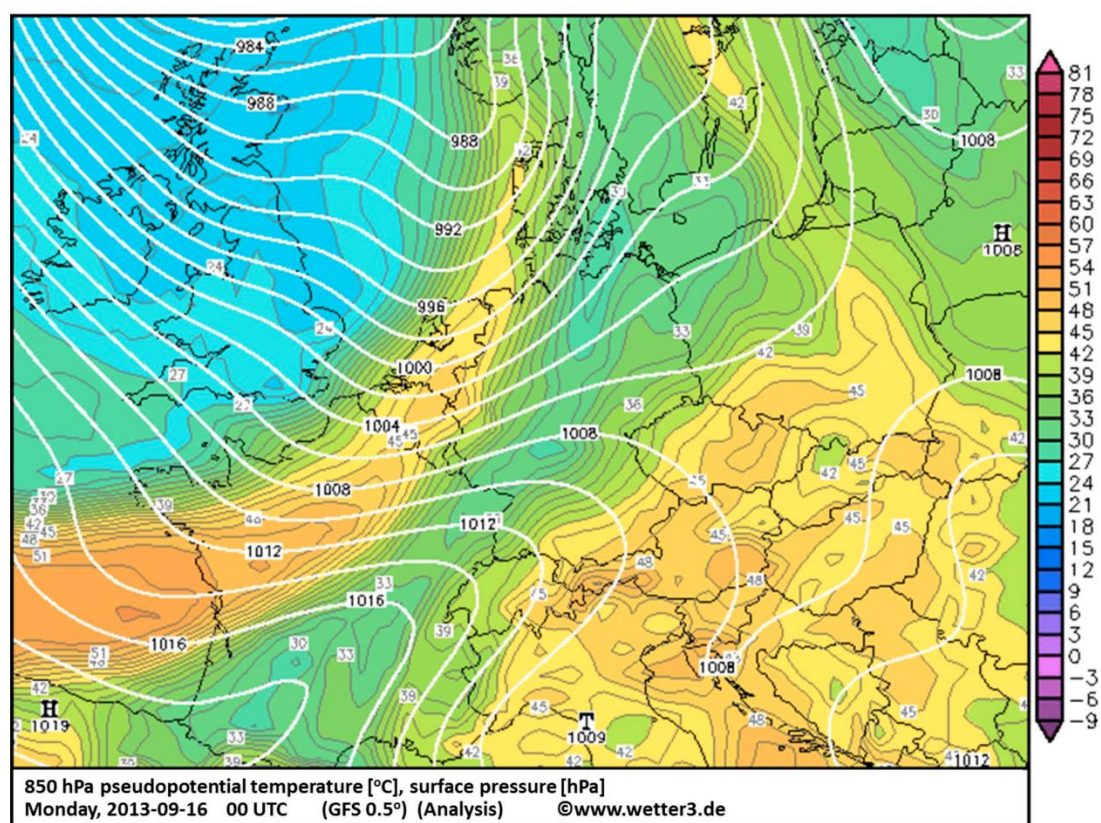
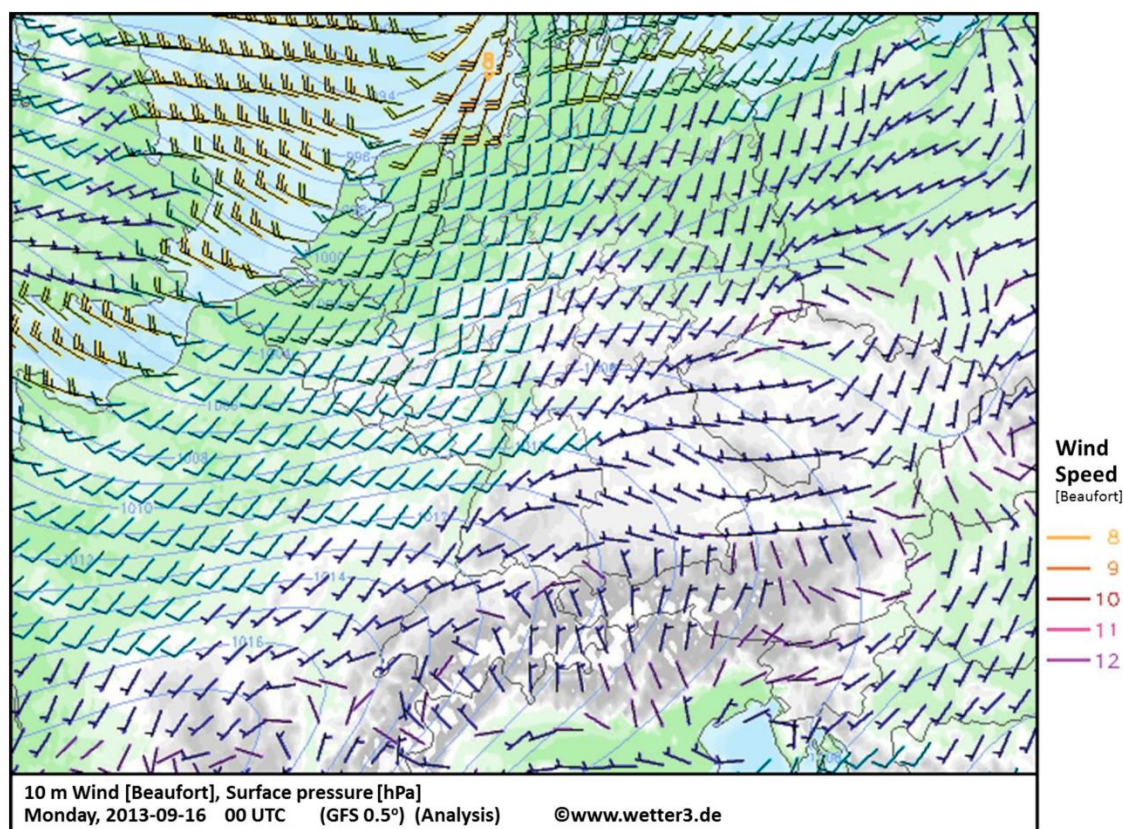


**Figure S2.** Three days back trajectories of Melpitz. The start time of back trajectories start from 2013-09-13 to 2013-09-19, with 6 hours interval. The back trajectories were calculated based on the GDAS (with  $0.5^\circ$  resolution) dataset with the Hysplit model ([http://www.arl.noaa.gov/HYSPLIT\\_info.php](http://www.arl.noaa.gov/HYSPLIT_info.php)).

## Results and Discussion



(a)



(b)



## Results and Discussion

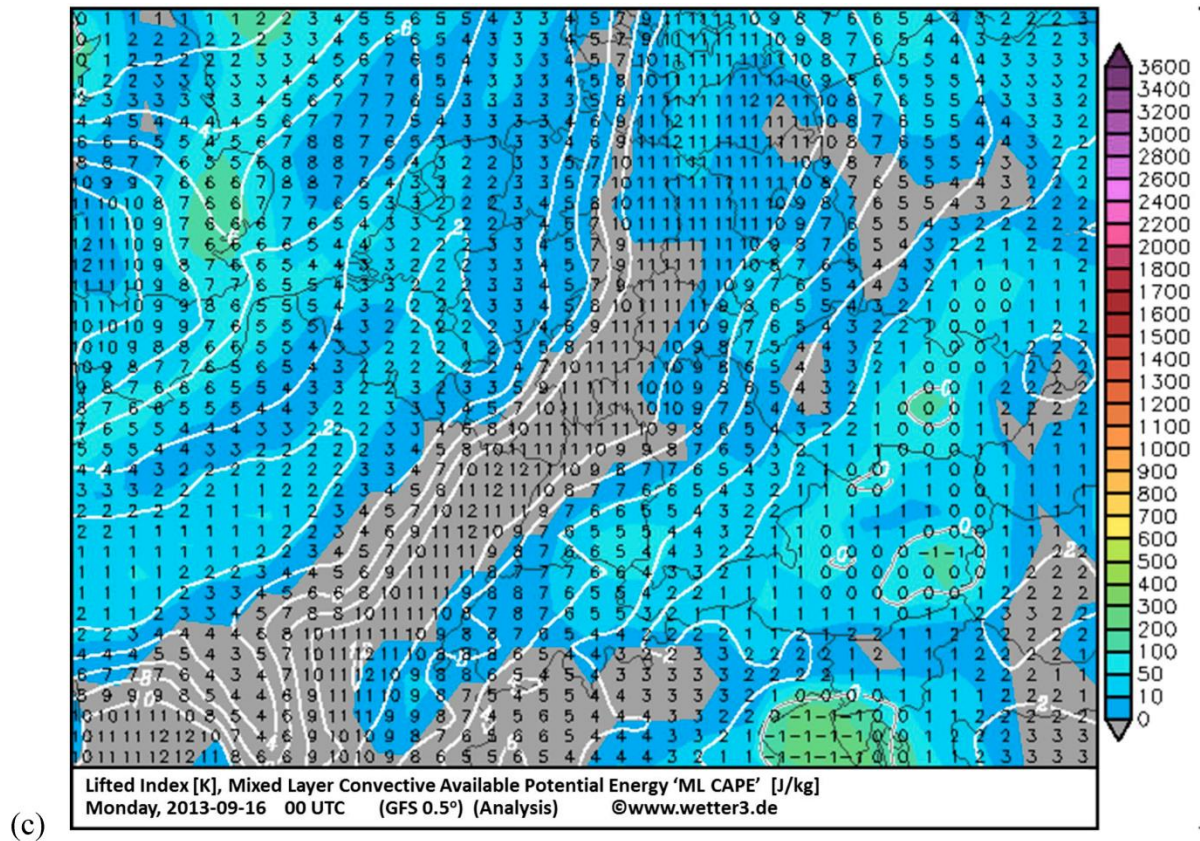


**Figure S3.** Weather map of Europe at 2013-09-16, 00:00 (UTC). (a) Surface pressure (white line) and pseudopotential temperature (color); (b) 10-meter wind field (arrows) and surface pressure (blue line); (c) lifted index (numbers and white line) and mixed layer convective available potential energy 'ML CAPE' (color)

Source: <http://www.wetter3.de/> (based on the GFS dataset with 0.5° resolution, last access: November 04<sup>th</sup>, 2015, reprint permission has been confirmed by [www.wetter3.de](http://www.wetter3.de/))

## Results and Discussion

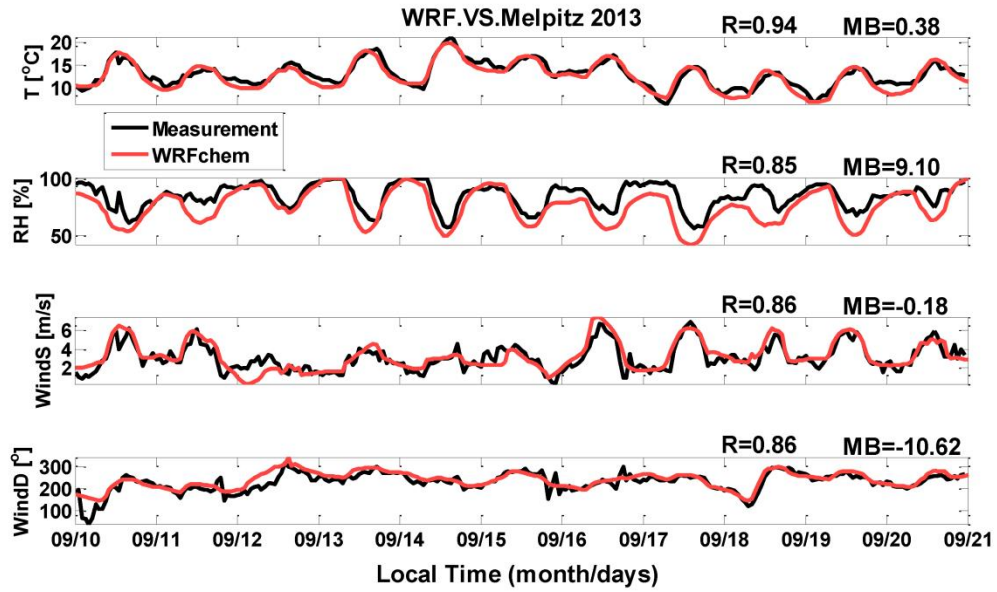


**Figure S4.** The comparisons between the simulation results and measurements at Melpitz near-ground layer. The correlation coefficient (R) and mean bias (MB) are marked on the top of each panel. (a) Temperature; (b) relative humidity (RH); (c) wind speed; (d) wind direction.

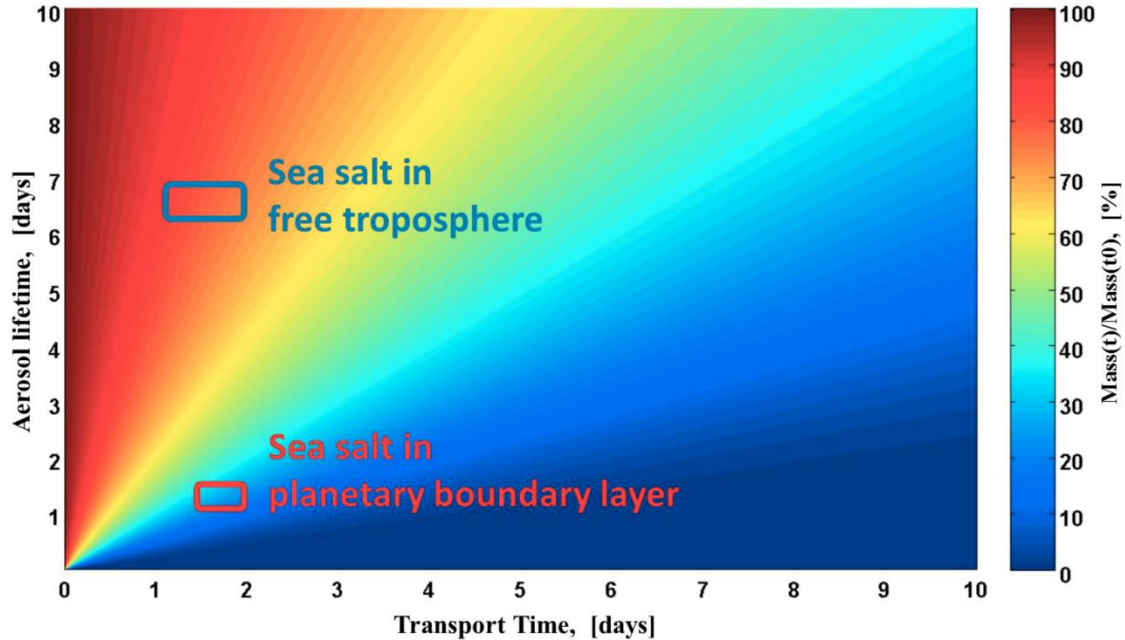


**Figure S5.** Sea salt mass residential rate with relationship of transport time and lifetime, based on the concept model (Chen et al., 2016). The color indicates the percentage of sea salt mass that can be transported from the coast to Melpitz

### Reference:

Chen, Y., Cheng, Y. F., Nordmann, S., Birmili, W., Denier van der Gon, H. A. C., Ma, N., Wolke, R., Wehner, B., Sun, J., Spindler, G., Mu, Q., Pöschl, U., Su, H., and Wiedensohler, A.: Evaluation of the size segregation of elemental carbon (EC) emission in Europe: influence on the simulation of EC long-range transportation, *Atmos. Chem. Phys.*, 16, 1823-1835, 10.5194/acp-16-1823-2016, 2016.

### 4. Summary and Conclusions

The overall goal of the present thesis is to figure out the reasons for gaps between the simulated and measured particle number/mass size distribution (PSD). This would help to improve the PSD simulation of different particle compositions in modelling studies, and therefore to refine the assessments of climate change. Simulations with a state-of-the-art fully online-coupled model WRF-Chem were performed during the HOPE-Melpitz campaign (September 10-20<sup>th</sup>, 2013). The modelled PSD is described by a sectional approach (MOSAIC) with eight isogradient (in logarithmic scale) discrete size bins (from about 39 nm to 10  $\mu\text{m}$ ) of dry particles. Extensive measurements of microphysical and chemical properties of size-resolved particles, gaseous pollutants mass concentration, and meteorological conditions, were performed at Melpitz during the campaign. I validated the PSD simulations of the most important absorbing (elemental carbon, EC) and scattering (nitrate) anthropogenic particles at the central Europe background site Melpitz. Although the meteorological conditions were well captured by the model, WRF-Chem significantly overestimated the coarse mode mass/number concentration of particles. This is mainly due to the overestimation of EC, sea salt aerosol (SSA) and nitrate. The main results referring to the addressed scientific questions/objectives are summarized as followed:

**Q1: Is the size distribution/segregation of EC (absorbing aerosol) well represented by the WRF-Chem model over Europe? What are the reasons for the uncertainties? (First publication)**

In my first published study (Chen et al., 2016a), the EUCAARI inventory of anthropogenic EC emission over Europe was evaluated, not only for the emission rate but also for the size segregation of EC emission. The coarse mode EC (EC<sub>c</sub>) emission fraction was substantially overestimated in Eastern Europe (e.g., Poland, Belarus etc.) and Russia by the EUCAARI inventory, with about 10–30% for Russia and 5–10% for the Eastern European countries. A concept model and a case study were designed to interpret the influence of this overestimation on EC long-range transport. Due to the overestimation of EC<sub>c</sub> emission fraction, The EC mass transported from Moskva to Melpitz would decrease by about 25–35% of the EC<sub>c</sub> mass concentration, and decrease by about 25–55% from Warsaw to Melpitz (Fig. 6). Since coarse mode particles have a shorter lifetime, they have less opportunity to be transported long-range and accumulated in the atmosphere. The March–April 2009 case (Nordmann et al., 2014) was re-

## Summary and Conclusions

simulated with adjusted ECc emission fraction in Eastern Europe, in order to validate the influence on EC transport. The result showed that the overestimation of ECc emission fraction in Eastern Europe may partly (~20-40%) explain the underestimation of EC in Germany when the air masses came from eastern direction in previous studies (Nordmann et al., 2014; Stern et al., 2008; Genberg et al., 2013). This result has a very significant scientific meaning, since it would help us to better understand the climate effect of the EC particle. Will the health and climatic effects of atmospheric EC particles be local, regional or global? This is to some extent determined by the transport of EC, which is largely influenced by its PSD. The PSD of EC should be carefully considered in the model validation and climate change evaluation studies. Unfortunately, the PSD information is not included in most of the current global EC emission inventories, and the PSD in EUCAARI only covers Europe and still has a high uncertainty.

Furthermore, the point sources of EC emission over Germany were also evaluated in my first publication. The comparisons of EC mass concentrations at the Melpitz, Leipzig-TROPOS and Bösels sites indicate that the EC point sources may be overestimated by factors of 2–10 with more than 60-90% of ECc. This also led to the overestimation of PSD in coarse mode when the EC plume hit Melpitz. The overestimation of EC point sources would give significant uncertainties in high resolution modelling studies.

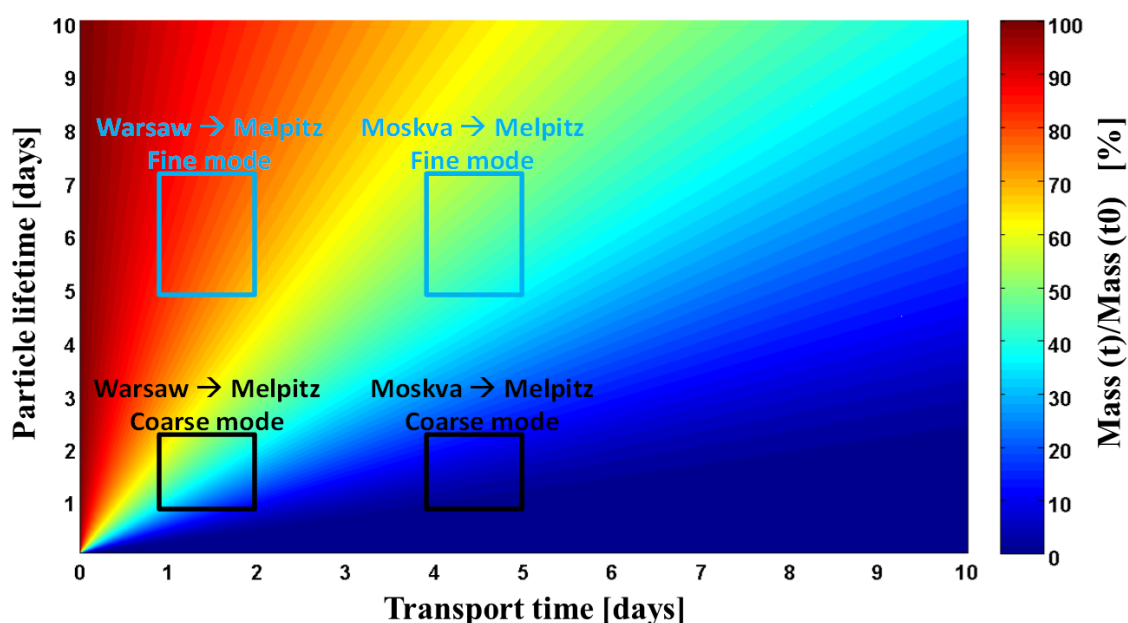


**Figure 6.** Aerosol mass residential rate in relation to the transport time and lifetime. Source: Chen et al. (2016a).



### **Q2: Is the chemical pathway of nitrate (scattering aerosol) well represented by the WRF-Chem model over Europe? What are the main reasons for the uncertainties? (Second publication)**

In my second published study (Chen et al., 2016b), I evaluated the SSA emission in WRF-Chem and investigated its influence on nitrate particle mass size distribution. In addition to EC, the overestimation of PSD in coarse mode was also contributed by SSA and nitrate. SSA mass concentrations were evaluated at four ground-based EMEP stations, including one continental inland station (Melpitz) and three coastal stations (Bilthoven, Kollumerwaard and Vredepeel). The day-to-day variations of SSA mass concentrations were well captured by the model despite an overestimation of SSA concentrations by factors of 8–20 due to the shortcoming of the WRF-Chem SSA emission scheme (Gong, 2003). In addition to the wind speed at 10 m above the ground, more parameters, such as sea surface temperature, salinity and wave data, might be needed for consideration in the SSA emission scheme to reduce its overestimation. The overestimation of SSA emissions did not only influence the release of primary SSA itself but also led to a significant overprediction of the coarse mode sodium nitrate (Fig. 7). Since most SSA is emitted as coarse particles, nitrate partitioning fraction of coarse mode was overestimated by ~20% when the SSA mass concentration was highly overestimated at Melpitz. This contributed to an overprediction of the coarse mode nitrate by around 140 %.

### **Q3: How can natural source particles (sea salt) influence the simulated anthropogenic nitrate particle mass size distribution? How wide can the influence of sea salt on nitrate particle mass size distribution be spread over Europe? (Second publication)**

Moreover, I investigated the influence of SSA on the simulated nitrate particle mass size distribution in my second publication. Nitrate can be “locked” in the particulate phase as the thermodynamically stable sodium nitrate, which is produced from the heterogeneous reaction of nitric acid on the surface of SSA. Although the nitrate partitioning fraction in coarse mode was overpredicted due to the overestimation of SSA, the nitrate partitioning fraction in fine mode was insensitive to the SSA emission. However, the increased consumption of the nitric acid, caused by the coarse mode nitrate formation on the surface of SSA, inhibited the fine mode ammonium nitrate formation (Fig. 7). The facilitation of coarse mode nitrate formation and



## Summary and Conclusions

inhibition of fine mode nitrate formation can shift the nitrate particle mass size distribution towards larger sizes.

Furthermore in my second publication, I demonstrated a mechanism that could transport SSA to the regions further inland, thus broadening its influence on the nitrate particle mass size distribution (Fig. 7). An “aloft bridge” between the marine planetary boundary layer (PBL) and the continental free troposphere can be formed over the coastal areas, due to the difference of nocturnal PBL structure between continental and marine regions. SSA can be mixed up by the marine PBL and injected into the continental free troposphere via the “aloft bridge”. Then it can more easily participate in the long-range transport, because the lifetime of particles can be about 5 times longer in the free troposphere than in the PBL. Later, downdrafts and turbulence of the fully developed continental PBL would mix the lifted SSA downwards to the surface layer of inland regions (e.g., central Europe), where a remarkable amount of NO<sub>x</sub> and ammonium nitrate is present.

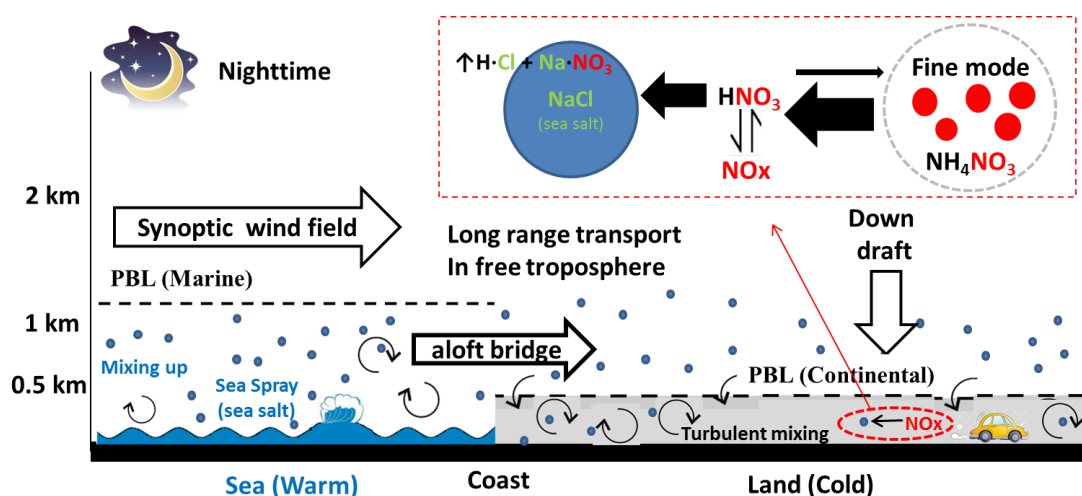


**Figure 7.** Schematic of sea salt transportation and its influence on coarse mode nitrate formation and nitrate particle mass size distribution. Source: Chen et al. (2016b).

### 5. Outlook

The present study has clearly demonstrated the need to further improve the simulation of PSD in models. The primary emissions and secondary formation processes are one of the most important contributors to the uncertainties of PSD simulations.

The present thesis highlights the importance of size distribution of EC particles, which is the most important absorbing particle. However, our understanding of EC size distribution is still limited. More measurements (e.g., online analysis by the Single Particle Soot Photometer (SP2), offline analysis of Berner/MOUDI samples, etc.) and long-term modelling studies are needed to further improve the PSD information of EC emission inventories. The size distribution of EC particles would influence its transport and optical properties, which is important for the assessment of EC climate effects, especially for the remote regions (e.g., Arctic and Himalayas).

For the scattering agent particulate nitrate: sea salt can alter the nitrate particle mass size distribution, which is crucial for nitrate optical properties thus for its direct radiative forcing. The change of nitrate particle mass size distribution can also influence the deposition processes of particulate nitrate, thus influencing the nitrogen cycle which is important for atmospheric chemistry. Furthermore, what is the influence on cloud formation and indirect radiative forcing due to the change of nitrate particle mass size distribution? This is also an interesting scientific question for future studies, although lots of laboratory and modelling studies are needed.

Moreover, this study also highlighted that the natural source coarse particles may have an impact on the PSD of anthropogenic source particles, via multi-phase chemistry. Many previous studies found that mineral dust can promote sulfate formation due to the heterogeneous reaction of SO<sub>2</sub> on its surface (e.g., Dentener et al., 1996; Harris et al., 2012 and 2013). Similar to sea salt and nitrate, this process can consume sulfuric acid which is the precursor of fine mode sulfate. Therefore, the sulfate particle mass size distribution may also be influenced by mineral dust. What is the influence of mineral dust on the cycle, transport and radiative forcing of anthropogenic sulfate? This could also be a very interesting question with remarkable scientific meanings.

## Appendix A

### A.1 Authors contribution to the two publications

#### **First publication: Evaluation of the size segregation of elemental carbon (EC) emission in Europe: influence on the simulation of EC long-range transportation**

In this publication, I conceived the study, performed the model simulations, conducted the data analysis and draft the manuscript with inputs from all co-authors. All co-authors discussed the results. Furthermore, Yafang Cheng carried out the main corrections of this publication and helped to prepare the emission inventory. Stephan Nordmann provided the data of 2009 case which was analyzed in this study. Wolfram Birmili improved the manuscript and provided the GUAN data used in this study. Hugo A. C. Denier van der Gon provided the emission inventory for the simulation. Nan Ma, Ralf Wolke, Birgit Wehner, Jia Sun, Gerald Spindler, Qing Mu, Ulrich Pöschl, Hang Su, and Alfred Wiedensohler made useful suggestions for the manuscript and the project.

#### **Second publication: Sea salt emission, transport and influence on size-segregated nitrate simulation: a case study in northwestern Europe by WRF-Chem**

In this publication, I conceived the study, performed the model simulations, conducted the data analysis and draft the manuscript with inputs from all co-authors. All co-authors discussed the results and provided useful suggestions. Furthermore, Yafang Cheng carried out the main corrections of this publication and helped to prepare the emission inventory. Hugo A. C. Denier van der Gon provided the emission inventory for the simulation. Gerald Spindler and Konrad Müller provided the DIGITEL filter chemical measurements at Melpitz. Bastian Stieger provided the MARGA measurements at Melpitz. Alfred Wiedensohler made useful suggestions for this project and the manuscript.

## **Bibliography**

- IPCC AR5: Climate Change 2013: The Physical Science Basis. Contribution of Working Group I to the Fifth Assessment Report of the Intergovernmental Panel on Climate Change, Report, edited by: Stocker, T. F., Qin D. H., Plattner, G. K., Tignor, M. M. B., Allen, S. K., Boschung, J., Nauels, A., Xia, Y., Bex, V., and Midgley, P. M., Cambridge University Press, New York, available at: <http://www.ipcc.ch/report/ar5> (last access: 10<sup>th</sup> September, 2016), 2013.
- Ackermann, I. J., Hass, H., Memmesheimer, M., Ebel, A., Binkowski, F. S., and Shankar, U.: Modal aerosol dynamics model for Europe: development and first applications, *Atmospheric Environment*, 32, 2981-2999, [http://dx.doi.org/10.1016/S1352-2310\(98\)00006-5](http://dx.doi.org/10.1016/S1352-2310(98)00006-5), 1998.
- Adams, P. J., Seinfeld, J. H., Koch, D., Mickley, L., and Jacob, D.: General circulation model assessment of direct radiative forcing by the sulfate-nitrate-ammonium-water inorganic aerosol system, *Journal of Geophysical Research: Atmospheres*, 106, 1097-1111, 10.1029/2000JD900512, 2001.
- Aquila, V., Hendricks, J., Lauer, A., Riemer, N., Vogel, H., Baumgardner, D., Minikin, A., Petzold, A., Schwarz, J. P., Spackman, J. R., Weinzierl, B., Righi, M., and Dall'Amico, M.: MADE-in: a new aerosol microphysics submodel for global simulation of insoluble particles and their mixing state, *Geosci. Model Dev.*, 4, 325-355, 10.5194/gmd-4-325-2011, 2011.
- Archer-Nicholls, S., Lowe, D., Utembe, S., Allan, J., Zaveri, R. A., Fast, J. D., Hodnebrog, Ø., Denier van der Gon, H., and McFiggans, G.: Gaseous chemistry and aerosol mechanism developments for version 3.5.1 of the online regional model, WRF-Chem, *Geosci. Model Dev.*, 7, 2557-2579, 10.5194/gmd-7-2557-2014, 2014.
- Athanasopoulou, E., Tombrou, M., Pandis, S. N., and Russell, A. G.: The role of sea-salt emissions and heterogeneous chemistry in the air quality of polluted coastal areas, *Atmos. Chem. Phys.*, 8, 5755-5769, 10.5194/acp-8-5755-2008, 2008.
- Barnard, J. C., Chapman, E. G., Fast, J. D., Schmelzer, J. R., Slusser, J. R., and Shetter, R. E.: An evaluation of the FAST-J photolysis algorithm for predicting nitrogen dioxide

## Bibliography

---

- photolysis rates under clear and cloudy sky conditions, *Atmospheric Environment*, 38, 3393-3403, <http://dx.doi.org/10.1016/j.atmosenv.2004.03.034>, 2004.
- Bauer, S. E., Koch, D., Unger, N., Metzger, S. M., Shindell, D. T., and Streets, D. G.: Nitrate aerosols today and in 2030: a global simulation including aerosols and tropospheric ozone, *Atmos. Chem. Phys.*, 7, 5043-5059, 10.5194/acp-7-5043-2007, 2007.
- Binkowski, F. S., and Shankar, U.: The Regional Particulate Matter Model: 1. Model description and preliminary results, *Journal of Geophysical Research: Atmospheres*, 100, 26191-26209, 10.1029/95JD02093, 1995.
- Birmili, W., Stratmann, F., and Wiedensohler, A.: Design of a DMA-based size spectrometer for a large particle size range and stable operation, *Journal of Aerosol Science*, 30, 549-553, [http://dx.doi.org/10.1016/S0021-8502\(98\)00047-0](http://dx.doi.org/10.1016/S0021-8502(98)00047-0), 1999.
- Birmili, W., Wiedensohler, A., Heintzenberg, J., and Lehmann, K.: Atmospheric particle number size distribution in central Europe: Statistical relations to air masses and meteorology, *Journal of Geophysical Research*, 106, 32005-32018, DOI: 10.1029/2000JD000220, 2001.
- Birmili, W., Weinhold, K., Rasch, F., Sonntag, A., Sun, J., Merkel, M., Wiedensohler, A., Bastian, S., Schladitz, A., Löschau, G., Cyrys, J., Pitz, M., Gu, J., Kusch, T., Flentje, H., Quass, U., Kaminski, H., Kuhlbusch, T. A. J., Meinhardt, F., Schwerin, A., Bath, O., Ries, L., Wirtz, K., and Fiebig, M.: Long-term observations of tropospheric particle number size distributions and equivalent black carbon mass concentrations in the German Ultrafine Aerosol Network (GUAN), *Earth Syst. Sci. Data*, 8, 355-382, 10.5194/essd-8-355-2016, 2016.
- Bond, T. C., Streets, D. G., Yarber, K. F., Nelson, S. M., Woo, J.-H., and Klimont, Z.: A technology-based global inventory of black and organic carbon emissions from combustion, *Journal of Geophysical Research: Atmospheres*, 109, 10.1029/2003JD003697, 2004.
- Bond, T. C., Bhardwaj, E., Dong, R., Jogani, R., Jung, S., Roden, C., Streets, D. G., and Trautmann, N. M.: Historical emissions of black and organic carbon aerosol from energy-related combustion, 1850–2000, *Global Biogeochemical Cycles*, 21, 10.1029/2006GB002840, 2007.
- Bond, T. C., Doherty, S. J., Fahey, D. W., Forster, P. M., Berntsen, T., DeAngelo, B. J., Flanner, M. G., Ghan, S., Kärcher, B., Koch, D., Kinne, S., Kondo, Y., Quinn, P. K., Sarofim, M.

## Bibliography

---

- C., Schultz, M. G., Schulz, M., Venkataraman, C., Zhang, H., Zhang, S., Bellouin, N., Guttikunda, S. K., Hopke, P. K., Jacobson, M. Z., Kaiser, J. W., Klimont, Z., Lohmann, U., Schwarz, J. P., Shindell, D., Storelvmo, T., Warren, S. G., and Zender, C. S.: Bounding the role of black carbon in the climate system: A scientific assessment, *Journal of Geophysical Research: Atmospheres*, 118, 5380-5552, 10.1002/jgrd.50171, 2013.
- Brüggemann, E., and Spindler, G.: Wet and dry deposition of sulphur at the site Melpitz in East Germany, *Water Air Soil Pollut* 109, 81-99, 1999.
- Carter, W. P. L.: Implementation of the SAPRC-99 chemical mechanism into the models-3 framework, US EPA report, available at: <http://www.engr.ucr.edu/~carter/pubs/s99mod3.pdf> (last access: 5 January 2017), 2000.
- Chapman, E. G., Gustafson Jr, W. I., Easter, R. C., Barnard, J. C., Ghan, S. J., Pekour, M. S., and Fast, J. D.: Coupling aerosol-cloud-radiative processes in the WRF-Chem model: Investigating the radiative impact of elevated point sources, *Atmos. Chem. Phys.*, 9, 945-964, 10.5194/acp-9-945-2009, 2009.
- Chen, Y., Zhao, C., Zhang, Q., Deng, Z. Z., Huang, M. Y., and Ma, X. C.: Aircraft study of mountain chimney effect of Beijing, china, *Journal of Geophysical Research: Atmospheres*, 114, 10.1029/2008JD010610, 2009.
- Chen, Y., Cheng, Y., Ma, N., Wolke, R., Nordmann, S., Schüttauf, S., Ran, L., Wehner, B., Birmili, W., van der Gon, H. A. C. D., Mu, Q., Barthel, S., Spindler, G., Stieger, B., Müller, K., Zheng, G. J., Pöschl, U., Su, H., and Wiedensohler, A.: Sea salt emission, transport and influence on size-segregated nitrate simulation: a case study in northwestern Europe by WRF-Chem, *Atmos. Chem. Phys.*, 16, 12081-12097, 10.5194/acp-16-12081-2016, 2016a.
- Chen, Y., Cheng, Y. F., Nordmann, S., Birmili, W., Denier van der Gon, H. A. C., Ma, N., Wolke, R., Wehner, B., Sun, J., Spindler, G., Mu, Q., Pöschl, U., Su, H., and Wiedensohler, A.: Evaluation of the size segregation of elemental carbon (EC) emission in Europe: influence on the simulation of EC long-range transportation, *Atmos. Chem. Phys.*, 16, 1823-1835, 10.5194/acp-16-1823-2016, 2016b.
- Cheng, Y., Zheng, G., Wei, C., Mu, Q., Zheng, B., Wang, Z., Gao, M., Zhang, Q., He, K., Carmichael, G., Pöschl, U., and Su, H.: Reactive nitrogen chemistry in aerosol water as a



## Bibliography

---

- source of sulfate during haze events in China, *Science Advances*, 2, 10.1126/sciadv.1601530, 2016.
- Cheng, Y. F., Su, H., Rose, D., Gunthe, S. S., Berghof, M., Wehner, B., Achtert, P., Nowak, A., Takegawa, N., Kondo, Y., Shiraiwa, M., Gong, Y. G., Shao, M., Hu, M., Zhu, T., Zhang, Y. H., Carmichael, G. R., Wiedensohler, A., Andreae, M. O., and Pöschl, U.: Size-resolved measurement of the mixing state of soot in the megacity Beijing, China: diurnal cycle, aging and parameterization, *Atmos. Chem. Phys.*, 12, 4477-4491, 2012.
- Chin, M., Rood, R. B., Lin, S.-J., Müller, J.-F., and Thompson, A. M.: Atmospheric sulfur cycle simulated in the global model GOCART: Model description and global properties, *Journal of Geophysical Research: Atmospheres*, 105, 24671-24687, 10.1029/2000JD900384, 2000.
- Chou, M.-D., Suarez, M. J., Ho, C.-H., Yan, M. M. H., and Lee, K.-T.: Parameterizations for Cloud Overlapping and Shortwave Single-Scattering Properties for Use in General Circulation and Cloud Ensemble Models, *Journal of Climate*, 11, 202-214, 10.1175/1520-0442(1998)011<0202:PFCOAS>2.0.CO;2, 1998.
- Croft, B., Pierce, J. R., and Martin, R. V.: Interpreting aerosol lifetimes using the GEOS-Chem model and constraints from radionuclide measurements, *Atmospheric Chemistry and Physics*, 14, 4313-4325, 2014.
- de Leeuw, G., Andreas, E. L., Anguelova, M. D., Fairall, C. W., Lewis, E. R., O'Dowd, C., Schulz, M., and Schwartz, S. E.: Production flux of sea spray aerosol, *Reviews of Geophysics*, 49, 10.1029/2010RG000349, 2011.
- Denier van der Gon, H. A. C., Bergström, R., Fountoukis, C., Johansson, C., Pandis, S. N., Simpson, D., and Visschedijk, A. J. H.: Particulate emissions from residential wood combustion in Europe – revised estimates and an evaluation, *Atmos. Chem. Phys.*, 15, 6503-6519, 10.5194/acp-15-6503-2015, 2015.
- Dentener, F. J., Carmichael, G. R., Zhang, Y., Lelieveld, J., and Crutzen, P. J.: Role of mineral aerosol as a reactive surface in the global troposphere, *Journal of Geophysical Research: Atmospheres*, 101, 22869-22889, 10.1029/96JD01818, 1996.
- EMEP: EMEP Manual for Sampling and Analysis, EMEP, available at: <http://www.nilu.no/projects/ccc/manual/index.html> (last access: 15 May 2016), 2014.

## Bibliography

---

- Emmons, L. K., Walters, S., Hess, P. G., Lamarque, J. F., Pfister, G. G., Fillmore, D., Granier, C., Guenther, A., Kinnison, D., Laepple, T., Orlando, J., Tie, X., Tyndall, G., Wiedinmyer, C., Baughcum, S. L., and Kloster, S.: Description and evaluation of the Model for Ozone and Related chemical Tracers, version 4 (MOZART-4), *Geosci. Model Dev.*, 3, 43-67, 10.5194/gmd-3-43-2010, 2010.
- Fast, J. D., Gustafson, W. I., Easter, R. C., Zaveri, R. A., Barnard, J. C., Chapman, E. G., Grell, G. A., and Peckham, S. E.: Evolution of ozone, particulates, and aerosol direct radiative forcing in the vicinity of Houston using a fully coupled meteorology-chemistry-aerosol model, *Journal of Geophysical Research: Atmospheres*, 111, 10.1029/2005JD006721, 2006.
- Foret, G., Bergametti, G., Dulac, F., and Menut, L.: An optimized particle size bin scheme for modeling mineral dust aerosol, *Journal of Geophysical Research: Atmospheres*, 111, 10.1029/2005JD006797, 2006.
- Forkel, R., Werhahn, J., Hansen, A. B., McKeen, S., Peckham, S., Grell, G., and Suppan, P.: Effect of aerosol-radiation feedback on regional air quality – A case study with WRF/Chem, *Atmospheric Environment*, 53, 202-211, <http://dx.doi.org/10.1016/j.atmosenv.2011.10.009>, 2012.
- Gelbard, F., and Seinfeld, J. H.: Simulation of multicomponent aerosol dynamics, *Journal of Colloid and Interface Science*, 78, 485-501, [http://dx.doi.org/10.1016/0021-9797\(80\)90587-1](http://dx.doi.org/10.1016/0021-9797(80)90587-1), 1980.
- Gelbard, F., Tambour, Y., and Seinfeld, J. H.: Sectional representations for simulating aerosol dynamics, *Journal of Colloid and Interface Science*, 76, 541-556, [http://dx.doi.org/10.1016/0021-9797\(80\)90394-X](http://dx.doi.org/10.1016/0021-9797(80)90394-X), 1980.
- Genberg, J., Denier van der Gon, H. A. C., Simpson, D., Swietlicki, E., Areskoug, H., Beddows, D., Ceburnis, D., Fiebig, M., Hansson, H. C., Harrison, R. M., Jennings, S. G., Saarikoski, S., Spindler, G., Visschedijk, A. J. H., Wiedensohler, A., Yttri, K. E., and Bergström, R.: Light-absorbing carbon in Europe – measurement and modelling, with a focus on residential wood combustion emissions, *Atmos. Chem. Phys.*, 13, 8719-8738, 10.5194/acp-13-8719-2013, 2013.

## Bibliography

---

- Ghan, S., Laulainen, N., Easter, R., Wagener, R., Nemesure, S., Chapman, E., Zhang, Y., and Leung, R.: Evaluation of aerosol direct radiative forcing in MIRAGE, *Journal of Geophysical Research: Atmospheres*, 106, 5295-5316, 10.1029/2000JD900502, 2001.
- Gong, S. L.: A parameterization of sea-salt aerosol source function for sub- and super-micron particles, *Global Biogeochemical Cycles*, 17, 10.1029/2003GB002079, 2003.
- Grell, G., Freitas, S. R., Stuefer, M., and Fast, J.: Inclusion of biomass burning in WRF-Chem: impact of wildfires on weather forecasts, *Atmos. Chem. Phys.*, 11, 5289-5303, 10.5194/acp-11-5289-2011, 2011.
- Grell, G. A., Peckham, S. E., Schmitz, R., McKeen, S. A., Frost, G., Skamarock, W. C., and Eder, B.: Fully coupled “online” chemistry within the WRF model, *Atmospheric Environment*, 39, 6957-6975, <http://dx.doi.org/10.1016/j.atmosenv.2005.04.027>, 2005.
- Grythe, H., Ström, J., Krejci, R., Quinn, P., and Stohl, A.: A review of sea-spray aerosol source functions using a large global set of sea salt aerosol concentration measurements, *Atmos. Chem. Phys.*, 14, 1277-1297, 10.5194/acp-14-1277-2014, 2014.
- Guenther, A., Karl, T., Harley, P., Wiedinmyer, C., Palmer, P. I., and Geron, C.: Estimates of global terrestrial isoprene emissions using MEGAN (Model of Emissions of Gases and Aerosols from Nature), *Atmos. Chem. Phys.*, 6, 3181-3210, 10.5194/acp-6-3181-2006, 2006.
- Hansen, J., Sato, M., Ruedy, R., Lacis, A., and Oinas, V.: Global warming in the twenty-first century: An alternative scenario, *Proceedings of the National Academy of Sciences*, 97, 9875-9880, 10.1073/pnas.170278997, 2000.
- Harris, E., Sinha, B., Foley, S., Crowley, J. N., Borrmann, S., and Hoppe, P.: Sulfur isotope fractionation during heterogeneous oxidation of SO<sub>2</sub> on mineral dust, *Atmos. Chem. Phys.*, 12, 4867-4884, 10.5194/acp-12-4867-2012, 2012.
- Harris, E., Sinha, B., van Pinxteren, D., Tilgner, A., Fomba, K. W., Schneider, J., Roth, A., Gnauk, T., Fahlbusch, B., Mertes, S., Lee, T., Collett, J., Foley, S., Borrmann, S., Hoppe, P., and Herrmann, H.: Enhanced Role of Transition Metal Ion Catalysis During In-Cloud Oxidation of SO<sub>2</sub>, *Science*, 340, 727-730, 10.1126/science.1230911, 2013.

## Bibliography

---

- Heintzenberg, J., Müller, K., Birmili, W., Spindler, G., and Wiedensohler, A.: Mass-related aerosol properties over the Leipzig Basin, *Journal of Geophysical Research: Atmospheres*, 103, 13125-13135, 10.1029/98JD00922, 1998.
- Hitzenberger, R., Ctyroky, P., Berner, A., Turšič, J., Podkrajšek, B., and Grgić, I.: Size distribution of black (BC) and total carbon (TC) in Vienna and Ljubljana, *Chemosphere*, 65, 2106-2113, <http://dx.doi.org/10.1016/j.chemosphere.2006.06.042>, 2006.
- Hitzenberger, R. and Tohno, S.: Comparison of black carbon (BC) aerosols in two urban areas - concentrations and size distributions, *Atmos. Environ.*, 35, 2153-2167, 2001.
- Hodnebrog, Ø., Stordal, F., and Berntsen, T. K.: Does the resolution of megacity emissions impact large scale ozone?, *Atmospheric Environment*, 45, 6852-6862, <http://dx.doi.org/10.1016/j.atmosenv.2011.01.012>, 2011.
- Hodnebrog, Ø., Solberg, S., Stordal, F., Svendby, T. M., Simpson, D., Gauss, M., Hilboll, A., Pfister, G. G., Turquety, S., Richter, A., Burrows, J. P., and Denier van der Gon, H. A. C.: Impact of forest fires, biogenic emissions and high temperatures on the elevated Eastern Mediterranean ozone levels during the hot summer of 2007, *Atmos. Chem. Phys.*, 12, 8727-8750, 10.5194/acp-12-8727-2012, 2012.
- Hong, S.-Y., Noh, Y., and Dudhia, J.: A new vertical diffusion package with an explicit treatment of entrainment processes, *Mon. Weather Rev.*, 134, 2318-2341, 2006.
- Im, U.: Impact of sea-salt emissions on the model performance and aerosol chemical composition and deposition in the East Mediterranean coastal regions, *Atmospheric Environment*, 75, 329-340, <http://dx.doi.org/10.1016/j.atmosenv.2013.04.034>, 2013.
- J. C. Barnard, J. D. F., G. Paredes-Miranda, W. P. Arnott, and A. Laskin: Technical Note: Evaluation of the WRF-Chem “Aerosol Chemical to Aerosol Optical Properties” Module using data from the MILAGRO campaign, *Atmos. Chem. Phys.*, 10, 7325-7340, doi:10.5194/acp-10-7325-2010, 2010.
- Jacobson, M. Z.: A physically-based treatment of elemental carbon optics: Implications for global direct forcing of aerosols, *Geophys. Res. Lett.*, 27, 217-220, doi:10.1029/1999GL010968, 2000.

## Bibliography

---

- Jacobson, M. Z.: Global direct radiative forcing due to multicomponent anthropogenic and natural aerosols, *Journal of Geophysical Research: Atmospheres*, 106, 1551-1568, 10.1029/2000JD900514, 2001.
- Jacobson, M. Z.: Atmospheric pollution: history, science, and regulation, Cambridge University Press, 2002.
- Jaeglé L., Quinn, P. K., Bates, T. S., Alexander, B., and Lin, J. T.: Global distribution of sea salt aerosols: new constraints from in situ and remote sensing observations, *Atmos. Chem. Phys.*, 11, 3137-3157, 10.5194/acp-11-3137-2011, 2011.
- Knutson, E. O.: Extended electric mobility method for measuring aerosol particle size and concentration. In B. Y. H. Liu (Ed.), *Fine particles: Aerosol generation, measurement, and sampling* (pp. 740-762), New York, NY: Academic Press., 1976.
- Koch, D., Schulz, M., Kinne, S., McNaughton, C., Spackman, J. R., Balkanski, Y., Bauer, S., Berntsen, T., Bond, T. C., Boucher, O., Chin, M., Clarke, A., De Luca, N., Dentener, F., Diehl, T., Dubovik, O., Easter, R., Fahey, D. W., Feichter, J., Fillmore, D., Freitag, S., Ghan, S., Ginoux, P., Gong, S., Horowitz, L., Iversen, T., Kirkevåg, A., Klimont, Z., Kondo, Y., Krol, M., Liu, X., Miller, R., Montanaro, V., Moteki, N., Myhre, G., Penner, J. E., Perlwitz, J., Pitari, G., Reddy, S., Sahu, L., Sakamoto, H., Schuster, G., Schwarz, J. P., Seland, Ø., Stier, P., Takegawa, N., Takemura, T., Textor, C., van Aardenne, J. A., and Zhao, Y.: Evaluation of black carbon estimations in global aerosol models, *Atmos. Chem. Phys.*, 9, 9001-9026, doi:10.5194/acp-9-9001-2009, 2009.
- Kohler, H.: The nucleus in and the growth of hygroscopic droplets, *Transactions of the Faraday Society*, 32, 1152-1161, 10.1039/TF9363201152, 1936.
- Kulmala, M., Asmi, A., Lappalainen, H. K., Baltensperger, U., Brenguier, J. L., Facchini, M. C., Hansson, H. C., Hov, Ø., O'Dowd, C. D., Pöschl, U., Wiedensohler, A., Boers, R., Boucher, O., de Leeuw, G., Denier van der Gon, H. A. C., Feichter, J., Krejci, R., Laj, P., Lihavainen, H., Lohmann, U., McFiggans, G., Mentel, T., Pilinis, C., Riipinen, I., Schulz, M., Stohl, A., Swietlicki, E., Vignati, E., Alves, C., Amann, M., Ammann, M., Arabas, S., Artaxo, P., Baars, H., Beddows, D. C. S., Bergström, R., Beukes, J. P., Bilde, M., Burkhardt, J. F., Canonaco, F., Clegg, S. L., Coe, H., Crumeyrolle, S., D'Anna, B., Decesari, S., Gilardoni, S., Fischer, M., Fjaeraa, A. M., Fountoukis, C., George, C.,

## Bibliography

---

- Gomes, L., Halloran, P., Hamburger, T., Harrison, R. M., Herrmann, H., Hoffmann, T., Hoose, C., Hu, M., Hyvärinen, A., Hõrak, U., Inuma, Y., Iversen, T., Josipovic, M., Kanakidou, M., Kiendler-Scharr, A., Kirkevåg, A., Kiss, G., Klimont, Z., Kolmonen, P., Komppula, M., Kristjánsson, J. E., Laakso, L., Laaksonen, A., Labonnote, L., Lanz, V. A., Lehtinen, K. E. J., Rizzo, L. V., Makkonen, R., Manninen, H. E., McMeeking, G., Merikanto, J., Minikin, A., Mirme, S., Morgan, W. T., Nemitz, E., O'Donnell, D., Panwar, T. S., Pawlowska, H., Petzold, A., Pienaar, J. J., Pio, C., Plass-Duelmer, C., Prévôt, A. S. H., Pryor, S., Reddington, C. L., Roberts, G., Rosenfeld, D., Schwarz, J., Seland, Ø., Sellegri, K., Shen, X. J., Shiraiwa, M., Siebert, H., Sierau, B., Simpson, D., Sun, J. Y., Topping, D., Tunved, P., Vaattovaara, P., Vakkari, V., Veefkind, J. P., Visschedijk, A., Vuollekoski, H., Vuolo, R., Wehner, B., Wildt, J., Woodward, S., Worsnop, D. R., van Zadelhoff, G. J., Zardini, A. A., Zhang, K., van Zyl, P. G., Kerminen, V. M., Carslaw, K., and Pandis, S. N.: General overview: European Integrated project on Aerosol Cloud Climate and Air Quality interactions (EUCAARI) – integrating aerosol research from nano to global scales, *Atmos. Chem. Phys.*, 11, 13061-13143, 10.5194/acp-11-13061-2011, 2011.
- Lamarque, J.-F., Bond, T. C., Eyring, V., Granier, C., Heil, A., Klimont, Z., Lee, D., Lioussé, C., Mieville, A., Owen, B., Schultz, M. G., Shindell, D., Smith, S. J., Stehfest, E., Van Aardenne, J., Cooper, O. R., Kainuma, M., Mahowald, N., McConnell, J. R., Naik, V., Riahi, K., and van Vuuren, D. P.: Historical (1850-2000) gridded anthropogenic and biomass burning emissions of reactive gases and aerosols: methodology and application, *Atmos. Chem. Phys.*, 10, 7017-7039, doi:10.5194/acp-10-7017-2010, 2010.
- Liao, H., and Seinfeld, J. H.: Global impacts of gas-phase chemistry-aerosol interactions on direct radiative forcing by anthropogenic aerosols and ozone, *Journal of Geophysical Research: Atmospheres*, 110, 10.1029/2005JD005907, 2005.
- Lin, Y., Farley, R., and Orville, H.: Bulk Parameterization of the Snow Field in a Cloud Model, *J. Clim. Appl. Meteorol.*, 22, 1065-1092, 1983.
- Liu, X., Easter, R. C., Ghan, S. J., Zaveri, R., Rasch, P., Shi, X., Lamarque, J. F., Gettelman, A., Morrison, H., Vitt, F., Conley, A., Park, S., Neale, R., Hannay, C., Ekman, A. M. L., Hess, P., Mahowald, N., Collins, W., Iacono, M. J., Bretherton, C. S., Flanner, M. G., and Mitchell, D.: Toward a minimal representation of aerosols in climate models: description

## Bibliography

---

- and evaluation in the Community Atmosphere Model CAM5, *Geosci. Model Dev.*, 5, 709-739, 10.5194/gmd-5-709-2012, 2012.
- Liu, Y., Zhang, S., Fan, Q., Wu, D., Chan, P., Wang, X., Fan, S., Feng, Y., and Hong, Y.: Accessing the Impact of Sea-Salt Emissions on Aerosol Chemical Formation and Deposition over Pearl River Delta, China, *Aerosol Air Qual. Res.*, 15, 2232–2245, 10.4209/aaqr.2015.02.0127, 2015.
- Macke, A., Seifert, P., Baars, H., Beekmans, C., Behrendt, A., Bohn, B., Bühl, J., Crewell, S., Damian, T., Deneke, H., Düsing, S., Foth, A., Di Girolamo, P., Hammann, E., Heinze, R., Hirsikko, A., Kalisch, J., Kalthoff, N., Kinne, S., Kohler, M., Löhnert, U., Madhavan, B. L., Maurer, V., Muppa, S. K., Schween, J., Serikov, I., Siebert, H., Simmer, C., Späth, F., Steinke, S., Trümner, K., Wehner, B., Wieser, A., Wulfmeyer, V., and Xie, X.: The HD(CP)2 Observational Prototype Experiment HOPE – An Overview, *Atmos. Chem. Phys. Discuss.*, 2016, 1-37, 10.5194/acp-2016-990, 2016.
- Maher, B. A., Ahmed, I. A. M., Karloukovski, V., MacLaren, D. A., Foulds, P. G., Allsop, D., Mann, D. M. A., Torres-Jardón, R., and Calderon-Garciduenas, L.: Magnetite pollution nanoparticles in the human brain, *Proceedings of the National Academy of Sciences*, 113, 10797-10801, 10.1073/pnas.1605941113, 2016.
- McConnell, J. R., Edwards, R., Kok, G. L., Flanner, M. G., Zender, C. S., Saltzman, E. S., Banta, J. R., Pasteris, D. R., Carter, M. M., and Kahl, J. D. W.: 20th-Century Industrial Black Carbon Emissions Altered Arctic Climate Forcing, *Science*, 317, 1381-1384, 2007.
- Meister, K., Johansson, C., and Forsberg, B.: Estimated Short-Term Effects of Coarse Particles on Daily Mortality in Stockholm, Sweden, *Environ. Health Persp.*, 120, 431-436, 2012.
- Ming, J., Cachier, H., Xiao, C., Qin, D., Kang, S., Hou, S., and Xu, J.: Black carbon record based on a shallow Himalayan ice core and its climatic implications, *Atmos. Chem. Phys.*, 8, 1343-1352, 10.5194/acp-8-1343-2008, 2008.
- Monahan, E. C., Spiel, D. E., and Davidson, K. L.: A model of marine aerosol generation via whitecaps and wave disruption, in: *Oceanic Whitecaps* edited by: Monahan, E. and Niocaill, G. M., D. Reidel, Norwell, Mass, 167-174, 1986.
- Myhre, G., Samset, B. H., Schulz, M., Balkanski, Y., Bauer, S., Bernsten, T. K., Bian, H., Bellouin, N., Chin, M., Diehl, T., Easter, R. C., Feichter, J., Ghan, S. J., Hauglustaine, D., Iversen, T., Kinne, S., Kirkevåg, A., Lamarque, J. F., Lin, G., Liu, X., Lund, M. T., Luo,



## Bibliography

---

- G., Ma, X., van Noije, T., Penner, J. E., Rasch, P. J., Ruiz, A., Seland, Ø., Skeie, R. B., Stier, P., Takemura, T., Tsigaridis, K., Wang, P., Wang, Z., Xu, L., Yu, H., Yu, F., Yoon, J. H., Zhang, K., Zhang, H., and Zhou, C.: Radiative forcing of the direct aerosol effect from AeroCom Phase II simulations, *Atmos. Chem. Phys.*, 13, 1853-1877, 10.5194/acp-13-1853-2013, 2013.
- Neumann, D., Matthias, V., Bieser, J., Aulinger, A., and Quante, M.: Sensitivity of modeled atmospheric nitrogen species and nitrogen deposition to variations in sea salt emissions in the North Sea and Baltic Sea regions, *Atmos. Chem. Phys.*, 16, 2921-2942, 10.5194/acp-16-2921-2016, 2016a.
- Neumann, D., Matthias, V., Bieser, J., Aulinger, A., and Quante, M.: A comparison of sea salt emission parameterizations in northwestern Europe using a chemistry transport model setup, *Atmos. Chem. Phys.*, 16, 9905-9933, 10.5194/acp-16-9905-2016, 2016b.
- Nordmann, S., Birmili, W., Weinhold, K., Müller, K., Spindler, G., and Wiedensohler, A.: Measurements of the mass absorption cross section of atmospheric soot particles using Raman spectroscopy, *J. Geophys. Res.-Atmos.*, 118, 12,075-012,085, doi:10.1002/2013JD020021, 2013.
- Nordmann, S., Cheng, Y. F., Carmichael, G. R., Yu, M., Denier van der Gon, H. A. C., Zhang, Q., Saide, P. E., Pöschl, U., Su, H., Birmili, W., and Wiedensohler, A.: Atmospheric black carbon and warming effects influenced by the source and absorption enhancement in central Europe, *Atmos. Chem. Phys.*, 14, 12683-12699, 10.5194/acp-14-12683-2014, 2014.
- Ntelekos, A. A., Smith, J. A., Donner, L., Fast, J. D., Gustafson, W. I., Chapman, E. G., and Krajewski, W. F.: The effects of aerosols on intense convective precipitation in the northeastern United States, *Quarterly Journal of the Royal Meteorological Society*, 135, 1367-1391, 2009.
- O'Dowd, C. D., Smith, M. H., Consterdine, I. E., and Lowe, J. A.: Marine aerosol, sea-salt, and the marine sulphur cycle: a short review, *Atmospheric Environment*, 31, 73-80, [http://dx.doi.org/10.1016/S1352-2310\(96\)00106-9](http://dx.doi.org/10.1016/S1352-2310(96)00106-9), 1997.
- Pakkanen, T. A., Hillamo, R. E., Aurela, M., Andersen, H. V., Grundahl, L., Ferm, M., Persson, K., Karlsson, V., Reissell, A., Røyset, O., Fløisand, I., Oyola, P., and Ganko, T.: Nordic

## Bibliography

---

- intercomparison for measurement of major atmospheric nitrogen species, *Journal of Aerosol Science*, 30, 247-263, [http://dx.doi.org/10.1016/S0021-8502\(98\)00039-1](http://dx.doi.org/10.1016/S0021-8502(98)00039-1), 1999.
- Petzold, A., and Kärcher, B.: Aerosols in the Atmosphere, in: *Atmospheric Physics*, edited by: Schumann, U., *Research Topics in Aerospace*, Springer Berlin Heidelberg, 37-53, DOI: 10.1007/978-3-642-30183-4\_3, 2012.
- Poulain, L., Spindler, G., Birmili, W., Plass-Dülmer, C., Wiedensohler, A., and Herrmann, H.: Seasonal and diurnal variations of particulate nitrate and organic matter at the IFT research station Melpitz, *Atmos. Chem. Phys.*, 11, 12579-12599, 2011.
- Pouliot, G., Pierce, T., Denier van der Gon, H., Schaap, M., Moran, M., and Nopmongcol, U.: Comparing emission inventories and model-ready emission datasets between Europe and North America for the AQMEII project, *Atmospheric Environment*, 53, 4-14, <http://dx.doi.org/10.1016/j.atmosenv.2011.12.041>, 2012.
- Putaud, J.-P., Raes, F., Van Dingenen, R., Brüggemann, E., Facchini, M. C., Decesari, S., Fuzzi, S., Gehrig, R., Hüglin, C., Laj, P., Lorbeer, G., Maenhaut, W., Mihalopoulos, N., Müller, K., Querol, X., Rodriguez, S., Schneider, J., Spindler, G., Brink, H. t., Tørseth, K., and Wiedensohler, A.: A European aerosol phenomenology—2: chemical characteristics of particulate matter at kerbside, urban, rural and background sites in Europe, *Atmospheric Environment*, 38, 2579-2595, <http://dx.doi.org/10.1016/j.atmosenv.2004.01.041>, 2004.
- Ramanathan, V., and Carmichael, G.: Global and regional climate changes due to black carbon, *Nature geoscience*, 1, 221-227, 2008.
- Reddington, C. L., McMeeking, G., Mann, G. W., Coe, H., Frontoso, M. G., Liu, D., Flynn, M., Spracklen, D. V., and Carslaw, K. S.: The mass and number size distributions of black carbon aerosol over Europe, *Atmos. Chem. Phys.*, 13, 4917-4939, 10.5194/acp-13-4917-2013, 2013.
- Rose, D., Wehner, B., Ketzel, M., Engler, C., Voigtländer, J., Tuch, T., and Wiedensohler, A.: Atmospheric number size distributions of soot particles and estimation of emission factors, *Atmos. Chem. Phys.*, 6, 1021-1031, 2006.
- Rosenthal, F. S., Kuisma, M., Lanki, T., Korhonen, M., Hussein, T., and Pekkanen, J.: Particulate Air Pollution Triggers Cardiac Arrest in Helsinki—Effect of Medical History and Two-pollutant Analysis, *Epidemiology*, 22, S53, 10.1097/01.ede.0000391825.03966.79, 2011.

## Bibliography

---

- Saide, P. E., Spak, S. N., Carmichael, G. R., Mena-Carrasco, M. A., Yang, Q., Howell, S., Leon, D. C., Snider, J. R., Bandy, A. R., Collett, J. L., Benedict, K. B., de Szoeki, S. P., Hawkins, L. N., Allen, G., Crawford, I., Crosier, J., and Springston, S. R.: Evaluating WRF-Chem aerosol indirect effects in Southeast Pacific marine stratocumulus during VOCALS-REx, *Atmos. Chem. Phys.*, 12, 3045-3064, 10.5194/acp-12-3045-2012, 2012.
- Saide, P. E., Carmichael, G. R., Liu, Z., Schwartz, C. S., Lin, H. C., da Silva, A. M., and Hyer, E.: Aerosol optical depth assimilation for a size-resolved sectional model: impacts of observationally constrained, multi-wavelength and fine mode retrievals on regional scale analyses and forecasts, *Atmos. Chem. Phys.*, 13, 10425-10444, 10.5194/acp-13-10425-2013, 2013.
- Schaap, M., Müller, K., and ten Brink, H. M.: Constructing the European aerosol nitrate concentration field from quality analysed data, *Atmospheric Environment*, 36, 1323-1335, [http://dx.doi.org/10.1016/S1352-2310\(01\)00556-8](http://dx.doi.org/10.1016/S1352-2310(01)00556-8), 2002.
- Schaap, M., Sauter, F., and Builtjes, P.: Chapter 5.10 On the direct aerosol forcing of nitrate over Europe: Simulations with the new LOTOS-EUROS model, in: *Developments in Environmental Science*, edited by: Carlos, B., and Eberhard, R., Elsevier, 582-591, 2007.
- Schaap, M., Otjes, R. P., and Weijers, E. P.: Illustrating the benefit of using hourly monitoring data on secondary inorganic aerosol and its precursors for model evaluation, *Atmos. Chem. Phys.*, 11, 11041-11053, 10.5194/acp-11-11041-2011, 2011.
- Schell, B., Ackermann, I. J., Hass, H., Binkowski, F. S., and Ebel, A.: Modeling the formation of secondary organic aerosol within a comprehensive air quality model system, *Journal of Geophysical Research: Atmospheres*, 106, 28275-28293, 10.1029/2001JD000384, 2001.
- Seinfeld, J. H., and Pandis, S. N.: *Atmospheric Chemistry and Physics: From Air Pollution to Climate Change*, John Wiley & Sons, New York, 2nd Edn., 2006.
- Shiraiwa, M., Yee, L. D., Schilling, K. A., Loza, C. L., Craven, J. S., Zuend, A., Ziemann, P. J., and Seinfeld, J. H.: Size distribution dynamics reveal particle-phase chemistry in organic aerosol formation, *Proceedings of the National Academy of Sciences*, 110, 11746-11750, 10.1073/pnas.1307501110, 2013.
- Skamarok, W., Klemp, J., Dudhia, J., Gill, D., Barker, D., Duda, M., Huang, X.-Y., Wang, W., and Powers, J.: *A Description of the Advanced Research WRF Version 3*, Report, National Center for Atmospheric Research, Boulder, Colorado, 2008.

## Bibliography

---

- Solazzo, E., Bianconi, R., Pirovano, G., Matthias, V., Vautard, R., Moran, M. D., Wyat Appel, K., Bessagnet, B., Brandt, J., Christensen, J. H., Chemel, C., Coll, I., Ferreira, J., Forkel, R., Francis, X. V., Grell, G., Grossi, P., Hansen, A. B., Miranda, A. I., Nopmongcol, U., Prank, M., Sartelet, K. N., Schaap, M., Silver, J. D., Sokhi, R. S., Vira, J., Werhahn, J., Wolke, R., Yarwood, G., Zhang, J., Rao, S. T., and Galmarini, S.: Operational model evaluation for particulate matter in Europe and North America in the context of AQMEII, *Atmospheric Environment*, 53, 75-92, <http://dx.doi.org/10.1016/j.atmosenv.2012.02.045>, 2012a.
- Solazzo, E., Bianconi, R., Vautard, R., Appel, K. W., Moran, M. D., Hogrefe, C., Bessagnet, B., Brandt, J., Christensen, J. H., Chemel, C., Coll, I., Denier van der Gon, H., Ferreira, J., Forkel, R., Francis, X. V., Grell, G., Grossi, P., Hansen, A. B., Jeričević, A., Kraljević, L., Miranda, A. I., Nopmongcol, U., Pirovano, G., Prank, M., Riccio, A., Sartelet, K. N., Schaap, M., Silver, J. D., Sokhi, R. S., Vira, J., Werhahn, J., Wolke, R., Yarwood, G., Zhang, J., Rao, S. T., and Galmarini, S.: Model evaluation and ensemble modelling of surface-level ozone in Europe and North America in the context of AQMEII, *Atmospheric Environment*, 53, 60-74, <http://dx.doi.org/10.1016/j.atmosenv.2012.01.003>, 2012b.
- Spindler, G., Brüggemann, E., Gnauk, T., Grüner, A., Müller, K., and Herrmann, H.: A four-year size-segregated characterization study of particles PM<sub>10</sub>, PM<sub>2.5</sub> and PM<sub>1</sub> depending on air mass origin at Melpitz, *Atmospheric Environment*, 44, 164-173, 2010.
- Spindler, G., Gnauk, T., Grüner, A., Iinuma, Y., Müller, K., Scheinhardt, S., and Herrmann, H.: Size-segregated characterization of PM<sub>10</sub> at the EMEP site Melpitz (Germany) using a five-stage impactor: a six year study, *J Atmos Chem*, 69, 127-157, [10.1007/s10874-012-9233-6](https://doi.org/10.1007/s10874-012-9233-6), 2012.
- Spindler, G., Grüner, A., Müller, K., Schlimper, S., and Herrmann, H.: Long-term size-segregated particle (PM<sub>10</sub>, PM<sub>2.5</sub>, PM<sub>1</sub>) characterization study at Melpitz -- influence of air mass inflow, weather conditions and season, *J Atmos Chem*, 70, 165-195, [10.1007/s10874-013-9263-8](https://doi.org/10.1007/s10874-013-9263-8), 2013.
- Stern, R., Builtjes, P., Schaap, M., Timmermans, R., Vautard, R., Hodzic, A., Memmesheimer, M., Feldmann, H., Renner, E., Wolke, R., and Kerschbaumer, A.: A model inter-comparison study focussing on episodes with elevated PM<sub>10</sub> concentrations,

## Bibliography

---

- Atmospheric Environment, 42, 4567-4588, <http://dx.doi.org/10.1016/j.atmosenv.2008.01.068>, 2008.
- Stockwell, W. R., Middleton, P., Chang, J. S., and Tang, X.: The second generation regional acid deposition model chemical mechanism for regional air quality modeling, *Journal of Geophysical Research: Atmospheres*, 95, 16343-16367, 10.1029/JD095iD10p16343, 1990.
- Stockwell, W. R., Kirchner, F., Kuhn, M., and Seefeld, S.: A new mechanism for regional atmospheric chemistry modeling, *Journal of Geophysical Research: Atmospheres*, 102, 25847-25879, 10.1029/97JD00849, 1997.
- Streets, D. G., Bond, T. C., Lee, T., and Jang, C.: On the future of carbonaceous aerosol emissions, *Journal of Geophysical Research: Atmospheres*, 109, 10.1029/2004JD004902, 2004.
- Streets, D. G., Shindell, D. T., Lu, Z., and Faluvegi, G.: Radiative forcing due to major aerosol emitting sectors in China and India, *Geophysical Research Letters*, 40, 4409-4414, 10.1002/grl.50805, 2013.
- ten Brink, H., Otjes, R., Jongejan, P., and Slanina, S.: An instrument for semi-continuous monitoring of the size-distribution of nitrate, ammonium, sulphate and chloride in aerosol, *Atmospheric Environment*, 41, 2768-2779, <http://dx.doi.org/10.1016/j.atmosenv.2006.11.041>, 2007.
- ten Brink, H. M., Kruisz, C., Kos, G. P. A., and Berner, A.: Composition/size of the light-scattering aerosol in the Netherlands, *Atmospheric Environment*, 31, 3955-3962, [http://dx.doi.org/10.1016/S1352-2310\(97\)00232-X](http://dx.doi.org/10.1016/S1352-2310(97)00232-X), 1997.
- Textor, C., Schulz, M., Guibert, S., Kinne, S., Balkanski, Y., Bauer, S., Berntsen, T., Berglen, T., Boucher, O., Chin, M., Dentener, F., Diehl, T., Easter, R., Feichter, H., Fillmore, D., Ghan, S., Ginoux, P., Gong, S., Grini, A., Hendricks, J., Horowitz, L., Huang, P., Isaksen, I., Iversen, I., Kloster, S., Koch, D., Kirkevåg, A., Kristjansson, J. E., Krol, M., Lauer, A., Lamarque, J. F., Liu, X., Montanaro, V., Myhre, G., Penner, J., Pitari, G., Reddy, S., Seland, Ø., Stier, P., Takemura, T., and Tie, X.: Analysis and quantification of the diversities of aerosol life cycles within AeroCom, *Atmos. Chem. Phys.*, 6, 1777-1813, 10.5194/acp-6-1777-2006, 2006.

## Bibliography

---

- Thomas, R. M., Trebs, I., Otjes, R., Jongejan, P. A. C., Brink, H. t., Phillips, G., Kortner, M., Meixner, F. X., and Nemitz, E.: An Automated Analyzer to Measure Surface-Atmosphere Exchange Fluxes of Water Soluble Inorganic Aerosol Compounds and Reactive Trace Gases, *Environmental Science & Technology*, 43, 1412-1418, 10.1021/es8019403, 2009.
- Timonen, K. L., Hoek, G., Heinrich, J., Bernard, A., Brunekreef, B., de Hartog, J., xe, meri, K., Ibal-Mulli, A., Mirme, A., Peters, A., Tiittanen, P., Kreyling, W. G., and Pekkanen, J.: Daily Variation in Fine and Ultrafine Particulate Air Pollution and Urinary Concentrations of Lung Clara Cell Protein CC16, *Occupational and Environmental Medicine*, 61, 908-914, 2004.
- Tuccella, P., Curci, G., Visconti, G., Bessagnet, B., Menut, L., and Park, R. J.: Modeling of gas and aerosol with WRF/Chem over Europe: Evaluation and sensitivity study, *Journal of Geophysical Research: Atmospheres*, 117, 10.1029/2011JD016302, 2012.
- U.S. EPA, O. o. R. a. D., . : Air Quality Criteria for Particulate Matter. Chapter 10: Dosimetry of Inhaled Particles in the Respiratory Tract. EPA/600/P-95/001bF, April 1996.
- Van Dingenen, R., Raes, F., Putaud, J.-P., Baltensperger, U., Charron, A., Facchini, M. C., Decesari, S., Fuzzi, S., Gehrig, R., Hansson, H.-C., Harrison, R. M., Hüglin, C., Jones, A. M., Laj, P., Lorbeer, G., Maenhaut, W., Palmgren, F., Querol, X., Rodriguez, S., Schneider, J., Brink, H. t., Tunved, P., Tørseth, K., Wehner, B., Weingartner, E., Wiedensohler, A., and Wählén, P.: A European aerosol phenomenology—1: physical characteristics of particulate matter at kerbside, urban, rural and background sites in Europe, *Atmospheric Environment*, 38, 2561-2577, <http://dx.doi.org/10.1016/j.atmosenv.2004.01.040>, 2004.
- van Dorland, R., Dentener, F. J., and Lelieveld, J.: Radiative forcing due to tropospheric ozone and sulfate aerosols, *Journal of Geophysical Research: Atmospheres*, 102, 28079-28100, 10.1029/97JD02499, 1997.
- Visschedijk, A., and Denier van der Gon, H.: EUCAARI deliverable : Pan-European Carbonaceous aerosol inventory, Report, TNO Built Environment and Geosciences, D42, Utrecht, Netherlands, 2008.
- Wang, R., Tao, S., Shen, H., Huang, Y., Chen, H., Balkanski, Y., Boucher, O., Ciais, P., Shen, G., Li, W., Zhang, Y., Chen, Y., Lin, N., Su, S., Li, B., Liu, J., and Liu, W.: Trend in

## Bibliography

---

- Global Black Carbon Emissions from 1960 to 2007, *Environmental Science & Technology*, 48, 6780-6787, 10.1021/es5021422, 2014.
- Wang, Z. B., Hu, M., Wu, Z. J., Yue, D. L., He, L. Y., Huang, X. F., Liu, X. G., and Wiedensohler, A.: Long-term measurements of particle number size distributions and the relationships with air mass history and source apportionment in the summer of Beijing, *Atmos. Chem. Phys.*, 13, 10159-10170, 10.5194/acp-13-10159-2013, 2013.
- Whitby, E. R., and McMurry, P. H.: Modal Aerosol Dynamics Modeling, *Aerosol Science and Technology*, 27, 673-688, 10.1080/02786829708965504, 1997.
- Whitby, K. T.: Proceedings of the International Symposium The physical characteristics of sulfur aerosols, *Atmospheric Environment*, 12, 135-159, [http://dx.doi.org/10.1016/0004-6981\(78\)90196-8](http://dx.doi.org/10.1016/0004-6981(78)90196-8), 1978.
- Wiedensohler, A., Birmili, W., Nowak, A., Sonntag, A., Weinhold, K., Merkel, M., Wehner, B., Tuch, T., Pfeifer, S., Fiebig, M., Fj äraa, A. M., Asmi, E., Sellegri, K., Depuy, R., Venzac, H., Villani, P., Laj, P., Aalto, P., Ogren, J. A., Swietlicki, E., Williams, P., Roldin, P., Quincey, P., Hüglin, C., Fierz-Schmidhauser, R., Gysel, M., Weingartner, E., Riccobono, F., Santos, S., Gröning, C., Faloon, K., Beddows, D., Harrison, R., Monahan, C., Jennings, S. G., O'Dowd, C. D., Marinoni, A., Horn, H. G., Keck, L., Jiang, J., Scheckman, J., McMurry, P. H., Deng, Z., Zhao, C. S., Moerman, M., Henzing, B., de Leeuw, G., Löschau, G., and Bastian, S.: Mobility particle size spectrometers: harmonization of technical standards and data structure to facilitate high quality long-term observations of atmospheric particle number size distributions, *Atmos. Meas. Tech.*, 5, 657-685, 10.5194/amt-5-657-2012, 2012.
- Wiedinmyer, C., Akagi, S. K., Yokelson, R. J., Emmons, L. K., Al-Saadi, J. A., Orlando, J. J., and Soja, A. J.: The Fire INventory from NCAR (FINN): a high resolution global model to estimate the emissions from open burning, *Geosci. Model Dev.*, 4, 625-641, 10.5194/gmd-4-625-2011, 2011.
- Wild, O., Zhu, X., and Prather, M. J.: Fast-J: Accurate Simulation of In- and Below-Cloud Photolysis in Tropospheric Chemical Models, *J. Atmos. Chem.*, 37, 245-282, 2000.
- Wolke, R., Schröder, W., Schrödner, R., and Renner, E.: Influence of grid resolution and meteorological forcing on simulated European air quality: A sensitivity study with the



## Bibliography

---

- modeling system COSMO–MUSCAT, *Atmospheric Environment*, 53, 110-130, <http://dx.doi.org/10.1016/j.atmosenv.2012.02.085>, 2012.
- Xu, L., and Penner, J. E.: Global simulations of nitrate and ammonium aerosols and their radiative effects, *Atmos. Chem. Phys.*, 12, 9479-9504, 10.5194/acp-12-9479-2012, 2012.
- Yang, Q., W. I. Gustafson, J., Fast, J. D., Wang, H., Easter, R. C., Morrison, H., Lee, Y. N., Chapman, E. G., Spak, S. N., and Mena-Carrasco, M. A.: Assessing regional scale predictions of aerosols, marine stratocumulus, and their interactions during VOCALS-REx using WRF-Chem, *Atmos. Chem. Phys.*, 11, 11951-11975, 10.5194/acp-11-11951-2011, 2011.
- Zanobetti, A., Schwartz, J., and Gold, D.: Are there sensitive subgroups for the effects of airborne particles?, *Environ Health Perspect*, 108, 841-845, Sep. 2000
- Zaveri, R. A., and Peters, L. K.: A new lumped structure photochemical mechanism for large-scale applications, *J. Geophys. Res.*, 104, 30387-30415, 1999.
- Zaveri, R. A., Easter, R. C., Fast, J. D., and Peters, L. K.: Model for Simulating Aerosol Interactions and Chemistry (MOSAIC), *Journal of Geophysical Research: Atmospheres*, 113, 10.1029/2007JD008782, 2008.
- Zhang, K., Wan, H., Wang, B., Zhang, M., Feichter, J., and Liu, X.: Tropospheric aerosol size distributions simulated by three online global aerosol models using the M7 microphysics module, *Atmos. Chem. Phys.*, 10, 6409-6434, 10.5194/acp-10-6409-2010, 2010a.
- Zhang, Y., Seigneur, c., Seinfeld, J. H., Jacobson, M. Z., and S., B. F.: Simulation of aerosol dynamics: a comparative review of algorithms used in air quality models, *AEROSOL SCIENCE AND TECHNOLOGY*, 31, 487-514, 1999.
- Zhang, Y., Wen, X. Y., and Jang, C. J.: Simulating chemistry–aerosol–cloud–radiation–climate feedbacks over the continental U.S. using the online-coupled Weather Research Forecasting Model with chemistry (WRF/Chem), *Atmospheric Environment*, 44, 3568-3582, <http://dx.doi.org/10.1016/j.atmosenv.2010.05.056>, 2010b.
- Zhang, Y., Sartelet, K., Zhu, S., Wang, W., Wu, S. Y., Zhang, X., Wang, K., Tran, P., Seigneur, C., and Wang, Z. F.: Application of WRF/Chem-MADRID and WRF/Polyphemus in Europe – Part 2: Evaluation of chemical concentrations and sensitivity simulations, *Atmos. Chem. Phys.*, 13, 6845-6875, 10.5194/acp-13-6845-2013, 2013.

## **Bibliography**

---

Zheng, G. J., Duan, F. K., Su, H., Ma, Y. L., Cheng, Y., Zheng, B., Zhang, Q., Huang, T., Kimoto, T., Chang, D., Pöschl, U., Cheng, Y. F., and He, K. B.: Exploring the severe winter haze in Beijing: the impact of synoptic weather, regional transport and heterogeneous reactions, *Atmos. Chem. Phys.*, 15, 2969-2983, 10.5194/acp-15-2969-2015, 2015.

# Acknowledgements

To spend 4 years as a PhD student in “Aerosol Group” of TROPOS is a true privilege. I would like to thank everyone in TROPOS to a friendly atmosphere and for all the help that you have given me, regarding scientific questions, computer problems, administration matters, German language problems and etc. Especially, I would like to mention my old friends: Nan Ma, Jia Sun, and Liang Ran for the great company and talks in the hard time during these 4 years, also for reading several manuscripts.

Most of all, I am grateful to my supervisor Prof. Dr. Alfred Wiedensohler for giving me the opportunity to work with this interesting topic in this extraordinary group. I have received many useful suggestions, ideas and advices by discussion with Alfred. It has been a great inspiration to work with a person who possesses such vast knowledge concerning atmospheric science. I also would like to thank my supervisor committee and PhD commission: Yafang Cheng, who gives me lots of inspirations, guides me scientific writing and reads all my manuscripts carefully; Ralf Wolke, for the helpful discussions about atmospheric chemistry modelling and guidance of model operation and development; Wolfram Birmili, whose fantastic ideas and enthusiasm on science and life really enlighten me a lot; and Prof. Dr. Ina Tegen and Prof. Dr. Johannes Quaas for the very helpful discussions and suggestions. In addition, I would like to further thank Prof. Dr. Gregory Carmichael for his acceptance to review this PhD thesis.

I also want to especially thank: Johannes Größ and Monique Teich for million times helping me with the German language problems; Jamie Banks and Andrew Reigert for the proof-reading of this thesis; Shan Huang and Kay Weinhold for helping me settle down at the first moment I arrived Germany; Stefanie Feuerstein, Robert Wagner, Stefanie Richters, Sebastian Duesing and Simonas Kecorius for all the activities we had together making these 4 years much more colorful; Stefanie Bauditz-Augustin and Sebastian Bley for together fighting with the new cumulative PhD regulation; Markus Hermann, Birgit Wehner, Sascha Pfeifer and Gerald Spindler for their precise advices; and all your friendship during my stay. I also want to thank Denier van der Gon for providing the high resolution European emission inventory used in this work. I would like to further thank Prof. Dr. Chunsheng Zhao for introducing me to aerosol science and TROPOS.

Finally, I would like to thank my family and all my friends for supporting me and making my life much happier. It is also the greatest luck that I met the best girlfriend in the world during my stay in “Aerosol Group” of TROPOS: Yu Wang. Thank you for supporting all the time!



## **Declaration of Independence**

Hereby I, Ying Chen, declare that I prepared this PhD Thesis without inadmissible aid and only by the usage of the specified resources. I also declare, that I marked the directly or indirectly adopted ideas from external references.

I insure that I do not get any assistance benefits from other persons in selection and evaluation of the material as well as in the preparation of the manuscript.

Furthermore, I hereby declare and confirm that this dissertation is entirely the result of my own investigations except where otherwise indicated. In particular, I insure that I did not make a claim on the aid of a doctoral consultant. Also I insure that no one has gained, from me or from other persons on behalf on me, immediately or indirectly pecuniary advantages, which are related to the content of this PhD dissertation.

Hereby I insure that this PhD Thesis was not submitted, neither in Germany nor in other countries, in an identical or similar design to another examination office for the purpose of a graduation or another examination procedure.

Hereby I state that I have not been involved in another PhD procedure.

Leipzig, 28.02, 2017

Leipzig, 28.02.2017

Ying Chen

Ying Chen



# *Curriculum Vitae*

## **Ying Chen**

Address: Günselstr. 2, 04329 Leipzig, Germany

Tel: +49 1577 8471405; +86 13611590970

Email: chen@tropos.de

## **Personal**

Date of birth: October 27, 1984

Place of birth: Fujian, China

Nationality: Chinese

## **Academic Education**

08/2013-present

### **Doctoral candidate**

at the Leibniz Institute for Tropospheric Research (TROPOS)  
supervised by Prof. Dr. Alfred Wiedensohler  
co-supervised by Dr. Wolfram Birmili, Dr. Ralf Wolke, and Dr.  
Yafang Cheng from Max Planck Institute for Chemistry

09/2006-07/2009

### **Master of Science in Atmospheric Physics at Peking University, Beijing, China**

Master's thesis: "Influence of local circulation on the pollutants  
distribution and transport over Beijing"  
Supervised by Prof. Dr. Chunsheng Zhao

09/2002-07/2006

### **Bachelor of Science in Atmospheric Science at Nanjing University of Information Science & Technology, China**

Bachelor's thesis: "Influence of aerosol particle mixing state on its  
optical properties"  
Supervised by Prof. Dr. Jun Yang



## Research Experience

- 02/2012-07/2013      **State Grid Electric Power Research Institute (SGEPRI), Nanjing, China**  
Scientific Researcher in the field: “Climate & renewable energy”
- 07/2009-02/2012      **China Electric Power Research Institute (CEPRI), Nanjing, China**  
Scientific Researcher in the field: “Climate & renewable energy”

## Publications

- Chen Y.**, et al., A Parameterization of Heterogeneous Hydrolysis of N<sub>2</sub>O<sub>5</sub> for 3-D Atmospheric Modelling: Improvement of Particulate Nitrate Prediction, *Atmos. Chem. Phys. Discuss.*, 2017, 1-23, 10.5194/acp-2017-105, 2017.
- Chen Y.**, et al., Evaluation of the size segregation of elemental carbon (EC) emission in Europe: influence on the simulation of EC long-range transportation, *Atmos. Chem. Phys.*, 16, 1823-1835, 10.5194/acp-16-1823-2016, 2016a.
- Chen Y.**, Sea salt emission, transport and influence on size-segregated nitrate simulation: a case study in northwestern Europe by WRF-Chem, *Atmos. Chem. Phys.*, 16, 12081-12097, 10.5194/acp-16-12081-2016, 2016b.
- Chen Y.**, et al., Aircraft Study of Mountain Chimney Effect of Beijing, China, *J. Geophys. Res.*, 114, D08306, 10.1029/2008JD010610, 2009.
- Chen Y.**, et al., A Regional Wind Power Forecasting Method Based on Statistical Upscaling Approach, *Automation of Electric Power Systems*, 37(7), 1-5, 10.7500/AEPS201207126, 2013 (in Chinese).
- Chen Y.**, et al., Improvement of Ultra-short Term Wind Power Forecast Model, *Automation of Electric Power Systems*, 35(15): 30-33, 2011 (in Chinese).
- He J., Mao H., Gong S., Yu Y., Wu L., Liu H., **Chen Y.**, et al., Investigation of particulate matter regional transport in Beijing based on numerical simulation, *Aerosol & Air Qual. Res.*, accepted (Feb. 2017).

## **Academic Conferences & Trainings:**

European Aerosol Conference 2016: “Evaluation of size-resolved elemental carbon emission in Europe and its influence on long-range transportation”

(Best Poster Award, September 2016, Tours France)

European Aerosol Conference 2015: “Evaluation of Particulate matter (PM) simulation ability in Central Europe by a regional chemistry-transport model: COSMO-MUSCAT”

(oral presentation, September 2015, Milano Italy)

Winter School: “Advanced analysis of atmospheric processes and feedbacks and biosphere-atmosphere interactions”, University of Helsinki, (March 2014, Hyytiälä Finland)

AASRI Conference on Power and Energy System: “A Statistical Approach of Wind Power Forecasting for Grid Scale” (oral presentation, June 2012, Hongkong China)

## **Patents**

**Chen Y.**, et al., Patent Number: CN2011100758472, A wind power curtail evaluation method based on the wind real-time measurement, 2013 (China)

**Chen Y.**, et al., Patent Number: CN102509028, Total Grid scale wind power forecasting algorithm based on statistical up-scale method, 2013 (China)

Chen Z.B., **Chen Y.**, et al., Patent Number: CN2012102504297, Method for establishing wind speed-power conversion probability model, 2013 (China)

Cheng X., **Chen Y.**, et al., Patent Number: CN2012101697767, Method of solar power forecast in regional scale, 2012 (China)

Chen Z.B., Cheng X., Zhou H., Ding J., Cui F., **Chen Y.**, et al., Patent Number: CN201210352973, Method of cloud movement forecasting for solar power prediction, 2012 (China)



## **Zusammenfassung der Dissertation**

# **Evaluation and Improvement of Particle Number/Mass Size Distribution Modelling in WRF-Chem over Europe**

der Fakultät für Physik und Geowissenschaften der Universität Leipzig

eingereicht von

M. Sc. Ying Chen

angefertigt am

Leibniz-Institut für Troposphärenforschung (TROPOS), Abteilung Experimentelle Aerosol- und  
Wolkenmikrophysik, supervised by Prof. Dr. Alfred Wiedensohler

Juni 2017

---

## **1. MOTIVATION**

Atmospheric aerosol particles play an important role in global climate, via direct radiative forcing (DRF, light scattering and absorption) and indirect radiative forcing (IRF, participating in cloud processes). The radiative forcing of aerosols still has the highest uncertainty among all climate change agents according to the recent IPCC assessment (IPCC AR5, 2013). The particle number/mass size distribution (PSD) is a key parameter that determines both the direct and indirect radiative forcing of aerosol (IPCC AR5, 2013). However, the simulation of PSD in 3-D models is very challenging and still highly uncertain (Aquila et al., 2011). Within all anthropogenic aerosol chemical compounds, elemental carbon (EC) and nitrate play an important role in climate warming and cooling over Europe, respectively (IPCC AR5, 2013). EC is the second strongest contributor to current global warming (Bond et al., 2007). Many previous studies (e.g., Nordmann et al., 2014) evaluated the EC inventories over Europe and reported significant uncertainties. However, they mainly focused on the bulk EC concentration and did not pay enough attention to evaluate the PSD of EC particles, which is important for the lifetime, transport and optical properties of EC particles. More modelling studies are needed to improve the PSD simulation of EC, thus refining the assessments of EC climate effects. Nitrate is an important anthropogenic scattering aerosol component, especially in western and central Europe (Schaap et al., 2011), where nitrate is mainly presented in the form of fine mode semi-volatile  $\text{NH}_4\text{NO}_3$ . The natural source sea salt may also play an important role in the coarse mode nitrate formation, due to the heterogeneous reaction of  $\text{HNO}_3$ . Thermodynamically stable  $\text{NaNO}_3$  is formed in the coarse mode with a consumption of  $\text{HNO}_3$ . This may influence the gas-particle equilibrium of fine mode  $\text{NH}_4\text{NO}_3$  and is expected to change the PSD of nitrate.

## 2. OBJECTIVES

Accordingly, the scientific questions of the present thesis are the following (Fig. 1):

- Q1: Is the size distribution/segregation of EC (absorbing aerosol) well represented by the WRF-Chem model over Europe? What are the reasons for the uncertainties?
- Q2: Is the chemical pathway of nitrate (scattering aerosol) well represented by the WRF-Chem model over Europe? What are the main reasons for the uncertainties?
- Q3: How can natural source particles (sea salt) influence the simulated anthropogenic nitrate particle mass size distribution/segregation? How wide can the influence of sea salt on nitrate particle mass size distribution (PMSD) be spread over Europe?

## 3. RESULTS AND CONCLUSIONS

Summarizing the results of this thesis, the answers to the above questions are the following:

The EC mass concentrations were highly overestimated by WRF-Chem at Melpitz, especially for the coarse mode. The uncertainties mainly stem from its emission inventory (EUCAARI), including the emission rate and the size-segregation. The inventory allocates too much EC emission in coarse mode over Eastern Europe and Russia. This can significantly reduce the lifetime of EC particles (Fig. 1). Hence, the simulated transport of EC with eastern originated air masses to Germany was reduced accordingly (First publication).

The particulate nitrate mass concentrations were highly overestimated by WRF-Chem as coarse mode  $\text{NaNO}_3$  at Melpitz. This was caused by the overestimation of coarse mode sea salt mass concentration, which is due to the shortcoming of its emission scheme. The overestimation of sea salt promoted the  $\text{NaNO}_3$  formation via heterogeneous reaction with  $\text{HNO}_3$  (Fig. 1), leading to the overprediction of coarse mode nitrate (Second publication).

As illustrated in Fig. 1, the overestimated natural source sea salt facilitated the coarse mode  $\text{NaNO}_3$  formation with a consumption of  $\text{HNO}_3$ . This can push the gas-particle equilibrium of fine mode  $\text{NH}_4\text{NO}_3$  lean to the gas-phase  $\text{HNO}_3$ . Eventually, the sea salt shifted the modelled nitrate PMSD towards larger sizes. A transport mechanism, derived from the planetary boundary layer structure, can broaden the influence of sea salt on the nitrate PMSD to central Europe, where a considerable amount of  $\text{NO}_x$  and  $\text{NH}_4\text{NO}_3$  is present (Second publication).

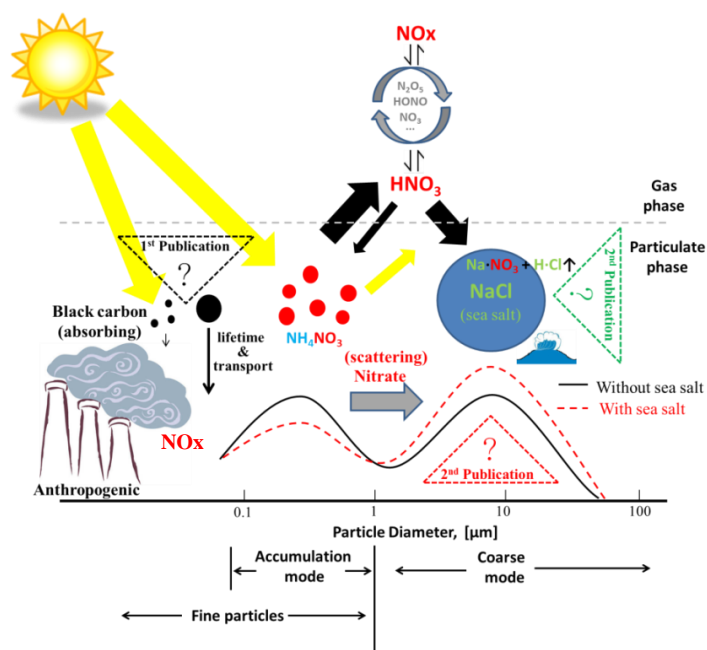


**Figure 1.** Schematic diagram of scientific objectives of the present thesis.

## References:

- Aquila, V., Hendricks, J., Lauer, A., et al.: MADE-in: a new aerosol microphysics submodel for global simulation of insoluble particles and their mixing state, *Geosci. Model Dev.*, 4, 325-355, 10.5194/gmd-4-325-2011, 2011.
- Bond, T. C., Bhardwaj, E., Dong, R., et al.: Historical emissions of black and organic carbon aerosol from energy-related combustion, 1850–2000, *Global Biogeochemical Cycles*, 21, n/a-n/a, 10.1029/2006GB002840, 2007.
- IPCC AR5: Climate Change 2013: The Physical Science Basis. Contribution of Working Group I to the Fifth Assessment Report of the Intergovernmental Panel on Climate Change, Report, edited by: Stocker, T. F., Qin D. H., Plattner, G. K., Tignor, M. M. B., Allen, S. K., Boschung, J., Nauels, A., Xia, Y., Bex, V., and Midgley, P. M., Cambridge University Press, New York, available at: <http://www.ipcc.ch/report/ar5> (last access: 10<sup>th</sup> September, 2016), 2013.
- Nordmann, S., Cheng, Y. F., Carmichael, G. R., et al.: Atmospheric black carbon and warming effects influenced by the source and absorption enhancement in central Europe, *Atmos. Chem. Phys.*, 14, 12683-12699, 10.5194/acp-14-12683-2014, 2014.
- Schaap, M., Otjes, R. P., and Weijers, E. P.: Illustrating the benefit of using hourly monitoring data on secondary inorganic aerosol and its precursors for model evaluation, *Atmos. Chem. Phys.*, 11, 11041-11053, 10.5194/acp-11-11041-2011, 2011.

## Publications List:

### First publication:

*“Chen, Y., Cheng, Y. F., Nordmann, S., Birmili, W., Denier van der Gon, H. A. C., Ma, N., Wolke, R., Wehner, B., Sun, J., Spindler, G., Mu, Q., Pöschl, U., Su, H., and Wiedensohler, A.: Evaluation of the size segregation of elemental carbon (EC) emission in Europe: influence on the simulation of EC long-range transportation, Atmos. Chem. Phys., 16, 1823-1835, 10.5194/acp-16-1823-2016, 2016a.”*

In this publication, I conceived the study, performed the model simulations, conducted the data analysis and draft the manuscript with inputs from all co-authors. All co-authors discussed the results. Furthermore, Yafang Cheng carried out the main corrections of this publication and helped to prepare the emission inventory. Stephan Nordmann provided the data of 2009 case which was analyzed in this study. Wolfram Birmili improved the manuscript and provided the GUAN data used in this study. Hugo A. C. Denier van der Gon provided the emission inventory for the simulation. Nan Ma, Ralf Wolke, Birgit Wehner, Jia Sun, Gerald Spindler, Qing Mu, Ulrich Pöschl, Hang Su, and Alfred Wiedensohler made useful suggestions for the manuscript and the project.

### Second publication:

*“Chen, Y., Cheng, Y., Ma, N., Wolke, R., Nordmann, S., Schüttauf, S., Ran, L., Wehner, B., Birmili, W., van der Gon, H. A. C. D., Mu, Q., Barthel, S., Spindler, G., Stieger, B., Müller, K., Zheng, G. J., Pöschl, U., Su, H., and Wiedensohler, A.: Sea salt emission, transport and influence on size-segregated nitrate simulation: a case study in northwestern Europe by WRF-Chem, Atmos. Chem. Phys., 16, 12081-12097, 10.5194/acp-16-12081-2016, 2016b.”*

In this publication, I conceived the study, performed the model simulations, conducted the data analysis and draft the manuscript with inputs from all co-authors. All co-authors discussed the results and provided useful suggestions. Furthermore, Yafang Cheng carried out the main corrections of this publication and helped to prepare the emission inventory. Hugo A. C. Denier van der Gon provided the emission inventory for the simulation. Gerald Spindler and Konrad Müller provided the DIGITEL filter chemical measurements at Melpitz. Bastian Stieger provided the MARGA measurements at Melpitz. Alfred Wiedensohler made useful suggestions for this project and the manuscript.



**Third publication (not contribute to this thesis):**

*“Chen, Y., Wolke, R., Ran, L., Birmili, W., Spindler, G., Schröder, W., Su, H., Cheng, Y., Tegen, I., and Wiedensohler, A.: A Parameterization of Heterogeneous Hydrolysis of N<sub>2</sub>O<sub>5</sub> for 3-D Atmospheric Modelling: Improvement of Particulate Nitrate Prediction, Atmos. Chem. Phys. Discuss., 2017, 1-23, 10.5194/acp-2017-105, 2017..”*

In this publication, I and Ralf Wolke conceived the study and performed the model simulations. I conducted the data analysis and draft the manuscript with inputs from all co-authors. All co-authors discussed the results and provided useful suggestions. Gerald Spindler provided the DIGITEL filter chemical measurements at Melpitz. Alfred Wiedensohler and Ina Tegen made useful suggestions for this project and the manuscript.

**Fourth publication (not contribute to this thesis):**

*He J., Mao H., Gong S., Yu Y., Wu L., Liu H., Chen Y., Jing B., Ren P., Zou C., Investigation of particulate matter regional transport in Beijing based on numerical simulation, Aerosol & Air Qual. Res., accepted (Feb. 2017).*

In this publication, I contributed to the scientific discussion, helped design and setup the modelling simulation, and made some corrections on the manuscript.

## **PhD commission:**

**Prof. Dr. Johannes Quaas** (Chairman)

from Institute for Meteorology, University of Leipzig, Leipzig, Germany  
johannes.quaas@uni-leipzig.de

**Professor Dr. Alfred Wiedensohler** (Supervisor)

from Leibniz Institute for Tropospheric Research, Leipzig, Germany  
ali@tropos.de

**Professor Dr. Ina Tegen**

from Leibniz Institute for Tropospheric Research, Leipzig, Germany  
itegen@tropos.de

## **Supervisor committee:**

**Prof. Dr. Alfred Wiedensohler** (First Supervisor)

from Leibniz Institute for Tropospheric Research, Leipzig, Germany  
ali@tropos.de

**Dr. Wolfram Birmili** (co-supervisor)

from Leibniz Institute for Tropospheric Research, Leipzig, Germany  
now at: German Federal Environment Agency (UBA), Berlin, Germany  
wolfram.birmili@uba.de

**Dr. Ralf Wolke** (co-supervisor)

from Leibniz Institute for Tropospheric Research, Leipzig, Germany  
wolke@tropos.de

**Dr. Yafang Cheng** (co-supervisor)

from Max Planck Institute for Chemistry, Mainz, Germany  
yafang.cheng@mpic.de